UNIVERSITA` DEGLI STUDI DI SASSARI

SCUOLA DI DOTTORATO IN SCIENZE BIOMOLECOLARI E BIOTECNOLOGICHE

Indirizzo Biochimica e Biologia Molecolare

CICLO XXIV

Direttore: Chiar.mo Prof. Bruno Masala

Molecular mechanisms involved in Amyotrophic Lateral Sclerosis: role of Bcl2-A1 and TDP-43 genes in motor neuron degeneration

Dottoranda

Dott.ssa Maria Elena Mura

Direttore:

Prof. Bruno Masala

Tutor:

Dott. Ciro Iaccarino

Anno Accademico 2010-2011

Index

Introduction

1. Amyotrophic Lateral Sclerosis (ALS)

Amyotrophic Lateral Sclerosis (ALS), also known as Lou Gherig's disease, is one of the most common neurodegenerative disorders, described for the first time by Jean-Martin Charcot in 1874. The pathology incidence is of 4-6 per 100.000 and the average age of onset is 50 years, but juvenile cases are also observed. The most typical feature of this progressive lethal disease is the degeneration of cortical, bulbar and spinal motor neurons, except for the neurons that control the bladder and the oculo-motoneurons (Fig. 1). This leads to generalized muscle weakness, fasciculations, muscle atrophy, speech and swallowing disabilities, progressive paralysis and, ultimately, death caused by respiratory failure (Bendotti et al., 2004). ALS may present as a predominantly lower motor neuron (LMN) form designates progressive muscular atrophy (PMA), a predominantly upper lower motor neuron (UMN) form called primary lateral sclerosis (PLS), or more commonly with mixed UMN and LMN deficits (Hand et al., 2002).

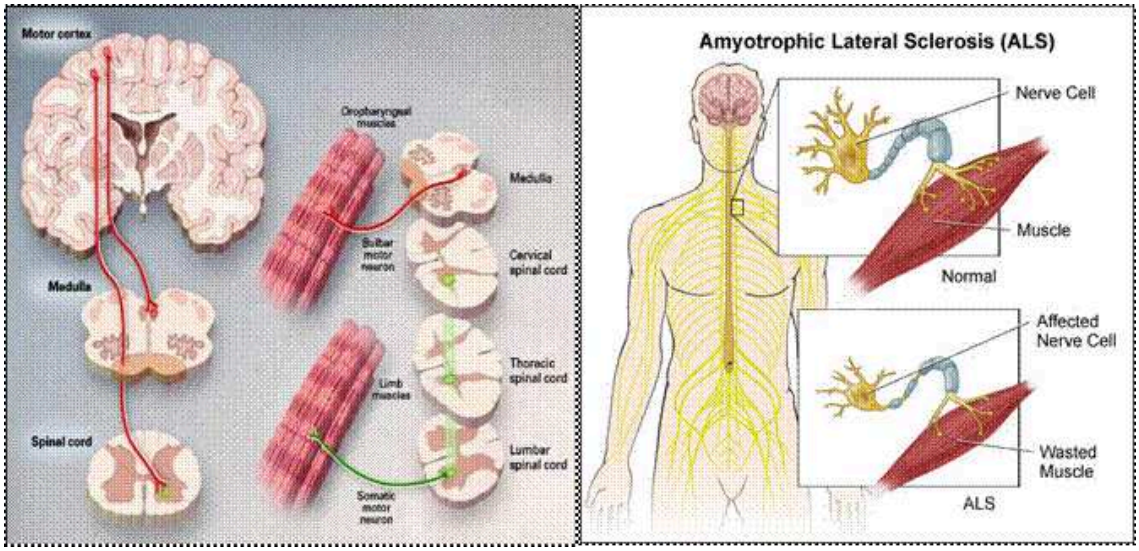

Fig. 1. Motor neurons involved in ALS and the consequent muscle atrophy.

Approximately 10% of ALS cases are inherited (familial ALS, FALS) and in the vast majority of patients, ALS is sporadic (SALS), although many cases labelled as sporadic may well have a family history (Andersen et al., 2011). Furthermore, SALS and FALS

are clinically indistinguishable and all genes found mutated in FALS cases have also been found mutated in SALS (Bendotti et al., 2004, Andersen et al., 2011). The male:female ratio is 1:1 in FALS and 1.7:1 in SALS, although this value decreases which increasing age at presentation, approaching 1:1 after 70 years of age. The duration of FALS is bimodal; a small percentage of patients have poor prognosis, with an average survival of < 2 years, whereas the remainder have a better prognosis than sporadic cases, with survival usually > 5 years (Hand et al., 2002). The development of effective therapeutics for ALS has been disappointing. Riluzole is the only approved medication shown in randomized controlled trials to benefit patients with SALS (Bensimon et al., 1994; Lacomblez et al., 1996). It is a neuroprotective drug that blocks glutamatergic neurotransmission in the CNS (Doble, 1996) but it has limited therapeutic benefits with minimal effects on survival (Miller et al., 2008) and no effect on muscle strength, quality of life or functional capacity (Lacomblez et al., 1996); it prolongs life by only 2 to 3 months (Miller et al., 2007). Other trials in the past year gave negative results, including lithium in combination with riluzole (Aggarwal et al., 2010), valproic acid (Piepers et al., 2009) and coenzyme Q10 (Kaufmann et al., 2009). In addition to pharmacotherapy, there are promising early developments with therapeutic implications in the areas of (i) RNA interference, (ii) stem cell therapies, (iii) viral vector-mediated gene therapy and (iiii) immunotheraphy (Mitsumoto et al., 2010).

(i) RNA interference (RNAi) is a process in which non coding miRNA inhibits and regulates gene expression by binding mRNA (Mello et al., 2004). This endogenous silencing mechanism is now being used to study its therapeutic application to autosomal dominant (heterozygous) disease that might be cured by effective silencing of the dominant mutant allele. Specific genes are experimentally target for silencing through the administration of siRNA produced *in vitro*, or miRNA using viral vectors.

(ii) Stem cell therapies might halt or slow the progression of motor neuron disease, by providing growth factors to host tissue, immunomodulation of host environment, anti-inflammatory effects of microglia and astrocytes, or even by replacing motor neurons or having trophic effects on neurons and neighboring cells. Several stem cell sources have been studied in ALS, including bone marrow transplant, mesenchymal stem cell (MSC) transplant, neural stem cell transplant, astrocyte precursor transplant, and induced pluripotent stem cells (iPSCs).

(iii) In diseases with identified genetic defects, there is ongoing research into using targeted gene therapy using viral vectors to improve abnormal protein synthesis. Whereas the large majority of human ALS is sporadic and without known mutation, another motor neuron disease, SMA, has a well defined genetic defect in the SMN1 gene. In 2010, Passini et al. described the use of a viral vector expressing human SMN that was injected into a mouse model of SMA. They described the successful expression of SMN in the mouse spinal cord, improved myofiber size and neuromuscular junction architecture, improvement in tests of muscle strength, and prolonged survival. This study is promising as a model for gene therapy in diseases of known genetic mutation and protein deficiency.

(iiii) Whereas RNAi therapy seems to reduce production of abnormal protein at transcriptional level, other studies are focusing on the use of antibody-mediated therapy to reduce the amount of abnormal protein. In follow-up to an earlier study demonstrating increased survival and delayed disease onset with SOD1 immunization (Urushitani et al., 2007), in other studies two monoclonal antibodies were tested against mutant SOD1 through passive intraventricular infusion in a mouse model (Gros Louis et al., 2010). One of the antibodies reduced the amount of mutant SOD1 in the spinal cord and prolonged survival. Passive antibody therapies may be safer but require further study.

2. Aetiology

Amyotrophic lateral sclerosis is likely to be a multifactorial and multisystem disease. The pathogenic mechanisms that underlie ALS remain largely unclear, but a large spectrum of aetiological factors have been considered including genetics, environmental factors, oxidative stress, glutamate excitotoxicity, mitochondrial damage, defective axonal transport, protein aggregation with TAR DNA-binding protein 43 as major constituent of the ubiquitinated protein inclusions found in surviving motor neurons in most forms of ALS, viral infection. Recently there has been growing interest in the role played by non-neuronal neighbourhood cells in the pathogenesis of motor neuron injury. Actually ALS is considered also a glial pathology and disruption of glial cell–motor neuron communication contribute to neurodegeneration and the propagation of motor neuron injury.

2.1 Environmental factors

Epidemiological studies demonstrate that there is a link between environmental factors and the onset of ALS. Environmental factors that have been associated with ALS risk include cigarette smoking (Chiba and Masironi, 1992; Weisskopf et al., 2004), exposure to heavy metals (Campbell et al., 1970; McGuire et al.; 1997; Kamel et al., 2002) and pesticides (Savettieri et al., 1991), intensive physical activity (Cruz et al., 1999; Longstreth, 1998; Chiò et al., 2005) and head injuries (Chen et al., 2007). A prospective study based on ALS mortality data found that an association with cigarette smoking was restricted to women (Weisskopf et al., 2005). Most of these factors have not been consistently implicated, but show variation in results across different studies. Nonetheless, there are indications that there may be causal links between different environmental toxicant, and a need for more research (Johnson and Atchison 2009; Schmidt et al., 2011).

2.2 Genetic factors

Although the underlying cause of the sporadic form of ALS remains unclear, progress in our understanding of disease mechanisms has been made through research into familial forms of ALS, which constitute 10% of cases (Bruijn et al., 2004).

Our understanding of the molecular and cellular pathology of ALS has progressed greatly since 1993, with the discovery that mutations in the gene coding for the Cu/Zn superoxide dismutase 1 (SOD1) underlie approximately 20% of FALS cases (Rosen, 1993). Mutations are inherited as an autosomal dominant trait (Deng et al., 1993). Subsequently, different Mendelian loci have been linked to FALS and several causative genes have been identified (Dion et al., 2009), including: ALSIN, that functions as an exchange factor for a small GTPase which regulates endosomal trafficking (Yang et al., 2001); VAPB, that encodes a vescicle-associated membrane protein-associated protein B (Nishimura et al., 2004); SETX, that encodes a DNA/RNA helicase (Chen et al., 2004); ANG, that causes a reduced neuroprotective activity against hypoxic injury (Greenway et al., 2006) and DCTN1, that is a component of the dynein complex that comprises the major axonal retrograde motor (Puls et al., 2003). Recently, much attention has been devoted to a gene coding for a DNA/RNA binding protein which has been implicated in the pathogenesis of ALS. In fact, a major shift in our understanding of ALS pathogenesis started in 2006 (Neumann et al., 2006; Arai et al., 2006) with the

identification of the 43 kDa transactive response (TAR) DNA-binding protein (TDP-43) as the main component of ubiquitinated protein aggregates found in sporadic ALS patients.

Dominant mutations in the TARDBP gene, which codes for TDP-43, were reported by several groups as a primary cause of ALS for 3% familial cases and 1.5% sporadic cases (Corrado et al., 2009; Kabashi et al., 2008). A list of genes involved in ALS is provided in Table 1.

Locus (chromosome)	Gene	Protein length (amino acids)	Number of mutations	Analysis type (initial)	Modes of inheritance	Phenotypic MND variants	Other features*	References
ALS1 (21q22.1)	*SOD1*	153×2	166	Linkage	Dominant–cp Dominant–icp Recessive *De novo* mutation	ALS PMA PBP (rare) BFA (rare)	Cognitive impairment (rare) Cerebellar ataxia Autonomic dysfunction (rare) FTD (rare)	Rosen *et al.* (1993)[31]
ALS2 (2q33.2)	*ALS2*	1,657	19	Linkage	Recessive	Juvenile PLS, juvenile ALS or infantile HSP	Unknown	Hadano *et al.* (2001)[42]
ALS3 (18q21)	Not identified	Unknown	None	Linkage	Dominant	ALS	NA	Hand *et al.* (2002)[122]
ALS4 (9q34)	*SETX*	2,677	9	Linkage	Dominant	ALS	AOA2, cerebellar ataxia, motor neuropathy‡	Chen *et al.* (2004)[43]
ALS5 (15q21.1)	*SPG11*	2,443	12	Linkage	Recessive	Juvenile ALS	NA	Orlacchio *et al.* (2010)[123]
ALS6 (16q11.2)	*FUS*	526	42	Linkage Candidate	Dominant–cp Dominant–icp *De novo* mutations Recessive	ALS ALS–FTD	Parkinsonism FTD	Vance *et al.* (2009)[80] Kwiatkowski *et al.* (2009)[81]
ALS7 (20p13)	Not identified	Unknown	None	Linkage	Dominant	ALS	NA	Sapp *et al.* (2003)[124]
ALS8 (20q13.3)	*VAPB*	99	3	Linkage	Dominant	ALS, PBP or PMA	Unknown	Nishimura *et al.* (2004)[86]
ALS9 (14q11.2)	*ANG*	147	17	Candidate	Dominant–cp Dominant–icp?	ALS PBP or ALS–FTD	Parkinsonism	Chen *et al.* (2010)[89]
ALS10 (1p36.2)	*TARDBP*	414	44	Candidate Linkage	Dominant–cp Dominant–icp Recessive (rare)	ALS ALS–FTD	PSP, PD FTD Chorea	Gitcho *et al.* (2008)[47] Sreedharan *et al.* (2008)[48] Kabashi *et al.* (2008)[49]
ALS11 (6q21)	*FIG4*	907	10	Candidate gene	Dominant	ALS PLS	CMT4J‡ Cognitive impairment	Chow *et al.* (2009)[110]
ALS12 (10p15–p14)	*OPTN*	577	5	Homozygosity mapping	Dominant–cp Recessive	ALS	POAG‡	van Es *et al.* (2009)[71]
ALS13 (12q24)	*ATXN2*	1,313	6 (intermediate length)	Candidate gene	Dominant	ALS	NA	Elden *et al.* (2010)[75]

*Other features reported in some but not all ALS patients with a particular mutation. ‡Clinical features reported in non-ALS patients with mutations not associated with ALS. Abbreviations: ALS, amyotrophic lateral sclerosis; AOA2, oculomotor apraxia type 2; BFA, benign focal amyotrophy; cp, documented complete penetrance; CMT4J, Charcot–Marie–Tooth disease type 4J; icp, documented incomplete penetrance; FTD, frontotemporal dementia; HSP, hereditary spastic paraparesis; MND, motor neuron disease; NA, information not available; PBP, progressive bulbar palsy; PD, Parkinson disease; PLS, primary lateral sclerosis; PMA, progressive muscular atrophy; PSP, progressive supranuclear palsy.

Table 1. Established ALS-associated genes as of June 2011 (Andersen and Al-Chalabi, 2011)

3 Superoxide dismutase 1 (SOD1)

3.1 Structure and function

Eukaryotic cells express three distinct forms of SOD. SOD 1 (Cu/Zn-SOD) is encoded on chromosome 21 (21q22.1)(Fig. 2) and localized to the cytoplasm. SOD 2 (Mn-SOD) is encoded on chromosome 6 and is located in the mitochondrial matrix, while SOD 3 (Fe-SOD) is an extracellular protein (Rosenfield et al., 1997).

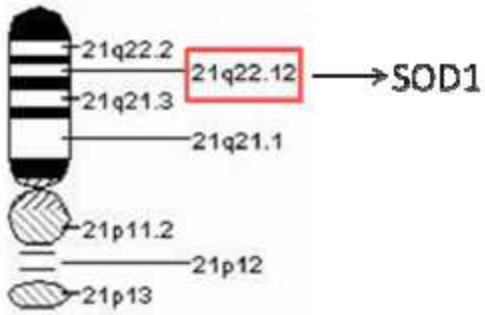

Fig. 2. SOD1 gene position on chromosome 21

SOD1 is an abundant protein in the CNS, accounting for about 1% of brain protein, but it is also ubiquitously expressed in all other tissues (Shaw et al., 2005). The product of the SOD1 gene, is a major antioxidant enzyme located predominantly in the cytosol, nucleus, and mitochondrial intermembrane space (IMS) of eukaryotic cells and in the periplasmic space of bacteria (Lyons et al., 1999; Matsumoto et al., 2001). The eukaryotic enzyme is a 32 kDa homodimer with a highly conserved amino acid sequence, and it contains one copper and one zinc-binding site, as well as a disulfide bond in each of its two subunits.

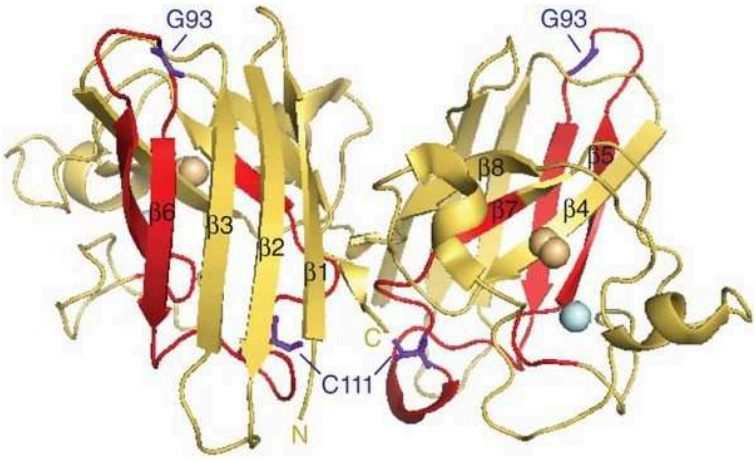

Fig. 3. The X-ray crystallographic structure of SOD1

Each of the two subunits of SOD1 forms an eight-stranded Greek key β-barrel and contains an active site that binds a catalytic copper ion (binding residues: His46, His48, His63 and His120) and a structural zinc ion (binding residues: His63, His71, His80 and Asp83) (Banci et al., 2008). The zinc ion is bound to three histidine residues and one aspartate residue. The copper atom is bound to four histidine residues. The two metal ions are connected via a histidine bridge (Fig. 4).

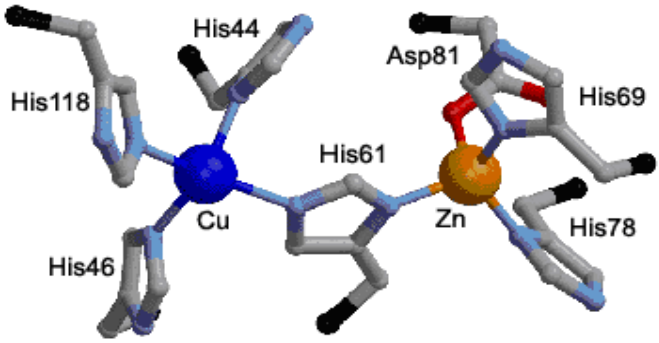

Fig. 4. Active site of SOD1

SOD1 catalyzes the disproportionation of superoxide, yielding hydrogen peroxide and dioxygen, thus reducing steady-state levels of superoxide in its surroundings, preventing the further generation of reactive oxygen species (ROS) (Dion et al., 2009). Attention has been focused on how mutations could affect these steps of SOD1 maturation. The mature, correctly folded and enzymatically active form of SOD1 is obtained in vivo through several post-translational modifications: acquisition of zinc and copper ions, disulfide bond formation, and dimerization (Culotta et al., 2006; Farnesano et al., 2004).

3.2 SOD1 mutations

To date, over 150 different mutations (mostly missense mutations) have been discovered in the SOD1 gene that account for 20% familial cases. Most of the individual mutations result in substitution of one single amino acid by another; such substitutions have been identified at over one third of the 153 amino acid residues of the wild-type Cu/Zn SOD protein. In addition to the individual amino acid substitutions, there are also a smaller group of mutations resulting in amino acid deletions and truncations. The mutations encompass all coding regions of the gene affecting over 70 positions with preponderance for exons 4 and 5 (Fig. 5).

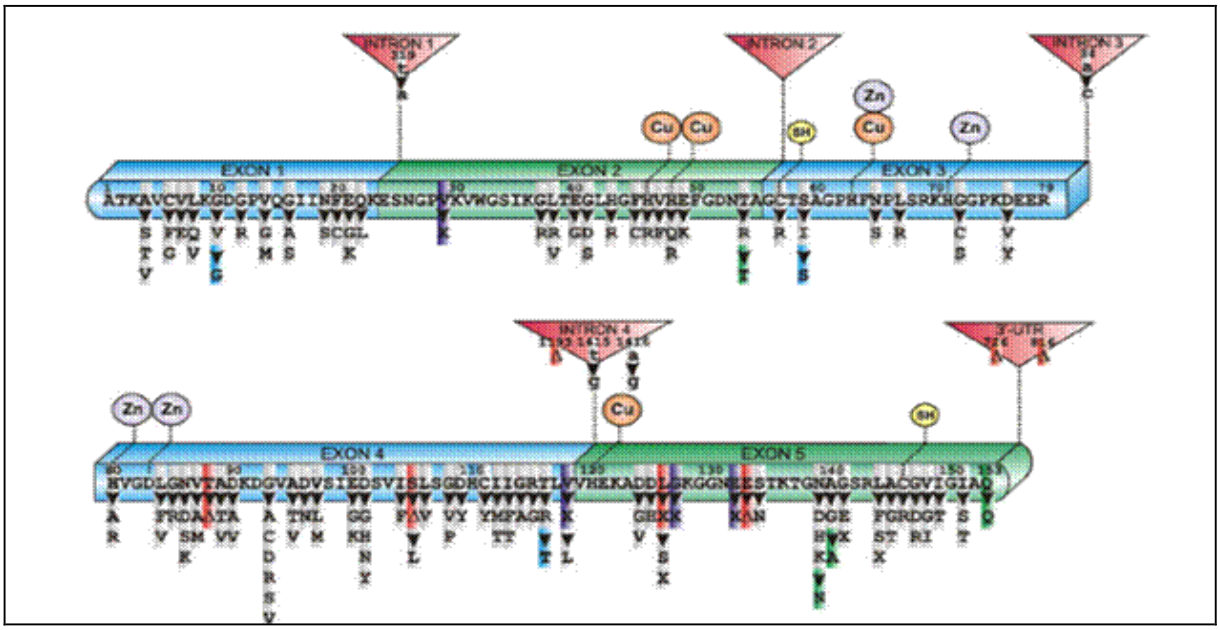

Fig. 5. Schematic diagram of human SOD1 primary sequence with exons, introns, metal binding domains (Cu, Zn), intramolecular disulfide bond (SH) and mutations linked to sporadic and familial ALS. Mutations are distributed throughout all exons with high prevalence in exons 4 and 5.No clear structure–function relationship to FALS appears evident. Mutation legend: grey, missense; purple, insertion; red, deletion; blue/green, silent; (D) in frame deletion; X, truncation (Turner and Talbot, 2008).

The mutations include some 110 missense, 8 nonsense, 7 sense and 3 in frame deletions in the coding sequence. Another 7 mutations occur in non coding sequence predicting aberrant mRNA splicing, although the precise functional effects of some of these mutations remains unclear (Restagno et al., 2005). Furthermore, the silent mutations are assumed to be non-pathogenic, although new data implicating the SOD1 transcript in ribonuclear protein complex stability suggests a plausible role for these variants in disease (Ge et al., 2006). Thus, the majority of SOD1 mutations encode polypeptides with single amino acid substitutions and a subset with C-terminal

truncation. All SOD1 mutations associate with dominant ALS, with the exception of N86S and D90A substitutions which also behave as recessive traits (Andersen et al., 1995; Hayward et al., 1998), although the former mutation was described in rare juvenile onset ALS. Compound mutations involving D90A and D96N were also reported in recessive FALS (Hand et al., 2001). SOD1-linked FALS is clinically heterogeneous both within and between affected families (Cudkowicz et al., 1997), hampering efforts to correlate disease onset and severity with mutation. Factors contributing to this include incomplete, low or age dependent penetrance and clinical anticipation (Iwai et al., 2002; Andersen, 2006). However, the most severe and prevalent mutation in America, A4V, reliably predicts short survival (Cudkowicz et al., 1997), while D90A, the most common SOD1 mutation worldwide and in the sporadic population, correlates with non-penetrant or slowly progressive disease (Andersen, 2006). Interestingly, D90A was first regarded as a neutral polymorphism in northern Scandinavian heterozygotes (Sjalander et al., 1995); however, homozygosity was later established in FALS pedigrees (Andersen et al., 1995). Remarkably, patients heterozygous for D90A were then discovered in the Belgian population (Robberecht et al., 1996), suggesting a protective haplotype in the Scandinavians. This ‘‘Viking haplotype’’ may have originated once from a common founder over 1000 years ago (Al-Chalabi et al., 1998) and is a linked to a cis-acting protective genetic factor presumed to be non coding SOD1 mutation (Parton et al., 2002), attempts at which to define have been unsuccessful to date. Curiously, only a single SALS patient with a de novo SOD1 mutation (H80A) has been reported (Alexander et al., 2002). This suggests that the strict division of FALS and SALS is problematic. In the absence of parental genotypes, an isolated case of ALS may be apparent SALS, dominant FALS with a low penetrant or de novo mutant SOD1 allele or recessive FALS as expertly reviewed recently (Andersen et al., 2006). It is important to note that some SOD1 mutations do not co-segregate with disease and carriers can remain asymptomatic throughout life, suggesting that not all SOD1 mutations cause ALS and some are rather polymorphisms. The clinical phenotype associated with a given mutation in the SOD1 gene is clearly not only dependent on the mutation itself, but may also be influenced by the genetic background of the patient, and possibly by environmental factors (Hayward et al., 1998). To date, there is no conclusive explanation on how mutations in the SOD1 gene cause ALS. Initially, it was hypothesized that mutations would impair the enzymatic activity of the protein, thus

resulting in increased cellular levels of reactive oxygen species, oxidative stress, and neuronal death (Deng et al., 1993). However, it has subsequently been shown that some mutants retain full catalytic activity, and that there is no correlation between residual enzymatic activity, clinical progression, and disease phenotype (Radunovic et al., 1997). Additional evidence against a loss-of-function hypothesis comes from animal models: SOD1 knockout mice do not develop motor neuron disease (Reaume et al., 1996), while transgenic mice (Gurney et al., 1994) and rats (Nagai et al., 2001) over-expressing the human mutant SOD1 gene do. Also, the expression of mutant SOD1 alleles in cell culture models induces apoptosis in neurons (Pasinelli et al., 1998). In both *in vitro* and *in vivo* models, dismutase activity appears to be normal or elevated, suggesting that SOD1 mutations may result into the acquisition of a novel function, toxic to motor neurons (gain-of function hypothesis). Several studies showed that mutant SOD1 is prone to misfolding and forms cytoplasmic aggregates. In turn, aggregates may lead to cell death by sequestering other cytoplasmic proteins essential for neuronal survival, by clogging the ubiquitin/proteasome system, by chaperones depletion, or by disrupting mitochondria, cytoskeleton and/or axonal transport (Ticozzi et al., 2011). The aggregation hypothesis is particularly attractive because protein aggregates are frequently associated with neurodegenerative diseases and are also observed in ALS (Bendotti et al., 2004). The discovery of mutations linked with fALS has made possible the development of aetiological models of the disease.

4. ALS10 and TDP-43

4.1 Structure and function of TDP-43

TARDBP, the gene encoding TDP-43, is located on chromosome 1p36.22, and is comprised of six exons (exon 1 is non-coding and of unknown function; exons 2–6 are protein coding) and is evolutionarily highly conserved. Cross-species comparisons of TDP-43 proteins from human, mouse, *Drosophila melanogaster*, and *Caenorhabditis elegans* showed a high degree of aminoacid sequence conservation (Ayala et al., 2005; Sreedharan et al., 2008).

The structure of TDP-43 was shown to resemble members of the heterogeneous ribonucleoprotein (hnRNP), RNA binding proteins, family (Lagier-Tourenne et al., 2010). TDP-43 contains five functional domains, which are illustrated in Figure 6. There are

two RNA recognition motifs (RRM1 and RRM2) and the greatest homology among species was shown to exist within these domains (Ayala et al., 2005). This suggests that proteins from human, mouse, worm and fly all share equivalent RNA and DNA recognition specificity. Further, these RRM domains have two highly conserved hexameric ribonucleoprotein 2 (RNP2), and octameric ribonucleoprotein (RNP1) regions, which are involved in binding to the TAR DNA sequence of HIV-1 and RNA sequences with UG repeats (Kuo et al., 2009). TDP-43 has a nuclear export signal (NES) and a nuclear localization signal (NLS) enabling it to shuttle between the nucleus and the cytoplasm, potentially transporting bound mRNAs (Banks et al., 2008). TDP-43 protein also has a glycine-rich sequence at the C-terminal, which has been shown to mediate protein–protein interactions (Lagier-Tourenne et al., 2010). However, this domain varies significantly between species and the low homology is presumed to reflect the differences in species-specific functions (Ayala et al., 2005).

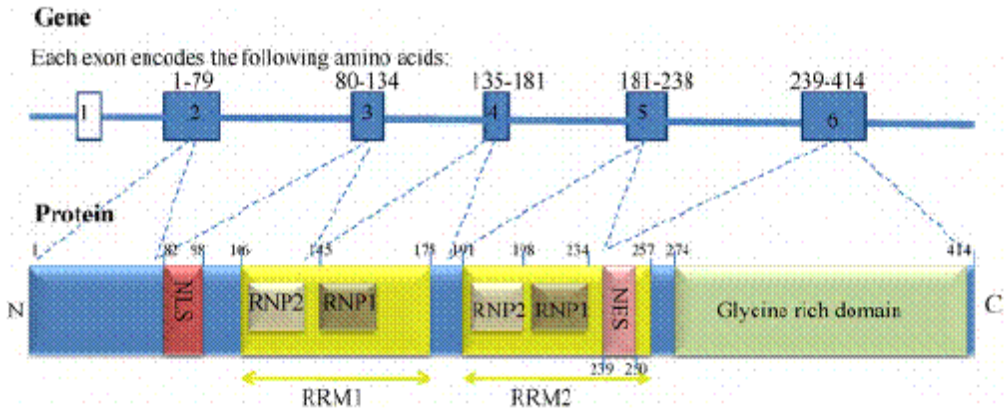

Fig. 6. Schematic diagram of the TARDBP gene and TDP-43 protein. Exon 1 of TARDBP is non-coding and exons 2–6 are protein coding. TDP-43 contains five known functional domains: nuclear localisation signal (NLS), nuclear export signal (NES), two RNA recognition motifs (RRM1 and RRM2) and a glycine-rich C-terminal region. Each RRM has two highly conserved regions, ribonucleoprotein 1 (RNP1) and ribonucleoprotein 2 (RNP2) (Warraich et al., 2010).

TDP-43 is a ubiquitously expressed protein in rodents and humans, with a possible species-specific difference in expression levels. Northern analysis showed that expression levels of human TDP-43 mRNA are heterogeneous among a variety of tissues, including pancreas, spleen, placenta, ovary, testis, lung, prostate, small intestine, kidney, colon, thymus, brain, and liver (Ou et al., 1995). TDP-43 is

predominantly localized to the nucleus with low levels in the cytoplasm (Banks et al., 2008). TDP-43 and some observed C-terminal fragments of the protein are degraded by both the ubiquitin proteasome system (UPS) and the autophagy-lysosomal pathway (ALP). Inhibition of the UPS or ALP was shown to cause cytoplasmic accumulation of TDP-43 in cell culture (Wang et al., 2010). TDP-43 has been found to associate with the ubiquitin-like protein, Ubiquilin 1, and binds and regulates the expression of histone deacetylase 6 (HDAC6), a protein associated with autophagasomal degradation (Fiesel et al., 2010; Lagier-Tourenne et al., 2010).

Most of the mutations identified are localized in the glycine-rich region encoded by exon 6. All the mutations are dominant missense changes with the exception of a truncating mutation at the extreme C-terminal of the protein (Y374X) (Daoud et al., 2009). Several variants lying in the non-coding regions of the TARDBP gene have been identified in patients but further studies are necessary to prove their pathogenic effect (Luquin et al., 2009; Gitcho et al., 2009). TDP-43 inclusions are not restricted to motor neurons but can be widespread in brain in ALS patients with or without dementia (Yokoseki et al., 2008; Van Deerlin et al., 2008; Pamphlett et al., 2009; Geser et al., 2008; Giordana et al., 2009).

Under normal conditions, TDP-43 is mainly localized within the nucleus, but abnormal TDP-43 distribution such as neuronal cytoplasmic or intranuclear inclusions and dystrophic neurites (Neumann et al., 2006; Arai et al., 2006), as well as glial cytoplasmic inclusions (Arai et al., 2006; Pamphlett et al., 2009; Dickson et al., 2007) have been reported. A very curious, and mechanistically unexplained, aspect of TDP-43 pathology is a significant TDP-43 nuclear clearance in a proportion of neurons containing cytoplasmic aggregates, suggesting that pathogenesis may be driven, at least in part, by loss of one or more nuclear TDP-43 functions (Neumann et al., 2006; Van Deerlin et al., 2008; Dickson et al., 2007; Igaz et al., 2008; Davidson et al., 2007). Immunoblotting of detergent-insoluble protein extracts from affected brain and spinal cord has defined a biochemical signature of disease that includes hyperphosphorylation and ubiquitination of TDP-43, and the production of several C terminal fragments (CTFs) around 25 kDa (Neumann et al., 2006; Arai et al., 2006).

The precise roles of TDP-43 is not fully elucidated. TDP-43 is structurally close to the family of heterogeneous ribonucleoproteins (hnRNPs) and has been involved in multiple levels of RNA processing including transcription, splicing, transport and translation (Fig.

7). Such multifunctional protein could have roles in coupling transcription with splicing and other RNA processes (Andersson et al., 2008; Bertolotti et al., 1999; Tan et al., 1999).

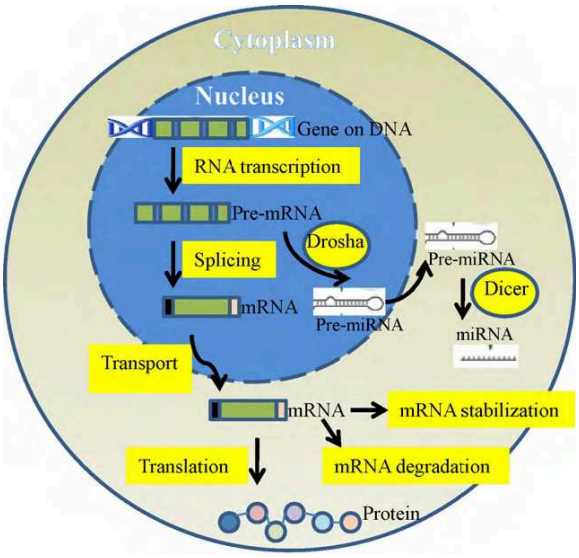

Fig. 7. Known biological functions of TDP-43. TDP-43 plays multiple roles in RNA processing (highlighted in yellow) in the nucleus and the cytoplasm (Warraich et al., 2010).

4.2 Role of TDP-43 in RNA metabolism

TDP-43 is widely implicated in many different aspects of RNA metabolism, including:

i) transcription

TDP-43 was cloned for the first time in 1995 as part of a research aimed at identifying novel HIV-1 inhibitors of transcription in correspondence to the TATA element of the viral LTR (Ou et al., 1995). The binding site of TDP-43 was identified as a polypyrimidine-rich region of the TAR DNA element and was hypothesized to repress the recruitment of transcriptional factors to this promoter. Unfortunately no follow up work has been reported in this system. More recently, a second promoter where TDP-43 has been described to play a functional role is in the mouse *SP-10* gene, which codes for an acrosomal protein, and whose expression is driven by a spermatid specific promoter (Lagier-tourenne et al., 2010). Also in this case, TDP-43 seems to mediate transcriptional repression in all mouse tissues with the exception of round spermatids (Buratti et al., 2010).

ii) Splicing

Evidence for a role of TDP-43 in splicing regulation came from the identification of their association with other splicing factors and that their depletion or over-expression affects the splicing pattern of specific targets. The association of TDP-43 with a number of

proteins involved in splicing (Buratti et al., 2005; Freibaum et al., 2010), is consistent with its function as a splicing regulator. These interactions are mediated by the C-terminal glycine-rich domain of TDP-43. Despite evidence that TDP-43 is involved in RNA splicing (Buratti et al., 2008; Law et al., 2006), few of its respective RNA targets has been identified and a comprehensive protein–RNA interaction map still needs to be defined. Recent technologies coupled with high-throughput sequencing have yielded a global insight into RNA regulation (Licatalosi et al., 2008; Yeo et al., 2009), and such approaches are eagerly anticipated to understand the role of TDP-43 in neurodegeneration. Indeed, disrupting the function of an RNA-binding protein can affect many alternatively spliced transcripts, and a growing number of neurological diseases have been linked to this process. Importantly, splicing alterations (Lin et al., 1998; Rabin et al., 2010) and mRNA-editing errors (Kawahara et al., 2004) have been reported in sporadic ALS patients. The observation of a widespread mRNA splicing defect in TDP-43 proteinopathies would reinforce the crucial role of splicing regulation for neuronal integrity and potentially identify candidate genes whose altered splicing is central to ALS pathogenesis.

iii) micro-RNA processing

TDP-43 may play roles in micro-RNA (miRNA) processing. It has been found (by mass spectrometry) to associate with Drosha (Gregory et al., 2004), the nuclear RNase III-type protein that mediates the first step in miRNA maturation (Kim et al., 2009). In addition, TDP-43 may be involved in the cytoplasmic cleavage step of miRNA biogenesis, mediated by the Dicer complex, as suggested by its association with proteins known to participate in these functions (Freibaum et al., 2010). Much more can be anticipated soon on the possible involvement of TDP-43 in miRNA processing.

Increasing evidence suggests that TDP-43 is integral components of RNA stress granules (SGs) (Andersson et al., 2008; Freibaum et al., 2010; Wang et al., 2008; Nishimoto et al., 2010), cytoplasmic, microscopically visible foci consisting of mRNA and RNP complexes that stall translation under stress conditions (Anderson et al., 2009). The role of these TDP-43-positive SGs remains unknown, but they were proposed to mediate the stabilization and transport of the low molecular weight neurofilament (NF-L) mRNA to the injury site for local translation of NF-L protein required for axonal repair (Strong et al., 2007, Moisse et al., 2009).

4.3 Cytosolic roles of TDP-43 in regulation of RNA subcellular localization, translation and decay

TDP-43 is also present in the cytosol where it is involved in diverse aspects of RNA metabolism, regulating the spatiotemporal fate of mRNA, i.e. subcellular localization, translation or degradation. Indeed, it has been shown by interspecies heterokaryon assays to shuttle between the nucleus and the cytoplasm (Ayala et al., 2008; Zinszner et al., 1997). In neurons, TDP-43 is found in RNA transporting granules translocating to dendritic spines upon different neuronal stimuli (Elvira et al., 2006; Wang et al., 2008). Collectively, these results suggest that both proteins could play a role in the modulation of neuronal plasticity by altering mRNA transport and local translation in neurons. The role of TDP-43 in the regulation of local translation is less well established; however, it has been shown to act as a translational repressor in vitro (Wang et al., 2008) and has extensive interactions with proteins participating in translation (Freibaum et al., 2010). Increasing evidence suggests that TDP-43 is integral components of RNA stress granules (SGs) (Andersson et al., 2008; Freibaum et al., 2010; Wang et al., 2008; Nishimoto et al., 2010), cytoplasmic, microscopically visible foci consisting of mRNA and RNP complexes that stall translation under stress conditions (Anderson et al., 2009). TDP-43 is neither essential for formation of SGs nor a neuroprotective factor in stress conditions (Colombrita et al., 2009). Nonetheless, in axotomized motor neurons *in vivo*, TDP-43 is found to translocate to the cytoplasm where it formed SGs that dissolved after neuronal recovery (Moisse et al., 2009; Sato et al., 2009). The role of these TDP-43-positive SGs remains unknown, but they are proposed to mediate the stabilization and transport of the low molecular weight neurofilament (NF-L) mRNA to the injury site for local translation of NF-L protein required for axonal repair (Strong et al., 2007, Moisse et al., 2009).

5 ALS experimental models

5.1 The SOD1 transgene

The discovery of gene mutations linked to human ALS has provided opportunities to develop model system for investigating mechanism of disease. The first models were cellular, mice and rats models mutant in the SOD1 gene.

Cellular models of SOD1 related ALS have been generated, which have helped to elucidate cellular mechanisms of disease (Shaw et al., 2005). In first models, SOD1 was inhibited chronically with either antisense oligodeoxynucleotides or diethyldithiocarbamate in spinal cord organotypic cultures. These studies showed that chronic inhibition of SOD1 resulted in the apoptotic degeneration of spinal neurons, including motor neurons, which. was markedly potentiated by the inhibition of glutamate transport (Rothstein et al., 1994). A limit of transient or stable transfection in human or mouse cells is the low endogenous gene expression level. This problem was solved by means of infection with replication-deficient recombinant adenoviruses. In an *in vitro* cell culture system, it has been shown that infection of mouse NSC-34 motor neuron-like cells with adenovirus containing mutant $SOD1^{G93A}$ gene increased cellular oxidative stress, mitochondrial dysfunction, cytochrome c release and motor neuron cell death (Liu et al., 2002).

In addition, several transgenic mouse and rat strains were created by the introduction of the sequence coding for human mSOD1 under the control of a promoter that enables ubiquitous expression of the transgene (Shibata et al., 2001). Unlike SOD1 knockouts, transgenic mice and rats with human fALS–SOD1 added to their own enzyme have a phenotype that closely resembles ALS (i.e. adult-onset progressive motor paralysis, muscle wasting and reduced lifespan). They also express almost all of the essential histopathological features of the human disease, including the selective degeneration of motor neurons in the spinal cord, the presence of ubiquitinated protein aggregates in motor axons and motor neuron perikarya, in addition to the fragmentation of the Golgi apparatus in motor neurons and the activation of microglia and astrocytes in the spinal cord and brainstem (Shibata et al., 2001). Moreover, several biochemical alterations observed in patients, such as the appearance of oxidative-stress markers, alterations of mitochondria in motor neurons and muscle and the activation of phosphorylation cascades are, in most cases, preserved in these models (Bendotti et al., 2001). There are, however, some differences between the various mutant SOD1 mouse strains (Valentine et al., 2005) and, depending on the mutation and copy number of the transgene, mutant SOD1 transgenic rodents die aged between 4 and 14 months. Transgenic mice recapitulate both the phenotype and the histopathology of patients and have the obvious advantage of a short lifespan of the animals. All FALS SOD1 rodents develop progressive muscular weakness and paralysis until death. Several transgenic

lines have been developed, carrying mutations at different positions in SOD1. Differences in the age of disease onset among those lines seem to depend predominantly on the transgene copy number, whereas the severity of the disease depends on the type of mutation. For example, the progression of the disease is much more rapid in mice that are transgenic for the G86R mutation of the mouse SOD1 (three days) or for the human G85R mutation (7–14 days) than in mice that are transgenic for human SOD1^{G93A} (60–110 days) (Shibata et al., 2001). Transgenic mice carrying 20 copies of SOD1 with the G93A mutation are the most widely studied. Figure 8 represents the progression of symptoms in these mice, which is preceded and paralleled by a sequence of alterations in the structure and function of motor neurons. As for many other diseases, the great advantage of an animal model that mimics the human pathology is the possibility to follow the stepwise progression of the disease, as well as for the design of potential therapeutics. However, the level of expression needed in heterozygous patients for mutant SOD1 to exert its toxic effect is much lower than for FALS transgenic rodents, in which a 10–30-fold increase of mutant protein level is necessary to induce the pathological phenotype. This is due to differences between mice and men; differences that should not be overlooked when using mice models (Carri et al., 2004).

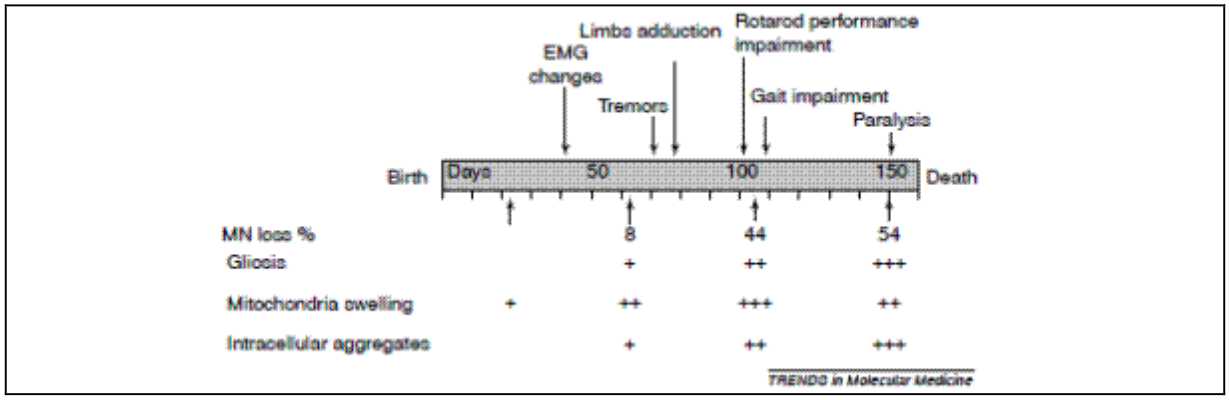

Fig. 8. Graphic representation of the behavioural and neuropathological progression of the disease in superoxide dismutase 1 SOD1^{G93A} transgenic mice. These mice develop the first signs of muscular dysfunction around two months of age, with an impairment of the evoked response tested electromiographically (EMG). Thereafter, tremors appear in the hind limb, associated with a progressive reduction in the extension reflex when the mice are raised by the tail. Atw4 months of age, the mice show a progressive muscular weakness starting from the hind limb, revealed by the increasing difficulty to stay on a rotating bar and by a reduction in stride length on an inclined ramp. At this stage, more than 50% of motor neurons (MN) of the lumbar spinal cord are lost and one month later these mice die. Mitochondrial vacuolisation and the swelling of motor neurons are among the earliest events and are accompanied by a decreased function of the mitochondria. Later, but still at the asymptomatic stage, the SOD1^{G93A} mice show signs of cytoskeletal disorganization in the motor neurons, with the accumulation of phosphorylated neurofilaments. The accumulation of detergent-insoluble proteins and ubiquitinated intracellular inclusions are particularly evident at advanced stages of the disease. Reactive gliosis, which involves hypertrophy and the activation of astrocytes, and the proliferation and activation of microglia, is detectable with the

degeneration of motor neurons and becomes prominent when the cell loss is remarkable. Hypertrophic astrocytes and reactive microglia are usually located around degenerating motor neurons (Bendotti and Carrì, 2004).

5.2 Cellular and animal models for TDP-43

The role of TDP-43 in the pathogenesis has not been established and both a gain of toxic property(ies) and a loss of function via its sequestration in aggregates are plausible. For TDP-43 the first outcomes modelling disease in fruit flies or mice have produced a confusing story that has not yet settled the key questions concerning mutant TDP-43-mediated pathogenesis. Consistently, increased cytoplasmic TDP-43 localization was found at presymptomatic stages in mice overexpressing wildtype TDP-43 (Wils et al., 2010) as well as in an acute rat model with adenovirus-mediated wild-type TDP-43 expression (Tatom et al., 2009).

In various cell culture experiments, the expression of TDP-43 proteins carrying mutations that disrupt its NLS (amino acids 78–84) led to localization primarily within the cytoplasm (Barmada et al., 2010; Winton et al., 2008). An elegant study utilized an automated microscopy system for long-term visualization and quantitative correlation between morphologic changes and survival of individual neurons to show that cytoplasmic TDP-43 is toxic for rat primary cortical neurons (Barmada et al., 2010). Although overexpression of wild-type TDP-43 led to increased cytoplasmic localization of TDP-43 and cell death independently of mutation, pathogenic TDP-43 mutations increased the proportion of cytoplasmic TDP-43 (Barmada et al., 2010). On the other hand, how forced synthesis of high levels of TDP-43 relates to actual pathogenic mechanism for the lower levels of TDP-43 in the physiologically relevant contexts is not established by such approaches. TDP-43 is likely to perform one or more cytoplasmic roles including contribution to neuronal recovery as illustrated by the rapid, transient cytoplasmic translocation of TDP-43 in response to stress (Moisse et al., 2009; Sato et al., 2009). These observations led to the hypothesis that prominent cytosolic localization in neurons of ALS patients may actually represent the typical response to stress rather than an initiating event in pathogenesis (Moisse et al., 2009; Sato et al., 2009). This could provide a partial explanation for the remarkably common incidence of cytoplasmic TDP-43 accumulation in a variety of neurodegenerative conditions of seemingly different origins. Increased cytoplasmic localization of TDP-43 is associated with the formation of intracellular aggregates in the affected areas in patients (Neumann et al.,

2006; Arai et al., 2006; Giordana et al., 2009) and in animal models including rats (Tatom et al., 2009), mice (Wils et al., 2010) and Drosophila (Li et al., 2010). In cell culture systems, increased cytoplasmic localization of TDP-43 was proposed to facilitate the formation of intracellular aggregates (Barmada et al., 2010; Winton et al., 2008; Nonaka et al., 2009). As in most neurodegenerative diseases where cytoplasmic aggregations are evident, an unresolved controversy is whether inclusions are neurotoxic or neuroprotective (Caughey et al., 2003), the latter presumably through the sequestration of smaller toxic species of misfolded proteins. The role of phosphorylation of TDP-43 in ALS patients has been explored with the help of phospho-specific antibodies that strongly bind to nuclear and cytoplasmic TDP-43. Using these, it has been identified as the major sites of phosphorylation on TDP-43 (Hasegawa et al., 2008) and was found highly phosphorylated in the proposed pathologic 25 kDa CTFs (Inukai et al., 2008; Hasegawa et al., 2008). Although a correlation between insolubility and phosphorylation of TDP-43 has been reported (Igaz et al., 2009), phosphorylation is not required for C-terminal cleavage, aggregation or toxicity, at least in cellular models (Zhang et al., 2009; Dormann et al., 2009). Fragments (20–25 kDa) containing the carboxy-proximal portion of TDP-43 accumulate in detergent (sarkosyl)-insoluble fractions derived from patient CNS tissues (Neumann et al., 2006; Arai et al., 2006). These CTFs originate, at least in part, from proteolytic cleavage at Arg208 (Igaz et al., 2009) and are more prominent in brains of ALS patients, whereas in the spinal cord of both groups, the predominant species within the inclusions are full-length TDP-43 (Igaz et al., 2008). When expressed in cells, the 25 kDa CTFs recapitulate some of the pathological features such as increased cytoplasmic accumulation, insolubility, hyperphosphorylation, polyubiquitination and cytotoxicity (Igaz et al., 2008; Zhang et al., 2009; Caccamo et al., 2009).

In transgenic mice expressing wild-type or mutant TDP-43, the appearance of the 25 kDa CTF (Wils et al., 2010; Wegorzewska et al., 2009) was shown to increase with disease progression, arguing for a pathogenic role (Wils et al., 2010). Curiously, in contrast to observations in patients (Neumann et al., 2006; Arai et al., 2006; Igaz et al., 2008) and in cell culture (Nishimoto et al., 2010; Zhang et al., 2009; Dormann et al., 2009; Zhang et al., 2007), where 25 kDa CTF is mainly cytoplasmic, the same fragment in transgenic mice was present solely in the nucleus where it formed intranuclear inclusions (Wils et al., 2010). Caspase-3, which is activated during apoptosis, has been

proposed to be the main protease generating the 25 kDa CTF in cells (Nishimoto et al., 2010; Zhang et al., 2009; Dormann et al., 2009; Zhang et al., 2007). The role of ubiquitination of TDP-43 in disease pathogenesis remains unknown, although it is likely to be a late event, since in patients the pre-inclusions and most TDP-43 inclusions are either weakly or not at all ubiquitinated (Giordana et al., 2009; Strong et al., 2007; Mori et al., 2008). Nevertheless, extensive ubiquitination of the pathologic CTFs in cells (Igaz et al., 2009) suggests that cellular degradation machineries such as the ubiquitin-proteasome system (UPS) and/or autophagy (reviewed in Levine et al., 2008) may be involved in removing TDP-43 aggregates.

6. Mechanisms in the pathogenesis of ALS

Current understanding of the neurodegenerative process in ALS suggests that there may be a complex interplay between multiple mechanisms including not only environmental and genetic factors but also oxidative stress, excitotoxicity, protein aggregation, and damage to critical cellular processes, including axonal transport and organelles such as mitochondria (Fig. 9).

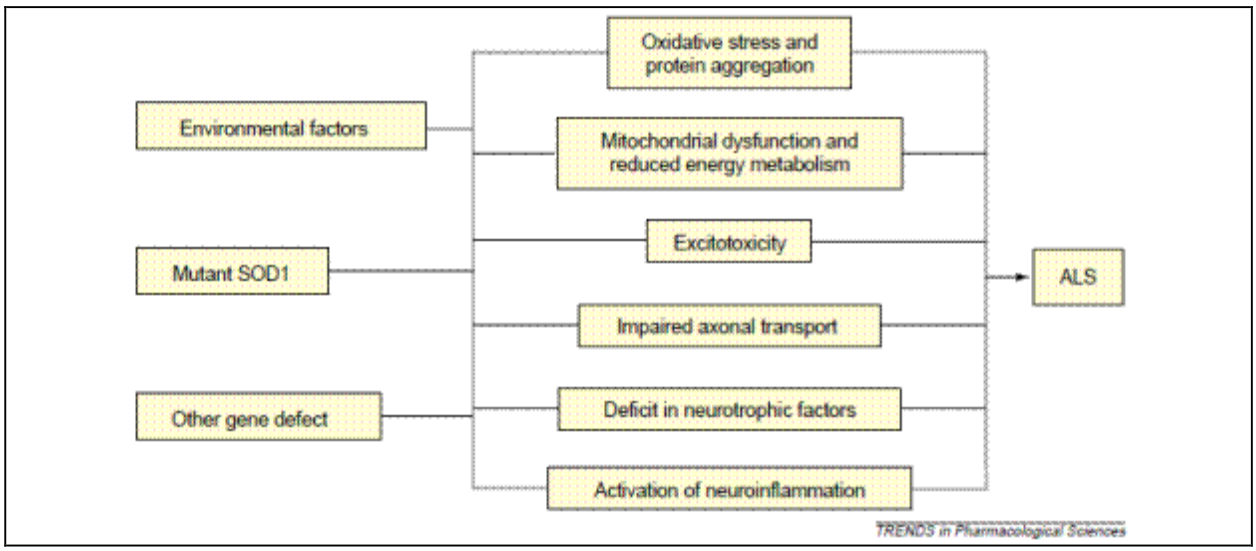

Fig. 9. Mechanisms in the pathogenesis of ALS. ALS occurs as both a sporadic disease and a familial disease that, in part because of the heterogeneity of onset and progression, are clinically indistinguishable. There is increasing evidence that cellular functions that are impaired as a consequence of the expression of mutant genes in fALS converge on pathways that can be activated in sALS by other 'environmental' toxic factors. Common pathways are represented by: (i) oxidative stress, which arises because of an imbalance between the production of ROS and the natural detoxifying defence and which might cause protein aggregation; (ii) mitochondrial dysfunction, which leads to oxidative stress, decreased activity of respiratory complexes, decreased ATP levels and cytochrome c release; (iii) excitotoxicity (the overstimulation of neurons by excitatory amino acid neurotransmitters such as glutamate), which causes the overloading of calcium ions into cellular compartments; (iv) defects in both

anterograde and retrograde axonal transport that impair axon–nuclear–axon communication; (v) deficit in neurotrophic growth factors, including brain-derived neurotrophic factor, ciliary neurotrophic factor, GDNF, IGF and VEGF; and (vi) neuroinflammation, which is a self-defence reaction that is aimed at neutralizing injurious stimuli that can become a harmful process. These pathways are activated in a complex neurotoxic cascade that involves molecular crosstalk between motor neurons and glia and between motor neurons and muscle, and leads to the non-cell-autonomous death of motor neurons. Therefore, intracellular and intercellular pathogenetic events represent possible 'points of intervention' for increasing the lifespan or improving the quality of life of patients, or both. It is interesting that overlapping mechanisms are thought to function in several other neurodegenerative disorders such as spinal cord injury, Alzheimer's disease, Huntington's disease and Parkinson's disease (Carrì et al., 2006).

Recently there has been growing interest in the role played by non-neuronal neighbourhood cells in the pathogenesis of motor neuron injury and in dysfunction of particular molecular signaling pathways (Fig.10).

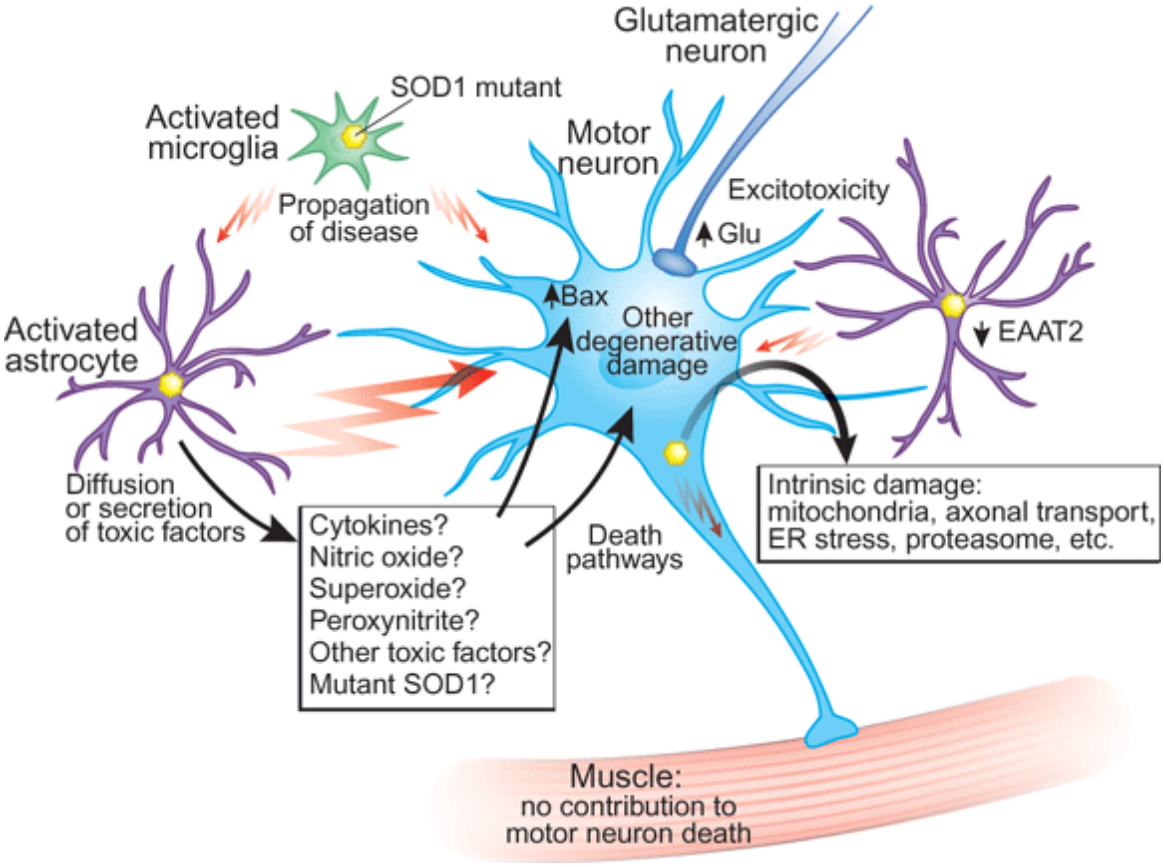

Fig. 10. Non–cell autonomous toxicity of mutant SOD1 produced by a combination of damage to different cell types. Mutant SOD1 caused intrinsic damage to motor neurons. The reduction of mutant SOD1 in motor neurons delays the onset of disease and extends the lifespan of transgenic ALS mice. Reduction of mutant SOD1 in microglia affects disease duration after onset, suggesting a role for microglia in the propagation of the disease. Although there is cell-autonomous damage caused by mutant SOD1 in the motor neurons, this may not be sufficient to trigger and propagate ALS pathogenesis (Julien 2007).

The relative importance of these different pathways may well vary in different subgroups of patients, and a very important task for clinicians and scientists in the future is to

further delineate the subcategories of motor neuronal diseases. Evidence has also accumulated that the final process of motor neuron death is likely to occur through a caspase dependent programmed cell death pathway resembling apoptosis (Shaw et al., 2005).

6.1 Oxidative stress

Oxidative stress causes structural damage and changes in redox-sensitive signaling. It arises from an imbalance between the generation and removal of reactive oxygen species (ROS), and/or from a reduction in the ability of the biological system to remove or repair ROS-induced damage (Ferraiuolo et al., 2011*)*. The effects of oxidative stress within non-dividing cells such as neurons may be cumulative, and cellular injury by free radical species is a major potential cause of the age related deterioration in neuronal function that occurs in neurodegenerative diseases. There has been particular interest in the role of oxidative stress in ALS, given that mutations in SOD1, which encodes a key cellular antioxidant defence protein, underlie around 20% of familial ALS cases. The close clinical and pathological similarity between sporadic and SOD1 related familial subtypes of motor neuronal diseases suggest that common pathophysiological mechanisms may be operating. In relation to the toxic gain of function of the mutant SOD1 protein, oxidative damage or metal mishandling, or both, have been strongly implicated. The main hypotheses have been that mutations alter the structure of the SOD1 protein, allowing greater access of abnormal substrates to the active copper site of the dimeric enzyme, resulting in the production of damaging free radical species including peroxynitrite and hydroxyl radicals. Both peroxynitrite and hydroxyl radicals are highly reactive and can cause oxidative damage to proteins, lipids and DNA. Such damage can alter protein conformations and disrupt enzyme active sites, change the properties of cellular membranes by oxidation of unsaturated fatty acids, and introduce mutations into DNA (Fig. 11) (Sian et al., 2006).

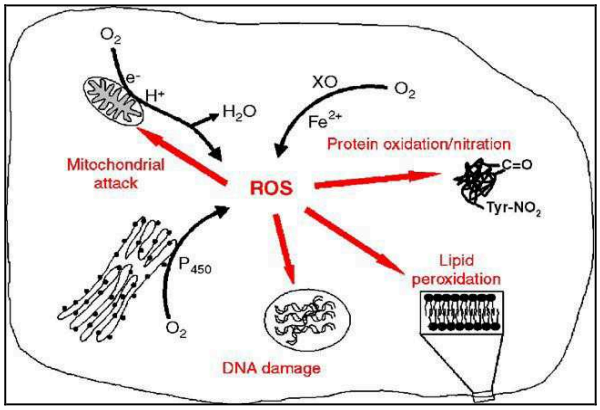

Fig. 11. Sources of reactive oxygen species and their targets. ROS are produced during oxidative phosphorylation in mitochondria, by oxidative enzymes including cytochrome P450 in the endoplasmic reticulum, and by xanthine oxidase (XO) and reduced metal ions in the cytosol. Cellular targets attacked by ROS include DNA, proteins, membrane lipids, and mitochondria (Barber et al., 2006).

Nitration of tyrosine residues on cellular proteins by peroxynitrite can have damaging consequences (Beckman et al., 1993). Some mutations in SOD1 render the protein more likely to form a zinc deficient variant (Crow et al., 1997; Estevez et al., 1999), which in turn makes the copper site more accessible to abnormal substrates. In vitro studies have shown that zinc deficient SOD1 causes peroxynitrite dependent cell death. Recently developed cellular models of mutant TAR DNA-binding protein 43 (TDP-43)-related ALS indicate that the presence of this mutant protein also induces oxidative stress in motor neuronal cell lines (Duan et al., 2010).

6.2 Excitotoxicity

Glutamate is the main excitatory neurotransmitter in the CNS and exerts its effects through an array of ionotropic and metabotropic postsynaptic receptors. The excitatory signal is terminated by removal of glutamate from the synaptic cleft by glutamate reuptake transporters, the most abundant of which is excitatory amino acid transporter 2 (EAAT2; also known as SLC1A2 or GLT1). Excitotoxicity is the term coined for neuronal injury induced by excessive stimulation of glutamate receptors, by mechanisms which include derangement of intracellular calcium homeostasis and excessive free radical production (Fig. 12). Motor neurons are particularly susceptible to toxicity through activation of cell surface AMPA receptors (Carriedo et al., 1996). A body of evidence, which is still circumstantial, has implicated glutamatergic toxicity as a contributory factor to motor neuron injury. The key findings are that the expression and function of the major glial glutamate reuptake transporter protein EAAT2 may be impaired in the CNS of ALS patients and that CSF (and therefore CNS extracellular fluid) levels of glutamate appear to be abnormally raised at least in a proportion of ALS patients (Rothstein et al., 1995; Fray et al., 1998; Shaw et al., 1995; Spreux-Varoquaux et al., 2002).

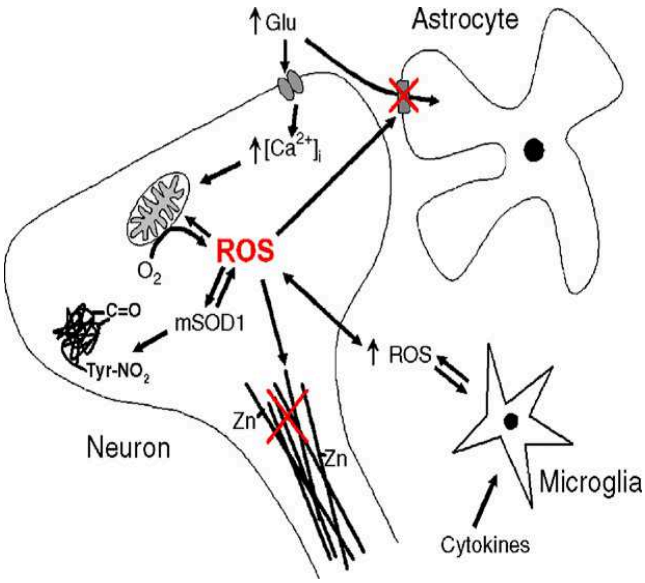

Fig. 12. Oxidative stress potentially influences other proposed mechanisms of neurodegeneration in ALS. Excitotoxicity leads to increased intracellular calcium levels that are buffered by mitochondria leading to increased ROS production. ROS, in turn, inhibit glutamate uptake through the EAAT2 transporter in glial cells. ROS can also cross the cell membrane and activate microglia, which respond by releasing cytokines and further ROS. Aberrant oxidative reactions catalysed by mutant SOD1 increase production of the highly reactive peroxynitrite and hydroxyl radical, causing nitration and aggregation of proteins including mutant SOD1 itself, and may also inhibit neurofilament assembly and cytoskeletal transport. Zinc binding to neurofilaments could deplete zinc binding to mutant SOD1 and exacerbate aberrant SOD1 chemistry (Barber et al., 2006).

The balance of evidence does not favour RNA mis-splicing as the cause of reduced EAAT2 expression as discussed above. Excitotoxicity has provided one of the few examples of a mechanistic link between mutant SOD1 mediated the sporadic form of the disease. The presence of mutant SOD1 increases the sensitivity of motor neurons to glutamate toxicity (Roy et al., 1998; Kruman et al., 1999), causes alteration in AMPA receptor subunit expression (Spalloni et al., 2003), and causes reduced expression of the major glutamate reuptake transporter EAAT2 (Bendotti et al., 2001). Whether as a primary or a propagating process, it appears that glutamate toxicity plays a contributory role to the injury of motor neurons in ALS.

6.3 Mitochondrial dysfunction

Mitochondria have a central role in intracellular energy production, calcium homeostasis and control of apoptosis. Several lines of evidence implicate mitochondrial dysfunction in ALS pathogenesis (Fig. 13).

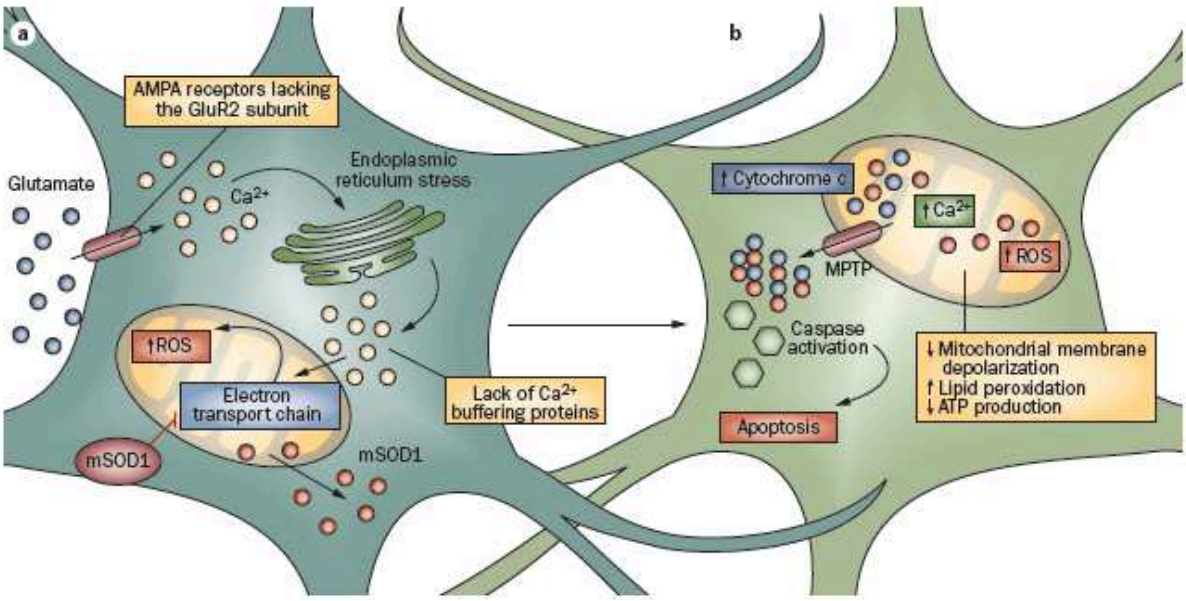

Fig. 13. Mitochondrial dysfunction in ALS. a) Studies on postmortem tissue and animal models of ALS have indicated a decrease in the activity of the complexes that form the mitochondrial electron transport chain, which may be caused by oligomers of mSOD1 associating with mitochondria. These oligomers could to lead to alterations in the mitochondrial redox state, damage to the mitochondrial protein import machinery, and sequestration of the antiapoptotic factor Bcl-2. Loss of EAAT2, and increased expression of calcium-permeable AMPA receptors lacking the edited form of the GluR2 subunit, leads to elevated intracellular calcium in motor neurons. High intracellular calcium concentrations may result in a toxic shift of calcium from the endoplasmic reticulum to the mitochondria, leading to excitotoxicity. Defective electron transport chain activity and calcium homeostasis are thought to underlie aberrant ROS generation. b) Together, these pathways result in depolarization of the mitochondrial membrane potential, reduced production of ATP, increased peroxidation of mitochondrial membrane lipids, opening of the MPTP channel, and initiation of apoptosis with release of cytochrome c into the cytoplasmic compartment. Abbreviations: ALS, amyotrophic lateral sclerosis; AMPA, α-amino-3-hydroxy-5-methyl-4-isoxazole propionic acid; EAAT2, excitatory amino acid transporter 2; MPTP, mitochondrial permeability transition pore; mSOD1, mutated superoxide dismutase 1; ROS, reactive oxygen species (Ferraiuolo et al., 2011)

Age related deterioration in mitochondrial function is considered a potentially important factor contributing to late onset neurodegenerative diseases. It is reviewed the existing evidence linking the expression of mutSOD1 to the many facets of mitochondrial dysfunction in ALS; recent studies suggests that the association and misfolding of the mutant protein (and possibly of the wild type protein as well) within these organelles is causally linked to their functional and structural alterations (Carrì and Cozzolino, 2001). The key evidence for mitochondrial dysfunction in human ALS includes the following:

- alteration in the morphology of mitochondria in hepatocytes, muscle and motor neurons;
- increased mitochondrial volume and calcium levels within motor axon terminals in muscle biopsies from sporadic ALS cases (Siklos et al., 1996);
- reduced complex IV activity in spinal motor neurons in sporadic ALS (Borthwick et al., 1999);

- high frequency of mitochondrial DNA mutations in motor cortex tissue in sporadic ALS (Dhaliwal et al., 2000);
- multiple mutations and decreased mitochondrial DNA in muscle and spinal cord in sporadic ALS (Wiedemann et al., 2002);
- ALS-like phenotype in one patient with a deletion in the cytochrome oxidase c subunit/gene (Comi et al., 1998).

Energy deficit, calcium mishandling and oxidative stress are paralleled by alteration in mitochondrial motility, dynamics and turnover and most probably lead to mitochondria-dependent cell death (Carrì and Cozzolino, 2011). Further evidence for the role of mitochondrial dysfunction as a contributory factor to motor neuron injury has come from the examination of cellular models of SOD1 related ALS. It has been demonstrated that mutant SOD1 proteins associated with the mitochondria tend to form cross-linked oligomers and that their presence causes a shift in the redox state of these organelles and results in impairment of respiratory complexes, this behaviour may explain the toxicity of ALS-mutant SOD1 proteins, which causes motor neurons to die (Ferri et al., 2006; Ferri et al., 2010). Expression of mutant (G93A) SOD1 in the NSC34 motor neuron cell line results in the development of morphologically swollen mitochondria, impaired activity of complexes II and IV of the mitochondrial respiratory chain, impaired cellular bioenergetic status, and alteration in the mitochondrial proteome (Takeuchi et al., 2002). Mitochondrial dysfunction has also been studied in mutant SOD1 transgenic mice. At least in some strains (for example, G93A) mitochondrial vacuolation within motor neurons is an early feature of the pathology (Wong et al., 1995). Whereas SOD1 was previously considered to be an exclusively cytosolic protein, it is now recognised also to reside in the intermembrane space of mitochondria (Higgins et al., 2002). SOD1 has been shown to accumulate in vacuolated mitochondria in mutant SOD1 mice (Jaarsma et al, 2001). It has been shown that the activities of several complexes of the mitochondrial respiratory chain are reduced before disease onset and that these changes increase with age. Neurodegeneration in motor neuron disease at the onset of the murine disease (Mattiazzi et al., 2002). Several groups have shown translocation of cytochrome C, an initiator of apoptosis, from the mitochondria to the cytosol during disease progression in the mouse (Guegan et al., 2001; Zhu et al., 2002). Partial deficiency of the mitochondrial form of SOD (MnSOD) exacerbates disease in transgenic SOD1 mice (Andreassen et al., 2000). Recently it has been reported that

mutant SOD1 is selectively and aberrantly recruited to the cytoplasmic face of mitochondria in spinal cord tissue from mutant SOD1 transgenic mice. Covalently damaged adducts of mutant SOD accumulated on the cytoplasmic face of mitochondria in the spinal cord (Liu et al., 2004). This tissue specific recruitment raises the possibility that mitochondrial abnormalities may be involved in the initiation of motor neuron injury. Recently it has been showed that the antiapoptotic protein Bcl2 may be entrapped within large protein aggregates of SOD1 in spinal cord tissue, which may result in reduction of the availability of this protein to regulate apoptosis (Pasinelli et al., 2004; Pedrini et al., 2010).

6.4 Cytoskeletal elements and axonal transport

Neurofilament proteins form a major component of the cytoskeleton of neurons, and important functions include maintenance of cell shape and axonal calibre, as well as axonal transport. Neurofilaments are the most abundant structural proteins in large cells with long axons such as motor neurons. Neurofilament subunits are assembled in the motor neuron cell body, and transported down the axon by slow axonal transport, with progressive phosphorylation during movement down the axon. Neurofilament subunits, classified according to their molecular weight as light (NF-L), medium (NF-M) or heavy (NF-H), have been identified as targets for oxidation by ROS produced by mutant SOD1. Accumulation and abnormal assembly of neurofilaments are common pathological hallmarks of ALS. Ubiquitinated inclusions with compact or Lewy bodylike morphology within surviving motor neurons in ALS may show immunoreactivity for neurofilament epitopes. The importance of neurofilaments in the normal functioning of motor neurons is demonstrated by the finding that approximately 1% of sporadic ALS cases have deletions of insertions in the KSP repeat region of the neurofilament heavy (NF-H) gene (Figlewicz et al., 1994; Tomkins et al., 1998). In addition, pathological changes within motor neurons develop in mice overexpressing NF-light or NF-heavy subunits, or in mice expressing mutations in the NF-light gene (Xu et al., 1993; Lee et al., 1994). Genetic manipulations to alter the expression of neurofilament proteins have been shown to alter the disease course in SOD1 transgenic mice. Increased expression of NF-heavy, which traps most neurofilaments within the cell body, robustly improves the disease course, by as much as six months in mutant SOD1 mice (Couillard-Despre's et al., 1998). The reasons for this somewhat counterintuitive effect are not

understood, though it has been suggested that excess neurofilaments within the cell body may function as a buffer for some other deleterious process, for example offering phosphorylation sites for dysregulated intracellular kinases, or reducing the burden of axonal transport (Lariviere et al., 2003). Motor neurons, which in the human nervous system may have axons up to one metre in length, are highly reliant on an efficient intracellular transport system with anterograde and retrograde components. It is interesting that in SOD1 mutant mice, axonal transport is demonstrably impaired several months before clinical disease onset (Williamson et al., 1992). The kinesin complex of proteins are important molecular motors for anterograde axonal transport on the microtubule system. Mutations of genes encoding several kinesin proteins have been shown to cause various types of motor neuron. The dynein–dynactin complex is the important motor for retrograde transport on the microtubule system, returning components (for example, multivesicular bodies and neurotrophic factors) back to the cell body. Mutations in dynein and the dynactin complex, which is an activator of cytoplasmic dynein, cause progressive motor neuron disease in mice (LaMonteet al., 2002; Hafezparast et al., 2003). As discussed in the genetics section, a dominant point mutation is the P150 subunit of dynactin, which causes a lower motor neuron disorder with vocal cord paresis in human subjects (Puls et al., 2003).

6.5 Inflammatory cascades and the role of non-neuronal cells

Recently there has been increasing interest in the possibility that non-neuronal cells, including activated microglia and astrocytes, may contribute to the pathogenesis or propagation of the disease process in ALS. Several studies in genetically engineered mouse models have indicated that expression of mutant SOD1 in neurons alone is insufficient to cause motor neuron degeneration and that participation of non-neuronal cells may be required (Pramatarova et al., 2001; Lino et al., 2002; Ferri et al., 2004). More recently Clement and colleagues produced several sets of chimeric mice which have both normal and mutant SOD1 expressing cells (Clement et al., 2003). Motor neurons expressing mutant SOD1 could escape disease if surrounded by a sufficient number of normal non-neuronal cells. Conversely normal motor neurons surrounded by mutant SOD1 containing non-neuronal cells developed signs of abnormality, with the development of ubiquitinated intraneuronal deposits. Astrocytes have many functions relevant to motor neuron physiology. First, they express the most important glutamate

transporter EAAT2/GLT-1, thus contributing to the clearance of this neurotransmitter; deficiency of astroglial EAAT2/GLT-1 causes severe motor neuron loss (Foran and Trotti, 2009) and alteration of this transporter has been repeatedly invoked as a cause contributing to ALS (Rothstein, 2009). Second, astrocytes are the major source of both trophic (Ekestern, 2004) and toxic factors (Ferri, 2004) for motor neurons. Several cytokines have been proposed to play a role in ALS as reinforcing signals from glia cells, including interleukin-6 (IL6), tumour necrosis factor α (TNFα), monocyte chemoattractant protein-1, monocyte colony-stimulating factor (MCSF) and transforming growth factor β1 (TGFβ1) that were found increased in cerebrospinal fluid, plasma and epidermis from ALS patients, although with sometimes conflicting results (Papadimitriou et al., 2010). In addition, the production of nitric oxide and the activation of cyclooxygenase type 2 (COX2) aggravate the toxic effects of mutant SOD1 in several experimental models for ALS. The production of all those proinflammatory mediators may be secondary to the induction of the transcription factor NF-κB, which is activated in the presence of reactive oxygen species (ROS) and by many other different signalling molecules associated with ALS onset and progression (Migheli et al., 1997; Kaltschmidt et al., 2005). NF-κB activation has been observed in astrocytes from ALS patients and in human cells expressing mutant SOD1 (Casciati, et al., 2002). NF-κB also regulates the expression of COX2 that may cause an increase in the synthesis of prostaglandins, which trigger astrocytic glutamate release and induce free radical formation, thus contributing to both excitotoxicity and oxidative damage. Indeed, treatment with COX2 inhibitors markedly protects motor neurones and significantly prolongs survival of ALS mice (Pramatarova et al., 2001). Surpriseling NF-κB downregulation in astrocytes, via espression of the dominant negative IκB-alpha-AA, fails to influence onset, severity, or progression of disease in a mutant SOD1-based ALS mice model (Crosio et al., 2006).
Recently it has been shown that also microglia play a critical role as resident immunocompetent and phagocytic cells within the CNS. Activation is associated with transformation to phagocytic cells capable of releasing potentially cytotoxic molecules including reactive oxygen species, nitric oxide, proteases, and proinflammatory cytokines such as interleukin-1B, tumour necrosis factor a (TNFα), and interleukin 6 (IL-6) (Gonzales-scarano et al., 1999). Given this, there is little doubt that activated microglia can inflict significant damage on neurons, but their role is complex and they are capable of stimulating neuroprotective as well as neurotoxic effects. Proliferation of

activated microglia is a prominent histological feature in the spinal ventral horn both in mutant SOD1 transgenic mice and in human ALS (Alexianu et al., 2001; Kauamata et al., 1992). In the mice, microglial activation is present before the onset of significant motor neuron loss or motor weakness. Various inflammatory cytokines or enzymes are upregulated in the spinal cord of ALS patients (IL-6, IL-1β, cyclo-oxygenase 2 (COX2), and prostaglandin E2 (PGE2)) or, in the spinal cord of mutant SOD1 mice (IL-1β, TNFα, COX2, PGE2) (Sekizawa et al., 1998; Hensley et al., 2002). Microglia appear to mediate the toxicity to neurons in patients with ALS by releasing factors that enhance glutamate toxicity (Brooks et al., 1995). It would be very relevant to identify molecules that contribute to this propagation and those released from activated microglia would clearly be plausible candidates. In a recent study D'Ambrosi and collegues have investigated about how mutant SOD1 affects P2 receptor-mediated proinflammatory microglial activation, considering that extracellular ATP is one of the most widespread microglia alarm signal endogenous to the CNS, and that ATP signaling evokes many proinflammatory functions of microglia. They observed up-regulation of P2X(4), P2X(7), and P2Y(6) receptors and down-regulation of ATP-hydrolyzing activities in mutant SOD1 microglia. This potentiation of the purinergic machinery reflected into enhanced sensitivity mainly to 2'-3'-O-(benzoyl-benzoyl) ATP, a P2X(7) receptor preferential agonist, and translated into deeper morphological changes, enhancement of TNF-α and cyclooxygenase-2 content, and finally into toxic effects exerted on neuronal cell lines by microglia expressing mutant SOD1 (D'Ambrosi et al., 2009). The purinergic activation of microglia may thus constitute a new route involved in the progression of ALS to be exploited to potentially halt the disease.

6.6 Protein aggregation

A recurring theme highlighted in research into neurodegenerative diseases has been the misfolding of mutant proteins with the formation of intracellular aggregates. Protein aggregates are found in motoneurons in models for ALS linked to a mutation in the gene coding for SOD1 and in ALS patients as well. Several hypotheses have been put forward to explain how mutant SOD1 aggregates could produce cellular toxicity. First, there might be sequestration of other proteins required for normal motor neuron function. Several additional proteins have been found present in SOD1 aggregates including CCS (copper chaperone for SOD1), ubiquitin neurofilaments, glial fibrillary

acidic protein, two neuronal glutamate transporters, Bcl2, and proteins involved in chaperone and proteosome functions (Pasinelli et al., 2004; Watanabe et al., 2001). Second, by repeatedly misfolding, the SOD1 aggregates may reduce the availability of chaperone proteins required for the folding and function of other essential intracellular proteins (Bruening et al., 2002). Third, the SOD1 mutant protein aggregates may reduce proteasome activity needed for normal protein turnover (Allen et al., 2003; Jhonston et al., 2000). Fourth, there could be inhibition of the function of specific organelles (for example, mitochondria) by aggregation on or within these organelles. Over-expression of chaperone proteins can reduce mutant SOD1 aggregation and enhances the survival and function of motor neurons in culture (Takeuchi et al., 2002). Aggregation of mutant SOD1 in the cytoplasm and/or into mitochondria has been repeatedly proposed as a main culprit for the degeneration of motor neurons. It is, however, still debated whether SOD1 aggregates represent a cause, a correlate or a consequence of processes leading to cell death. It has been demonstrated in a recent study that the over-expression of Grx1 increases the solubility of mutant SOD1 in the cytosol but does not inhibit mitochondrial damage and apoptosis induced by mutant SOD1 in neuronal cells (SH-SY5Y) or in immortalized motor neurons (NSC-34). Conversely, the over-expression of Grx2 increases the solubility of mutant SOD1 in mitochondria, interferes with mitochondrial fragmentation by modifying the expression pattern of proteins involved in mitochondrial dynamics, preserves mitochondrial function and strongly protects neuronal cells from apoptosis (Ferri et al., 2010).

The identification of TDP-43 as the major protein constituent of these inclusions initiated a major shift in our understanding of the patho-biology of ALS. As I have said before, under normal conditions, TDP-43 is predominantly localized in the nucleus, and loss of nuclear TDP-43 staining is seen in most cells containing TDP-43-positive cytoplasmic inclusions (Neumann et al., 2006). TDP-43 inclusions are not restricted to motor neurons, and it seems that cytoplasmic redistribution of TDP-43 is an early pathogenic event in ALS (Giordana et al., 2010). Similarly, cytoplasmic inclusions containing mutant fused in sarcoma (FUS) protein have been observed in some patients with FUS-related FALS (Groen et al., 2010; Hewitt et al, 2010).

Proteins found in aggregates in ALS provide several important clues about the disease pathogenesis. Loss of nuclear TDP-43 and/or aggregation of the protein in cytoplasmic inclusions may be key pathogenic processes in both SALS and FALS.

6.7 DNA/RNA metabolism

Identification of TDP-43, a ubiquitously expressed RNA–DNA binding protein, as a major component of the ubiquitinated inclusions in ALS focused attention on altered RNA processing as an important potential pathophysiological mechanism in this disease (Fig. 14).

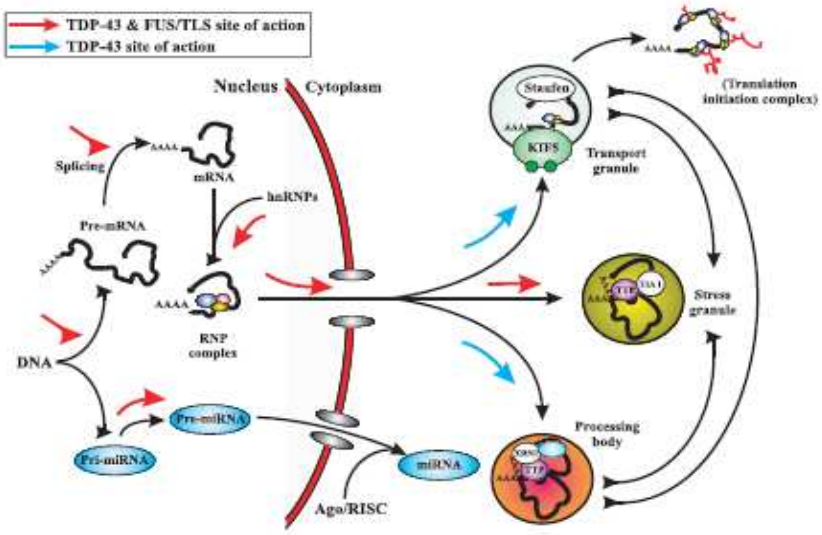

Fig. 14. Schematic diagram of the mRNA metabolism pathway from transcription through to degradation. Pre-mRNA is generated from DNA by RNA polymerase II and then processed by the spliceosome into mRNA. mRNA is incorporated into an RNP complex which is then shuttled to the cytosolic compartment where it is further modified into either transport granules, translationally quiescent stress granules or processing bodies in which mRNA is targeted to degradation. There is significant interchange of mRNAs, however, between each of these compartments, with each having the capacity to return the mRNA to a translationally active polysome. mRNA degradation is modulated, in part, by the incorporation of miRNA into the mRNP complex. Complete complementarity with the target mRNA will lead to mRNA degradation, while incomplete complementarity will lead to translational inactivation but not necessarily degradation. Sites at which both TDP-43 and FUS can impact on RNA metabolism are shown as red arrows, while those at which only TDP-43 has been identified to interact are shown as blue arrows. Note the many steps at which FUS/TLS and/or TDP-43 may have an effect on the pathway, each of which may manifest as overall changes in the cellular phenotype (Strong and Volkening, 2011).

The mRNA is first produced as a pre-mRNA from which non-coding sequences (introns) are removed by the spliceosome, a large RNP complex in which both TDP-43 and FUS/TLS can be found (Freibaum et al., 2010; Sephton, et al. 2011). Once spliced, mature mRNA is transported from the nucleus (Iko et al., 2004). With the inclusion of molecular motors including dynein (retrograde transport) or kinesin (anterograde transport), the resulting transport granules shuttle mRNA to the location at which it is required for translation. Under conditions of cellular stress, transport granules and translation initiation complexes may be quickly converted into translationally quiescent granules known as stress granules (SGs). Typically, SGs are believed to store mRNA

that is required in response to cellular stress or injury until such time as the mRNA is required to be translationally competent, or they may serve as locations to repair abnormal translational complexes that are inoperative (Buchan et al., 2009). Regardless of purpose, mRNA sequestered to SGs is translationally quiescent. Interestingly, dynein and kinesin appear to play opposing roles in SG dynamics, with knock-down of dynein impairing SG formation while kinesin is required for SG dissolution (Loschi et al., 2009). SGs exist in a dynamic equilibrium with processing bodies (P-bodies), cytoplasmic RNA granules that mediate RNA degradation through a mechanism involving decapping followed by XRN1 digestion of the mRNA (Parker et al., 2007; Sheth et al., 2003). These structures are also translationally inactive. In addition to this route of mRNA degradation, AU-rich mRNA and RNA that does not satisfy quality control mechanisms in the cell are commonly degraded by the exosome in a 3'–5' manner (Mukherjee et al.. 2002; Houseley et al., 2006; Chen et al., 2001). Targeting of mRNA for silencing or degradation is also controlled by the incorporation of microRNA (miRNA) into mRNA containing granules. miRNA is transcribed from DNA as pri-miRNA, processed by DGCR8/Drosha, exported as pre-miRNA and further processed by Dicer/TRB in association with Argonaut proteins (Macfarlane and Murphy 2010; Fiesel and Kahle, 2011). It is then incorporated into the RNA-induced silencing complex (RISC) where removal of the complementary strand yields the mature miRNA that is incorporated into the mRNA-containing granule (Gregory et al., 2004; Liu et al., 2008; Pillai 2005; Jabri 2005). Complete complementarity results in rapid degradation of the mRNA while incomplete complementarity translationally silences the mRNA (Nelson et al., 2008).

However, it must be noted that this is not an absolute as some miRNA may cause an increase in translation (Orom et al., 2008). From the description of the RNA metabolism pathway above, it is clear that a very important part of this process is the dynamic nature in which regulatory factors such as miRNA and proteins interact with the mRNA throughout this process and the effects this can have on RNA stability, compartmentalization (Chaudhury et al 2010) and the ultimate fate of the mRNA (Singh and Valcarcel, 2005). This concept of dynamic plasticity of the RNP granule is unfortunately often put aside in the discussion of any single RNA binding protein and its relevance to ALS (Strong and Volkening, 2011).

A further recent study indicates that mutant TDP-43 dysregulates alternative splicing of mRNA (Highley et al., 2010). Fibroblast cell lines derived from patients with TARDBP-

related ALS showed the expected loss of nuclear expression of TDP-43, together with widespread changes in RNA splicing, including changes in transcripts of other RNA-processing genes and genes that have been previously implicated in ALS. The authors concluded that splicing dysregulation associated with loss of nuclear TDP-43 is likely to contribute to the pathophysiology of ALS.

Further evidence of dysfunctional RNA metabolism in ALS emerges from the presence of mutations in angiogenin (ANG) (Greenway et al., 2006) and the DNA–RNA helicase senataxin (SETX) in some cases. ANG, the expression of which is increased during hypoxia to promote angiogenesis, also acts as a transfer RNA-specific ribonuclease and regulates ribosomal RNA transcription (Kieran et al., 2008). A proposed mechanism by which ANG normally prevents cell death is inhibition of the translocation of apoptosis-inducing factor into the nucleus (Li et al., 2011). Mutations in ANG are likely to have a deleterious effect through loss of function, as over-expression of ANG extends the lifespan of mSOD1 mice (Kieran et al., 2008). SETX autosomal dominant mutations are associated with juvenile-onset FALS (Chen et al. 2004). The SETX protein is predicted to be a component of large ribonucleoprotein complexes, with roles in maintaining DNA repair in response to oxidative stress, and RNA processing (Chen et al. 2004). The mechanisms by which mutant SETX causes ALS remain to be determined.

Additional evidence that dysregulated RNA processing may contribute to motor neuron injury in ALS arises from the detection of biomarkers of RNA oxidation in human ALS and mSOD1 mice (Chang et al., 2008), and the transcriptional repression within motor neurons that occurs in the presence of mSOD1 (Kirby et al., 2005; Ferraiuolo et al., 2007).

7. Motor neuron death in ALS: a role for apoptosis

Cell death can occur by different possible mechanisms, including autophagy, necrosis and apoptosis. Autophagy seems to prevail as a protein clearing system over other multienzymatic pathways such as the proteasome within motor neurons. The evidence which links an altered autophagy to the onset of motor neuron death proposes that this biochemical pathway might represent a final common mechanism underlying both inherited and sporadic forms of ALS (Crippa et al., 2010; Nassif and Hetz, 2010; Pasquali et al., 2010).

Necrosis is the classically recognised form of cell death and is characterised by high amplitude swelling of the mitochondria, nuclear flocculation and uncontrolled cell lysis. Tissue necrosis is normally seen following severe trauma to cells. The alternative form of cell death is via a programmed sequence of events and is termed apoptosis.

The pathways of apoptosis play an integral part in many biologic events, including morphogenesis, cell turnover, and the removal of harmful cells, and balanced apoptosis is crucial to ensuring good health. Cell death via apoptosis follows the activation of effector proteases called caspases, which participate in enzymic cascades that terminate in cellular disassembly (Los et al., 2001; Green et al., 1999). This action can occur through several routes, including mitochondria independent and -dependent pathways. Cells undergoing apoptosis commit suicide in an orderly fashion by cutting themselves into membrane-packaged parcels after cleavage of their chromosomal DNA, and then they are removed by phagocytic cells. Two major cells for clearing and degrading apoptotic bodies and necrotic material are dendritic cells (DCs) and macrophages. The highly orchestrated form of cell death and clearance is critical to the health of many organisms during development, and also for maintaining the normal function of the immune system. The importance of regulation of cell numbers and/or the removal of aged, damaged, or autoimmune cells to minimize inflammatory or immune reactions is discussed (Fields et al., 2001). There are two pathways of activation: intrinsic and extrinsic pathway. In the extrinsic one, the activation of apoptotic pathways and programmed cell death are initiated by the binding of a specific protein ligand to a cell surface transmembrane receptor (Fig. 15).

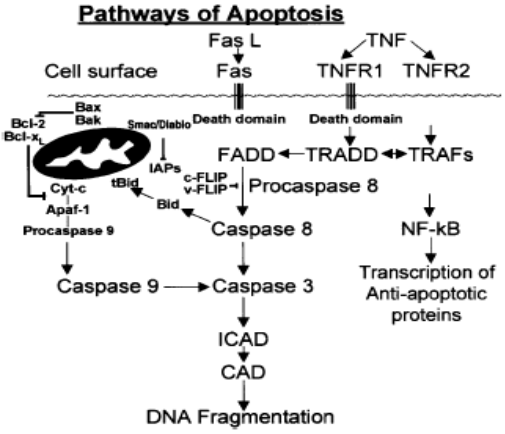

Fig. 15. The 2 major pathways of apoptosis—the extrinsic (Fas and other TNFR superfamily members and ligands) and the intrinsic (mitochondria-associated) pathways. Both pathways lead to activation of caspase-3, giving rise to apoptotic cell death. Only a few examples of proteins that directly affect cell death and the resulting DNA fragmentation are shown in the simplified diagram. Most of the effector and control proteins are written as acronyms (Schultz and Harrington, 2003).

Apoptotic signals are transmitted to target cells via the TNF superfamily of death receptors (DRs), the members characterized by a conserved extracellular cysteine-rich motif. Each DRs has an intracellular death domain (DD) that function as a protein-protein binding module after recruiting various cytosolic signaling molecole that comprise the specific apoptotic pathways. The DD of the receptor then recruits so-called adaptor proteins that also have DDs. This protein, which has a DD at its C-terminus and a second protein-protein interaction domain, called a death-effector domain, at its N-terminus. The death effector domain of the adaptor protein binds to the death-effector domain, or prodomain, of caspase-8, and a complex termed the death-inducing signaling complex (DISC) is formed which subsequently signals proteolysis and endonucleolytic cleavage. Activated caspase-8 then activates a series of downstream caspases, such as caspase-3, that result in cleavage of structural and regulatory intracellular proteins, DNA fragmentation and cell death. In the intrinsic pathway caspases are activated by perturbance of the mitochondria, and this may lead to the opening of the mitochondrial permeability transition pore complex with organelle swelling, and then rupture of the outer membrane. This results in release of the apoptosis-stimulating molecules cytochrome c and apoptosis-inducing factor (AIF). A second mechanism allows direct release of cytochrome c and the other factors without evidence that the permeability transition pore complex has been opened to the environment. Bcl-2, a protein inhibitor of programmed cell death, blocks both the permeability transition pore opening and the release of cytochrome c (Susin et al., 1996). Released cytochrome c induces multimerization of apoptosis protease-activating factor (Apaf)-1 to activate procaspases-9 and -3, The Bcl-2 family of proteins, located in the outer mitochondrial membrane, is important in preventing and permitting apoptosis, and is instrumental in controlling the release of cytochrome c (Monaghan et al., 1992; de Jong et al., 1994). In fact, all mitochondrial activities in apoptosis can be blocked by overexpression of Bcl-2 or Bcl-XL but overexpression is an experimental phenomenon that may not occur under normal physiologic conditions. Cytochrome c is a required cofactor and forms a complex with Apaf-1, procaspase-9, and deoxyadenosine monophosphate (dATP) (Li et al., 1998). The large complex is called the apoptosome. Apaf-1 is an adaptor protein that binds procaspase-9 through the caspase activation and recruitment domain, resulting in caspase-9 auto-activation in the presence of cytochrome c and ATP or dATP. After caspases-9 and -8 are activated, cleavage and

activation of additional upstream caspases in amplifying loops may occur, or this action allows caspase-9 to activate downstream caspases such as caspase-3, leading to endonuclease-fragmentation of the cell's DNA (Schultz et al., 2003). The balance between pro- and anti-apoptotic proteins (Bcl-2 family members) expressed in the outer mitochondrial membrane probably determines whether programmed cell death is initiated or whether the cell will survive (Pellegrini et al., 1999; Antonsson et al., 2000). It was later determined that Bcl-2 family members interact with one another, forming heterodimers and, occasionally, homodimers. Members of this family either inhibit or promote cell death, and together with mitochondria, cytochrome c (a required co-factor for Apaf-1), AIF, intracellular balances of dATP or ATP, and caspases, are involved in the initiation and execution of the intrinsic pathway (Oltvai et al., 1993; Korsmeyer et al., 1999). The relative concentration of family members acts as a gauge for cell death. This family comprises nearly 20 proteins divided into two main groups. Antiapoptotic members such as Bcl-2, Bcl-xL, Bcl-w, Bfl-1, and Mcl-1 promote cell survival, whereas proapoptotic members such as Bax and Bak function as death effectors (Schultz et al., 2003).

7.1 Evidences for apotosis during ALS progression

Neuronal apoptosis has been suggested to underlie the neurodegeneration of motor neurones expressing mutant SOD1. In fact while wild-type SOD1 is anti-apoptotic in neuronal cultures and a determinant of lifespan in *Drosophila* (Rothstein et al., 1994; Rabizadeh et al., 1995; Greenlund et al., 1995; Parkes et al., 1998), mutant SOD1 proteins are pro-apoptotic both *in vitro* and *in vivo* (Durham et al., 1997; Pasinelli et al., 1998; Pasinelli et al., 2000). Thus, alteration in the expression of the pro- and anti-apoptotic genes, activation of caspases and release of cytochrome-c have been found in the spinal cord of transgenic mice expressing SOD1 with the G93A mutation and in human ALS patients without SOD1 mutations (Vukosavic et al., 1999; Pasinelli et al., 1998; Pasinelli et al., 2000; Guegan et al, 2003). In addition, survival of the $SOD1^{G93A}$ ALS mice is prolonged by overexpression of Bcl2 (Kostic et al., 1997), by inhibition of caspase-1 (Friedlander et al., 1997), and by treatment with the pancaspase inhibitor ZVAD-fmk (Li et al., 2000). Moreover we have demonstrated that overexpression of $SOD1^{G93A}$ requires the expression of Apaf1 to induce cell death (Cozzolino et al., 2004). Intriguingly it has been demonstrated that both WT and mutant SOD1 can bind Bcl2,

providing evidence of a direct link between SOD1 and an apoptotic pathway (Pasinelli, 2004).

Experimental evidences have demonstrated that, in ALS patients, motor neurons die for apoptosis. Crosio and collegues have investigated expression of the Bcl2 family members in spinal cords of transgenic $SOD1^{G93A}$, $SOD1^{WT}$ and non-transgenic mice and it is resulted that Bcl2-A1 is the only member of this family to be upregulated in both asymptomatic and symptomatic G93A mice, with a tendency to decrease in the final stages of disease. Interestingly, this upregulation is tissue specific, as Bcl2-A1 mRNA is increased neither in the brain nor in the muscle of G93A transgenic mice. Moreover, induction of Bcl2-A1 in $SOD1^{G93A}$ transgenic mice occurs via NF-kB-independent pathway (Crosio et al., 2006). It has been shown that Bcl2-A1 has various effects in response to TNF-α in different cell cultures: it acts as an antiapoptotic in immune-derived cell lines (Zong et al., 1999), in microvascular endothelial cells (Wang et al., 1999) and in HT1080 fibrosarcoma cells (Karsan et al., 1996), whereas it is clearly pro-apoptotic in B cells (Kucharczak et al., 2005). In different cell cultures (NSC-34, undifferentiated and differentiated ETNA cells and primary cultures from spinal cords), the overexpression of Bcl2-A1 and $SOD1^{G93A}$ increases the level of cell death after exposure to TNF-α, a situation mimicking the condition of neuroinflammation occurring in ALS (Crosio et al., 2006).

For the important involvement of Bcl2-A1 in the motor neurons destiny, I have recently focused my attention on the gene Bcl2-A1.

7.2. Bcl2-A1

Bcl2-A1 (also known as Bcl2-related protein A1, BFL1; A1; Bfl-1/A1) was originally identified as a murine hematopoietic-specific, granulocyte-macrophage colony-stimulating factor-inducible gene product (Choi et al., 1995; Karsan et al., 1996). The human Bcl2-A1 gene codes for a 175-amino acid Bcl2 family protein that has an anti-apoptosis activity and is expressed abundantly in bone marrow and at a low level in several other tissues (Hung-Ha et al., 1998). Unlike other Bcl2 family proteins, expression of Bcl2-A1 permits limited cell proliferation over an extended period of time when cells are induced to undergo apoptosis (D'Sa-Eipper et al., 1998). Human Bcl2-A1 can be considered as a homologue of mouse A1, because the two proteins share about 72% amino acid identity (Choi et al., 1995; Karsan et al., 1996). Bcl2-A1 appears to be

induced by inflammatory cytokines, tumor necrosis factor and interleukin-1 (Karsan et al., 1996), and it has been shown to be a direct transcriptional target of NF-kB that is overexpressed in many human tumors and is a means by which NF-kappaB inhibits apoptosis (Zong et al., 1999; Wang et al, 1999; Simmons et al., 2008). Like Bcl2, Bcl2-A1 can prolong cell survival in some experimental paradigms, e.g. it retards tumor necrosis factor-induced apoptosis in the human dermal microvascular cell line, HMEC-1 (Karsan et al., 1996) and p53-induced apoptosis in the primary rat kidney cells (D'Sa-Eipper et al., 1996). However, the function of Bcl2-A1 seems to be distinct from that of Bcl-2, because Bcl2-A1 permits cell proliferation (D'Sa-Eipper et al., 1996; D'Sa-Eipper, 1998). It has also been demonstrated that Bcl2-A1 is the only known Bcl-2 family member to be induced by the inflammatory cytokines TNFα and IL-1β (Karsan et al., 1996; Duriez et al., 2000). This unique characteristic of Bcl2-A1 prompted us to study the role of this protein in ALS, given all the above-mentioned links between neuroinflammation and disease progression.

Recent studies have demonstrated that distinct subcellular localizations of this protein are correlated with its funtion. A previous research demonstrated that Bcl2-A1 does not contain a well-defined C-terminal transmembrane domain and deletion of the C-terminal 24 amino acid region (corresponding to the transmembrane domain of other Bcl2 family proteins) partially reduces the various activities of Bcl2-A1 (D'Sa-Eipper et al., 1998). Recent independent studies, with Bcl2-A1-overexpressing cells, suggested that Bcl2-A1 localizes to the mitochondria (Werner et al., 2002; Kucharczak et al., 2005; Duriez et al., 2000) and that the C-terminal end of Bcl2-A1 is important for anchoring Bcl2-A1 to the mitochondria (Duriez et al., 2000; Ko et al., 2003), moreover it has been found that C-terminal region of Bcl2-A1 induces cell death that accompanies caspase activation when fused with GFP. (Yang et al., 2005). Brien and collegues have demonstrated that Bcl2-A1 may co-exist in two distinct conformational states, the first one with its C-terminal helix 9 (residues 155–175) inserted in the hydrophobic groove formed by the BH1–3 domain of Bcl2-A1, and the second one with its C-terminal tail. Interestingly, thay have demonstrated that helical wheel projection of the C-terminal helix of Bcl2-A1 highlights its amphipathic character, a feature of transmembrane helices or membrane anchors, and that both the anchorage of Bcl2-A1 to the mitochondria and the anti-apoptotic function of the protein are dependent on the amphipathic nature of the C-terminal helix. These data suggested that even though Bcl2-A1 may co-exist in two

distinct conformational states, most of the endogenous Bcl2-A1 seems to be tightly associated with the mitochondria via its C-terminal end and that the amphipathic nature of helix 9 is critical for that localization (Fig. 16, Brien et al, 2003).

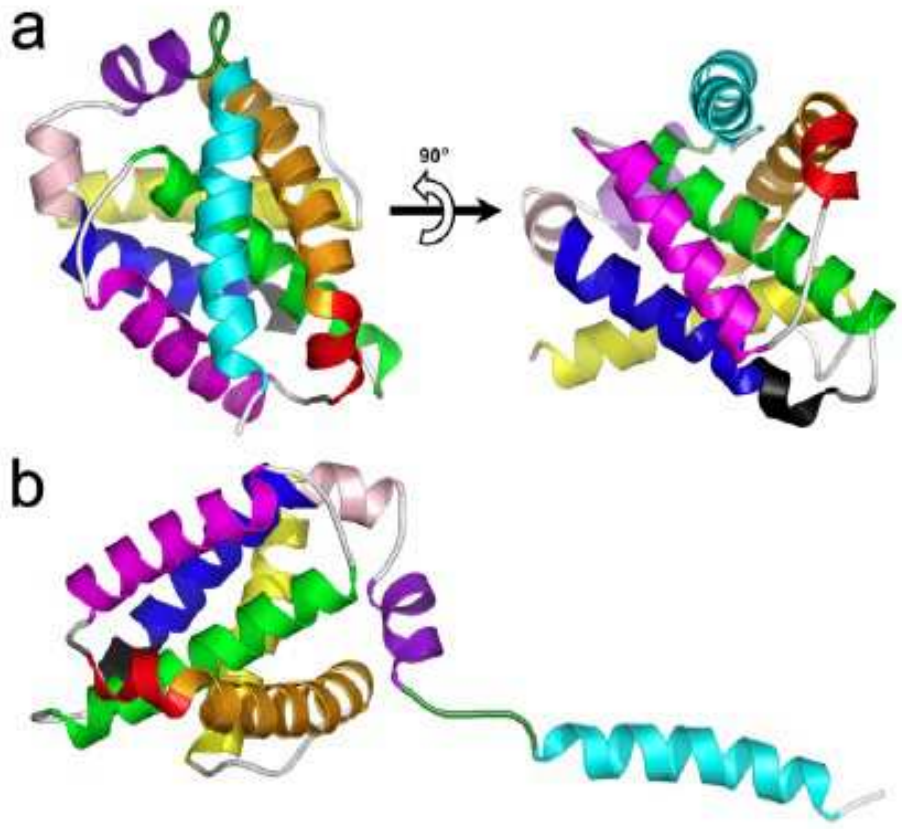

Fig. 16. Three-dimensional model of full length human Bfl-1. (a) Ribbon representations of Bfl-1 in its compact form with helix α9 placed in the hydrophobic BH3-binding cleft. (b) Bfl-1 in its extended form with helix α9 protruding from the globular core. α-helices are colored sequentially from N- to C-terminal ends as follows: yellow, α1 (aa 2-21); orange, α2 (aa 32-51); red, α3 (aa 53-58); purple, α4 (aa 64-79); green, α5 (aa 86-106); blue, α6 (aa 116-130); pink, α7 (aa 132-136); magenta, α8 (aa 139-148); cyan, α9 (aa 155-173). The 310 helix (aa 113-115) is shown in black. The loop connecting α8 and α9 is shown in dark green (aa 149-154). Orientation of the model in figure (b) is deduced from that of left figure (a) by a90° clockwise rotation in the plane of the paper(Brien et la., 2009).

Material and Methods

1. Material

1.1 The bacterial strain

Competent cells used are E. coli DH5 α. Bacterial cells are defective for the restriction and have mutations in relA1 and recA1 genes, to improve the stability and quality of recombinant plasmids.

1.2 Cell lines

NSC34 cell line: Spinal Cord Neuronal Clone 34 (Durham et al., 1993).

The NSC34 cell hybrids are obtained by fusion of neuroblastoma cells with mouse embryonic motor neuron cells. Even in the absence of specific agents exhibit characteristics of motor neuron differentiation and maintain the ability to proliferate actively in culture.

SH-SY5Y cell line (Biedler et al., 1978): SH-SY5Y cells (ATCC number CRL-2266) are human cells derived from neuroblastoma cell line.

HEK293 cell line: HEK293 are human embryonic kidney cells (Graham et al., 1977).

1.3 Animals

I used $SOD1^{G93A}$ transgenic mice (strain B6.Cg-Tg(SOD1–G93A)-1Gur from The Jackson Laboratory, 99.99% C57BL/6 genetic, 50% survive at 157.1±9.3 days, http://jaxmice.jax.org/strain/004435.html). Non-transgenic littermates were used as control.

1.4 Plasmid constructions and oligonucleotides

pGL2-promBcl2-$A1^{WT}$: a fragment corresponding to mouse Bcl2-A1b gene promoter (ch NCBIM37:9:89093447:89103264:1), spanning from − 2017 to + 129 was isolated by RT-PCR and was cloned in pGL2-Basic (Promega) (Adlam et al., 2003; Sung-Kyun et al., 2011). Oligonucleotides, used to amplify the promoter, had the XhoI recognition site (highlighted nt) used to digest pGL2-Basic vector:

NAME	SEQUENCE
Promoter Bcl2a1-b forward	5′AAACTCGAGTTAAGGCAATAGGTGGGAGC3′
Promoter Bcl2a1-b reverse	5′AAACTCGAGTTCCCTGGCAGAGCTGACT3′

pGL2-promBcl2-A1$^{Nf\text{-}kB/AP1}$: Mutations of NF-κB and AP1 binding site (highlighted nt) were generated in the Bcl2-A1b promoter using the Quickchange site-directed mutagenesis kit (Stratagene). Oligonucleotides used to mutagenize the promoter were:

NAME	SEQUENCE
Promoter Bcl2-A1b A1$^{Nf\text{-}kB}$	5'CTTGCTGCTGTTTCAGGTCATAACAGGTTTCGTCTCAGCG3'
Promoter Bcl2-A1b^{AP1}	5'TTAAGGACTAGAGAGGTAAAAGACTCAGGAATTAAG3'

GST-Bcl2-A1: a PCR fragment, corresponding to mouse Bcl2-A1b coding sequence (NM_007534.3), was cloned into BamHI and SmaI restriction sites of the pGEX-3 vector (GE healthcare) (Johnson et al., 1989; Fikrig et al*.,* 1990).

pCMV-mouse/human pro-caspase3: coding sequences corresponding to mouse (NM_009810) and human (NM_004346) pro-caspase 3 were isolated by RT-PCR and cloned into HindIII (for mouse pro-caspase3) or EcoRI (for human pro-caspase3) downstream to 3xFlag repeats (p3xFlag-CMV-10 vector, Sigma- Aldrich) (Andersson et al., 1989; Thomsen et al, 1984)

NAME	SEQUENCE
pCMV-mouse pro-caspase3 forward	5'-ATCGAATTCAATAGTGTTTGTCAGGTTCAAC-3'
pCMV-mouse pro-caspase3 reverse	5'-ATCAAGCTTGGAAACAACAAAACCTCAGTG-3'
pCMV-human pro-caspase3 forward	5'ATCGAATTCAGAGAACACTGAAAACTCAGT3'
pCMV-human pro-caspase3 reverse	5'ATCGAATTCCTTTAGTGATAAAAATAGAGTTC3'

pCMV-SOD1$^{WT/G93A}$: coding sequences corresponding to SOD1^{WT}, SOD1^{G93A} were isolated by RT-PCR from tissues of transgenic mice and cloning into Hind III and XbaI restriction sites of the pRc/CMV vector (Invitrogen) (Xing et al., 1996; Goldberg et al., 1993).

5xMyc-mouse Bcl2-A1b (Crosio et al., 2006; Ferri et al., 2006): coding sequence corresponding to mouse Bcl2-A1b (NM_007534.3) was obtained by cloning a PCR fragment corresponding to mouse Bcl2-A1b into StuI and XhoI restriction sites of pCS2-MTK vector (Roth et al., 1991).

mBcl2-A1b$^{\Delta\alpha1/\Delta\alpha1\text{-}3/\Delta\alpha7\text{-}9/\Delta\alpha9}$: Bcl2-A1 deletion mutants were obtained by mutagenesis, using the Quickchange site-directed mutagenesis kit (Stratagene), starting from 5xMyc-mBcl2-A1b plasmid described above. Oligonucleotides used to mutagenize the gene were:

NAME	DELETION	SEQUENCE
mBcl2-A1b$^{\Delta\alpha1}$ forward	(Δaa 4–34)	5'GCTGAGTACGAGGTGCTACAAAGAG3'
mBcl2-A1b$^{\Delta\alpha1}$ reverse	(Δaa 4–34)	5'CTCTTTGTAGCACCTCGTACTCAGC3'
mBcl2-A1b$^{\Delta\alpha1\text{-}3}$ forward	(Δaa 4–64)	5'GCTGAGTACGAGACCGCCAGAATAAT3'
mBcl2-A1b$^{\Delta\alpha1\text{-}3}$ reverse	(Δaa 4–64)	5'ATTATTCTGGCGGTCTCGTACTCAGC3'
mBcl2-A1b$^{\Delta\alpha7\text{-}9}$ forward	(Δaa 130–168)	5'TCAATAACACAGGATTTCTCCTCAAGTA3'
mBcl2-A1b$^{\Delta\alpha7\text{-}9}$ reverse	(Δaa 130–168)	5'TACTTGAGGAGAAATCCTGTGTTATTGA3'
mBcl2-A1b$^{\Delta9}$ forward	(Δaa 150–168)	5'AGTTTGAACCCAAATTTCTCCTCAAGTA3'
mBcl2-A1b$^{\Delta9}$ reverse	(Δaa 150–168)	5'TACTTGAGGAGAAATTTGGGTTCAAACT3'

5xMyc-human Bcl2-A1 (Crosio et al., 2006; Ferri et al., 2006): coding sequence corresponding to human Bcl2-A1 (NM_004049.3) was obtained by cloning a PCR

fragment corresponding to human Bcl2-A1 into EcoRI restriction site of pCS2-MTK vector.

NAME	SEQUENCE
hbcl2a1 forward	5'GAAGTCATGCTTGGACAATG3'
hbcl2a1 reverse	5'TAGAAAAGTCATCCAGCCAG3'

hTDP-43$^{WT/Q331K/M337V/A382T}$: Coding sequences corresponding to human TDP-43 (NM_007375.3) were isolated by RT-PCR and cloned downstream to 5xMyc repeats into XhoI restriction site of the pCS2-MTK vector. Mutants were obtained by mutagenesis starting from hTDP-43, using the Quickchange site-directed mutagenesis kit (Stratagene), Oligonucleotides used to amplify the gene WT and to mutagenize it were:

NAME	SEQUENCE
hTDP-43^{WT} forward	5'AATTCTCGAGCCTCTGAATATATTCGGGTAACC3'
hTDP-43^{WT} reverse	5'AATTCTCGAGCTACATTCCCCAGCCAGAA3'
hTDP-43^{Q331K}	5'CCAGGCAGCACTAAAGAGCAGTTGGGG3'
hTDP-43^{M337V}	5'CAGTTGGGGTATGGTGGGCATGTTAGC3'
hTDP-43^{A382T}	5'AATTCTGGTGCAACAATTGGTTGGG3'

2. Methods

2.1 Preparation of competent cells

Plated on an agar plate E. coli DH5 α cells (10 g/L of tryptone, 5 g/L yeast extract, 10 g/L NaCl, 15 g/L agar) in the absence of antibiotics. After 12 hours collect a single colony to grow for 14-16 hours in 2 ml of LB (10 g/L of tryptone, 5 g/L yeast extract, 10 g/L NaCl) at 37 °C in agitation. Inoculate the cells into 100 ml of LB and shake at 37 °C. Check bacterial growth by reading in a spectrophotometer at a wavelength of 600 nm until reaching an optical density (OD) of 0.4. Centrifuge the cell suspension is at 4000 rpm for

10’ at 4 °C. Remove supernatant and resuspend the pellet in a volume of 10 ml of $CaCl_2$ 0.1 mM, and centrifuge the cell suspension as above. Resuspend the pellet in 4 ml of cold $CaCl_2$ 0.1 mM, 10% glycerol, put on ice for 15’ and store in aliquots at -80 °C.

2.2 Cell cultures

NSC cells and SH-SY5Y are cultured in Dulbecco MEM/F12 ground (Gibco BRL), HEK293 in Dulbecco MEM, always in the presence of 10% fetal calf serum, free of tetracycline contamination (Tet-free FCS, Clontech) and inactivated at 56 °C for 30’. Medium contains 100 units/ml penicillin G and 100 µg/ml streptomycin (Gibco BRL). The cells are grown in an incubator at 37 °C in a humidified atmosphere containing 5% CO_2. Trypsin (0.5 g/ml, 68 mM EDTA) is added to split cells, then diluted in fresh medium.

2.3 Tissue dissection

All animal procedures have been performed according to the European Guidelines for the use of animals in research (86/609/CEE) and the requirements of Italian laws (D.L. 116/92). At early symptomatic stage of the disease (120 days), mice are anesthetized with chloral hydrate 500 mg/kg, sacrificed and tissue dissected. Spinal cord is manually dissected and stored dried at −80 °C. Lymphocytes are isolated from 1 ml heparinated blood samples by standard centrifugation on a Ficoll gradient. All efforts are made to minimize suffering. All animals have been raised and crossed in the indoor animal house in a 12 h light/dark cycle in a virus/antigen-free facility with controlled temperature and humidity and have been provided with water and food ad libitum.

2.4 Use of restriction and modification enzymes

The digestion reactions are usually assembled with 3 units enzyme/µg DNA and a specific buffer. The incubation is performed for one hour at 37 °C. After the digestion with appropriate enzymes, vectors are digested, at 37 °C for one hour, by CIP (Calf Intestinal Phosphatase,1 unit/µl, Promega), to remove phosphate to 5' ends of the linearized plasmid.

2.5 Agarose gel electrophoresis

Dissolve the agarose (1%) in TAE (40 mM Tris-HCl, pH [8.5], 1 mM EDTA, 20 mM acetic acid) and add ethidium bromide (EtBr) at a final concentration of 0.04 µg/ml. Dilute samples in water and loading buffer (0.04% bromophenol blue, 0.04% xylene cianol, 30% glycerol). Load samples to a voltage of 120V. Visualize Nucleic acid bands under UV light. The size of the fragments are estimated in the presence of a ladder of known molecular weight.

2.6 DNA purification from agarose gel

Kit Wizard ® SV Gel and PCR Clean-Up System (Promega) is used to isolate a DNA fragment. Following electrophoresis, excise DNA band from gel and place gel slice in a 1.5 ml microcentrifuge tube. Add Membrane Binding Solution (10µl/10mg of gel slice). Vortex and incubate at 50–65°C until gel slice is completely dissolved. Insert SV Minicolumn into Collection Tube. Transfer dissolved gel mixture to the Minicolumn assembly. Incubate at room temperature for 1'. Centrifuge at 16,000 ×g for 1'. Discard flowthrough and reinsert Minicolumn into Collection Tube. Add 700µl Membrane Wash Solution (ethanol added). Centrifuge at 16,000 ×g for 1'. Discard flowthrough and reinsert Minicolumn into Collection Tube. Repeat Step 4 with 500µl Membrane Wash Solution. Centrifuge at 16,000 ×g for 5'. Empty the Collection Tube and recentrifuge the column assembly for 1' with the microcentrifuge lid open (or off) to allow evaporation of any residual ethanol. Carefully transfer Minicolumn to a clean 1.5 ml microcentrifuge tube. Add 50 µl of Nuclease-Free Water to the Minicolumn. Incubate at room temperature for 1'. Centrifuge at 16,000 ×g for 1'. Discard Minicolumn and store DNA at 4°C or –20°C.

2.7 Ligation reaction

Ligase reaction is set up as follows: in a final volume of 15 µl, incubate 40-80 ng of linearized plasmid and a variable quantity of insert in the presence of 1 unit of T4 DNA ligase (Promega) in an appropriate buffer (Ligase buffer 10X, Promega). Evaluate, for each cloning, the optimal ratio vector/insert for the reaction. After an incubation O/N at 16°C, transform E. coli DH5 α cells with 5 µl of the reaction.

2.8 Bacterial transformation

Add 5 µl of a ligation reaction to 80 µl of competent cells. After incubation on ice for 30', shock the cells at 37 °C for 3', then incubate at room temperature for 10'. Add 500 µl of LB and incubate at 37 °C for 50', centrifuge for few seconds to obtain a pellet and, eliminated 500 ml of LB, resuspend the pellet. Plate cells on a selective solid medium (LB agar and appropriate antibiotic) and incubate O/N at 37 °C.

2.9 Plasmid DNA purification (Miniprep)

Wizard®Plus SV Minipreps DNA Purification System (Promega) is used to purify plasmidic DNA. Pellet 1–10 ml of overnight culture for 5'. Thoroughly resuspend pellet with 250 µl of Cell Resuspension Solution. Add 250 µl of Cell Lysis Solution to each sample; invert 4 times to mix. Add 10 µl of Alkaline Protease Solution; invert 4 times to mix. Incubate 5 minutes at room temperature. Add 350 µl of Neutralization Solution; invert 4 times to mix. Centrifuge at top speed for 10' at room temperature. Insert Spin Column into Collection Tube. Decant cleared lysate into Spin Column. Centrifuge at top speed for 1' at room temperature. Discard flowthrough, and reinsert Column into Collection Tube. Add 750 µl of Wash Solution (ethanol added). Centrifuge at top speed for 1'. Discard flowthrough and reinsert column into Collection Tube. Repeat Step 10 with 250 µl of Wash Solution. Centrifuge at top speed for 2' at room temperature. Transfer Spin Column to a sterile 1.5 ml microcentrifuge tube, being careful not to transfer any of the Column Wash Solution with the Spin Column. If the Spin Column has Column Wash Solution associated with it, centrifuge again for 1' at top speed, then transfer the Spin Column to a new, sterile 1.5 ml microcentrifuge tube. Add 100 µl of Nuclease-Free Water to the Spin Column. Centrifuge at top speed for 1' at room temperature. Discard column, and store DNA at –20°C or below.

2.10 Transfection of eucariotic cells

Transient expression of each plasmid (1.5 µg DNA/5–7×10^5 cells) is obtained transfecting cells with LipofectAMINE LTX and PLUS reagent (Invitrogen). Dilute the optimized amount of plasmid DNA in OPTIMEM (Gibco BRL) and add the optimized volume of PLUS™ Reagent directly to the diluted DNA. Mix gently and incubate for 5' at room temperature. Add the optimized volume of Lipofectamine™ LTX directly to the

diluted DNA, incubate for 30' at room temperature. DNA-lipid complexes are stable for 6 hours at room temperature. Add DNA-lipid complex dropwise to the well containing cells, mixing gently. Medium may be changed after 4–6 hours.

2.11 DNA extraction and precipitation

Add an equal volume of phenol-chloroform-isoamyl alcohol 25:24:1 [pH 8.0] to the lysis product. Mix carefully and centrifuge at 12000 rpm for 10' at room temperature. Recover the aqueous phase containing DNA. Add 0.1 volumes of 3M sodium acetate [pH 5.5] and 2.5 volumes of ethanol (EtOH) absolute to prepitate DNA. Mix by vortex and store the sample at -80 °C for 20'. Centrifuge for 15'at 12000 rpm and wash the pellet with EtOH 80% and centrifuge for 10' at 12000 rpm. Eliminate the EtOH and air-dry the pellet. Resuspend in distilled H_2O.

2.12 RNA extraction

Lyse cells directly in a culture dish by adding TRIZOL Reagent (1 ml per 10 cm2) to dish, and passing the cell lysate several times through a pipette. Incubate the homogenized samples for 5' at 15-30°C to permit the complete dissociation of nucleoprotein complexes. Add 0.2 ml of chloroform per 1 ml of TRIZOL Reagent. Shake tubes vigorously for 15'' and incubate them at 15-30°C for 2-3'. Centrifuge the samples at 12,000 ×*g* for 15' at 2-8°C. Following centrifugation, the mixture separates into a lower red, phenol-chloroform phase, an interphase, and a colorless upper aqueous phase. RNA remains exclusively in the aqueous phase. Transfer the aqueous phase to a fresh tube. Precipitate the RNA from the aqueous phase by mixing with isopropyl alcohol (0.5 ml/1 ml of TRIZOL Reagent). Incubate samples at 15-30°C for 10' and centrifuge at 12,000 ×*g* for 10' at 2-8°C. The RNA precipitate, often invisible before centrifugation, forms a gel-like pellet on the side and bottom of the tube. Remove the supernatant. Wash the RNA pellet once with 75% ethanol (1 ml/1 ml of TRIZOL Reagent). Mix the sample by vortex and centrifuge at 7,500 ×*g* for 5' at 2-8°C. At the end of the procedure, briefly dry the RNA pellet and dissolve RNA in RNase-free water.

2.13 UV spectrophotometry

Dilute 5 µl of sample in 1 ml of H_2O into a quartz cuvette. Measure the absorbance at a wavelength of 260 nm and 280 nm by spectrophotometry. Absorbance (OD) of the sample at 260 nm provides a measure of the amount of nucleic acids present in the sample considering 1 OD=50µg/ml for DNA and 1 OD=40 µg/ml for the RNA, the absorbance at 280 nm estimated the amount of protein contaminants.

2.14 Reverse transcription reaction

The reverse transcription reaction is set up as follows:

RNA	1µg
Random primers (100ng/µl)	1,25µl

Incubate for 5 minutes at 65-75 °C.

First-strand Buffer 5X	5 µl
DTT 0.1 M	2,5 µl
dNTPs 2mM	2,5 µl
SuperScript II RT (200 U/µl)	0,5 µl
RNase OUT (40U/µl)	0,5 µl
H_2O	To 25 µl

Incubate 5' at room temperature, one hour at 37 °C and 5' at 95 °C to inactivate reverse transcriptase.

2.15 PCR reaction

The PCR reaction to amplify gene is set up in the following manner:

DNA/cDNA	2 µl
Colorless GoTaq Reaction Buffer 5X (Promega)	4 µl
dNTP 2mM	2 µl
Oligonucleotide forward 10µM	1 µl
Oligonucleotide reverse 10µM	1 µl

GoTaq DNA polimerase 5 U/µl (Promega)	0,5 µl
H_2O	To 20 µl

The PCR reaction for mutagenesis is set up as follows:

DNA	2 µl
Pfu Turbo Buffer 10x (Stratagene)	2,5 µl
dNTP 2mM	2,5 µl
Oligo forward 10µM	1 µl
Oligo reverse 10µM	1 µl
Pfu Turbo 5 U/µl (Stratagene)	0,5 µl
H_2O	To 25 µl

Amplification conditions are:

1. 3’ at 94 °C.
2. 30’’ at 94 °C for denaturation,
3. 30’’ at the specific annealing temperature of the primer,
4. 1’ at 72 °C per kb of DNA for the extension
5. 10’ at 72 °C.

Steps 2-3-4 are repeated for 30 cycles

2.16 Detection of Bcl2-A1 subtype mRNA by RT-PCR

Bcl2-A1a, Bcl2-A1b, Bcl2-A1d are amplified from mouse cDNA, obtained by retro-transcription of spinal cord and lymphocyte total RNA from $SOD1^{G93A}$ transgenic mouse and control mice. Specific primers for all the three mRNAs are used for the amplification (5′ACTCCCTGGCTGAGCACTA3′; 5′AGTTTCCAGTTTTGTGGCA3′) and the product is analyzed by single and double digestion with Pst I and Bgl II.

2.17 Luciferase assay

Lyse transfected NSC-34 cells in Lysis Reagent (25 mM Tris-phosphate [pH 7.8], 2 mM DTT, 2 mM 1.2-diaminocyclohexane-N,N,N′,N′-tetraacetic acid, 10% glycerol, 1% Triton X-100). Incubate equal amount of protein extracts with 100 µl of Luciferase Assay Reagent (Promega) and determine luminescence using the Victor 5 Wallace workstation (PerkinElmer) according to manufacturer's instruction.

2.18 GST pull-down assay

Express the GST-Bcl2-A1 fusion protein in E. coli BL21. After induction with 0.5 mM IPTG for 3 h at 30 °C, collect bacteria, wash twice in PBS 1X and lyse in lysis buffer (50 mM Tris HCl [pH 8.0], 1 mM EDTA, 150 mM NaCl, 1% Triton X100, 1 mM PMSF, protease inhibitor cocktail 1X, lysozime 200 µg/ml). Keep bacterial cell lysates on ice for 30′ and sonicate for 5″ at 100W for 3 times. Purify GST-proteins on glutathione–Sepharose 4 fast flow resin (GE Healthcare). Incubate aliquots (500 ng) of GST-Bcl2-A1 or GST alone with 2 mg of total spinal cord protein extracts from $SOD1^{G93A}$ transgenic mice, obtained by homogenization in lysis buffer (50 mM Tris–HCl [pH 8.0], 150 mM NaCl, 1% NP-40, 1 mM PMSF, protease inhibitor cocktail 1X). After an overnight incubation at 4 °C, collect GST-Bcl2-A1 or GST alone by adding to the mixture 10 µl of glutathione-Sepharose 4 fast flow resin for 2 h at 4 °C. After five washes in lysis buffer, resuspend the beads in Laemmli Buffer 1X (50 mM Tris-HCl [pH 6.8], 1% β-mercaptoethanol, 10% glycerol, 1% SDS, bromophenol blue) and load on SDS/PAGE acrylamide gel. Stain SDS/PAGE loaded with GST-pulldown with Mass Compatible Super Blue Stain Kit (Nurex srl, Sassari) or analyzed by Western blot as described below.

2.19 In-gel digestion and matrix-assisted laser desorption/ionization (MALDI) mass spectrometry (MS) analysis

Excise proteins of interest with a sterile scalpel and destain with 100 µl of 5 mM NH_4HCO_3/50% acetonitril. Dehydrate gel pieces with acetonitrile, dry at room temperature and reswoll with 10 µl of 5 mM NH4 HCO3 containing 10 ng/µl trypsin for 40’ on ice. Subsequently, remove excess of digestion buffer and substitute with an equal volume of 5 mM NH4HCO3. Conduct tryptic digestion over night at 37 °C. Store

the peptide mixtures at 4 ◦C. Mix the peptides extracted from the gel pieces with an equal volume of 10mg/ml α-cyano-4-hydroxy-cinnamic acid in 40% (v/v) acetonitrile/0.1% (v/v) trifluoroacetic acid and apply the mixed solution as a microcrystalline thin film onto a 96-spot MALDI target. Performe MALDI-MS using a Micromass Tof-Spec 2E spectrometer (Manchester, UK), equipped with a 337nm nitrogen laser. The instrument operates in the positive ion reflectron mode at 20 kV accelerating voltage with time-lag focusing. Each mass spectrum is generated by accumulating data from 100 to 120 laser shots (Lepedda et al., 2009). The MS spectra acquired is submitted to MASCOT (Matrix Science, London UK).

2.20 SDS-PAGE and Western blot analyses

Prepare protein extracts by addition of Laemmli buffer (50 mM Tris-HCl, pH [6.8], 1% β-mercaptoethanol, 10% glycerol, 1% SDS, bromophenol blue), denature at 95 °C for 5' and resolve by standard SDS-polyacrylamide gel electrophoresis (SDS-PAGE). Load protein extracts in a stacking gel 4% acrylamide/bisacrilamide (37.5:1) and in a running gel. Perform electrophoresis in running buffer (25 mM Tris HCl, pH [7.8], 200 mM glycine, 0.1% SDS), by applying a current of 80 V for the stacking or 100 V for the running gel. Analyze proteins by Western blot: electroblot samples onto Protan nitrocellulose (Schleicher & Schuell GmbH). Incubate membranes for 16 h at 4°C with 3% low-fat milk in PBS 1X/Tween-20 0.05 % solution and the following antibodies: anti-Flag M2 monoclonal antibody (Sigma-Aldrich), anti-myc monoclonal antibody 9E10 (Sigma-Aldrich), anti-βactin monoclonal antibody AC-15 (Sigma-Aldrich), rabbit polyclonal anti-Cu-ZnSOD antibody (Stressgen), rabbit polyclonal anti-human MnSOD antibody (Stressgen), rabbit anti-cleaved caspase-3 (Cell signaling), rabbit anti-caspase-3 (Cell signaling), rabbit anti-PARP (Cell signaling), rabbit anti-CREB (Cell signaling). Secondary antibodies (peroxidase-conjugated) are obtained from Invitrogen. After membrane washing, visualize proteins by enhanced chemioluminescence (GE Healthcare) followed by Densitometric analyse, performed using Quantity One software program (Bio-Rad Laboratories) and normalized against the signal obtained by re-probing the membranes with an antibody against mouse β-actin. Student's t test is used for data analysis and differences is considered statistically significant if pb0.05. All statistical computations is performed using GraphPad Prism 4.0 (GraphPad Software).

2.21 Immunoprecipitations

At 48 h after transfection, lyse HEK293 cells in 1 ml of lysis buffer. After centrifugation at 12,000 g for 10 min at 4 °C, pre-clear the supernatants at 4 °C for 1 h with protein A-Sepharose. Add the anti-Myc or the anti–Flag antibodies at 1:1000 dilution, and after an overnight incubation at 4 °C, collect the immunoprecipitates by adding 20 µl of protein A-Sepharose. Wash the beads five times in lysis buffer, resuspend in Laemmli Buffer 1X and analyze by Western blotting.

2.22 Subcellular fractioning

5×10^6 HEK293 are transfected with plasmids coding for WT or the deletion mutant Δα9 of murine Bcl2-A1 and the human Bcl2-A1. 48 h after transfection harvest cells, wash in 1 ml of ice-cold PBS 1X with 1 mM EDTA and centrifuge at 600 ×g for 5′ at 4 °C. Solubilize the pellet in 1 ml of mitochondrial buffer (210 mM mannitol, 70 mM sucrose, 1 mM EDTA, 10 mM Hepes-KOH [pH 7.5]) containing protease inhibitors cocktail (Sigma-Aldrich). Store 50 µl of the solubilized (total) fraction and homogenize the remaining in a glass-teflon potter homogenizer (10–15 strokes) and centrifuge at 600 ×g for 5′ at 4 °C. Harvest the supernatant and centrifuge again in the same conditions. Following an additional centrifugation at 10,000 ×g for 10′ at 4 °C, collect the supernatant (cytosolic fraction) and wash the mithocondrial pellet in 1 ml of mitochondrial buffer and centrifuge at 10,000 ×g for 10′ at 4 °C. Resuspend the pellet carefully in 100 µl of lysis buffer (50 mM Tris–HCl [pH 8.0], 150 mM NaCl, 1% NP- 40) and protease inhibitors, incubate for 10′ on ice and centrifuge at 10,000 ×g for 10′ at 4 °C; store the supernatant (mitochondrial fraction) at −20 °C. Evaluate protein concentration using Coomassie Protein Assay Reagent (Fluka Analytical) and load 10 µg of each fraction on SDS/PAGE followed by Western Blot analysis.

2.23 Nuclear-cytoplasmic separation of TDP-43

1×10^6 SH-SY5Y are transfected or not (-) with a plasmid coding for WT or mutants Q331K-M337V-A382T of TDP-43. 48 h after transfection wash cells twice with cold PBS 1X, harvest in 500 µl of PBS and centrifuge at 3000 rpm for 3’ at 4 °C. Resuspend the pellet gently in 500 µl of S1 buffer (10 mM Hepes [pH 7.9], 10 mM KCl, 1,5 mM $MgCl_2$, 0,1 mM EGTA [pH 7.0], 1 M DTT (1 µl/2ml), syringe ten times at 4 °C, centrifuge at

3000 rpm for 3' at 4 °C, collect supernatant (cytoplasmic fraction) and resuspend the pellet gently in 500 µl of S1 buffer. Centrifuge at 3000 rpm for 3' at 4 °C, resuspend the pellet with 30 µl of S1. Shake for 30' at 4 °C, centrifuge for 10' at 4 °C at 12000 rpm and collect the supernatant (nuclear fraction).

2.24 TDP-43 solubility

1×10^6 SH-SY5Y are transfected or not (-) with a plasmid coding for WT or mutants Q331K-M337V-A382T of TDP-43. 72 h after transfection scrape cells off the plate in culture medium, collect by centrifugation, wash with PBS 1X, and resuspend in 500 ml of buffer A (10mM Tris-HCl [pH 8.0], 1mM EDTA [pH 8.0], 100mM NaCl, 1% Triton X-100 containing protease inhibitors cocktail (Sigma-Aldrich). After 10 min of ice incubation, centrifuge the lysates at 20,000 g for 10', and collect the supernatants as detergent soluble fractions, whereas wash the pellet (insoluble fractions) in buffer A, centrifuge again as before and resuspend in 150 µl of Laemmli buffer 1X.

2.25 Immunofluorescence

Wash 1×10^5 NSC-34 cells, grown on a cover-glass, twice with PBS 1X and then fix with 1 ml of 4% paraformaldehyde/PBS 1X for 10'. Permeabilize cells with 0.1% Triton X-100 in PBS and block non-specific binding with 5% bovine serum albumin, 0.1% Triton X-100 diluted in PBS for 1 h at room temperature. Incubate cells with primary antibodies (mouse anti-myc diluted 1:1000, Sigma-Aldrich, rabbit anti-MnSOD diluted 1:2000, Stressgene) diluted in blocking solution, overnight at 4 °C and then with secondary antibodies Alexa 594- and Alexa 488-conjugated (Molecular Probe, Invitrogen) diluted 1:1000 in blocking solution for 1 h at room temperature. Analyze cells with a Leica TCS SP5 confocal microscopy with LAS lite 170 image software.

2.26 In vitro assay for caspase-3 activation

To test caspase-3 activation in vitro I use a protocol modified from Deveraux et al. (1997). Incubate aliquots of 2 µg of HEK293 cells transfected with Flag-pro-caspase-3 with scalar quantity of myc immunoprecipitates from HEK293 cells transfected or not (−) with 5xmyc-Bcl2A1 at 30 °C for 30′ in a final volume of 20 µl. Add 50 ng of recombinant active caspase-8 (Sigma-Aldrich) and incubate the reaction for additional 15′ at 30 °C.

Stop the reactions by adding of 6 µl Laemmli Buffer 5X. The samples are finally analyzed by Western Blot.

2.27 Assessment of cell death

Quantification of apoptotic cells is obtained by direct visual counting after nuclear staining of 4% paraformaldehyde-fixed cells with the fluorescent probe Hoechst 33342 (1 µg/ml, Sigma). One hundred cells is analyzed in each examined field at 20× magnification, and eight randomly chosen fields for each experimental condition are counted. Only the cells containing clearly picnotic or fragmented nuclei are considered apoptotic.

Results

Theme 1: Molecular dissection of Bcl2-A1 role during ALS onset and progression in SOD1 models of the disease

Expression of mutant SOD1 typical of familial amyotrophic lateral sclerosis induces the expression of Bcl2-A1, a member of the Bcl2 family of proteins, specifically in motor neurons of transgenic mice. In this work, I have used immortalized motor neurons (NSC-34) and transgenic mice expressing mutant SOD1 to unravel the molecular mechanisms and the biological meaning of this up-regulation. I report that up-regulation of Bcl2-A1 by mutant SOD1 is mediated by activation of the redox sensitive transcription factor AP1 and that Bcl2-A1 interacts with pro-caspase-3 via its C-terminal helix α9. Furthermore, Bcl2-A1 inhibits pro-caspase-3 activation in immortalized motor neurons expressing mutant SOD1 and thus induction of Bcl2-A1 in ALS mice represents a pro-survival strategy aimed at counteracting the toxic effects of mutant SOD1. These data provide significant new insights on how molecular signaling, driven by expression of the ALS causative gene SOD1, affects regulation of apoptosis in motor neurons and thus may have implications for ALS therapy, where prevention of motor neuronal cell death is one of the major aims.

1. Mutant SOD1 induces Bcl2-A1 expression via AP1

It has been demonstrated that Bcl2-A1 is specifically induced in motor neurons of $SOD1^{G93A}$ mice (Crosio et al., 2006). Since mice have multiple Bcl2-A1 genes (the isoforms -a, -b and -d consist of two exons and encode a full length protein, while isoform -c lacks putative exon 2 and it is most likely a pseudogene), in a preliminary experiment I carried out the classification and relative quantification of Bcl2-A1a, -A1b and -A1d mRNA subtypes in spinal cord and lymphocytes of mice expressing wild-type (WT) or mutant (G93A) SOD1. Semiquantitative RT-PCR shows that Bcl2-A1 is induced only in the spinal cord of $SOD1^{G93A}$ mice, since lymphocytes of both genotypes have comparable levels of Bcl2-A1 mRNA (Fig. 1A). The amplicons were subjected to digestion with restriction enzymes that allow discrimination of Bcl2-A1 isoforms, as

reported by Hatakeyama et al. (1998) (Fig. 1B). In the spinal cord, all three isoforms are induced, although isoform A1b is clearly the most abundant (Figs. 1C and D). Previous reports have demonstrated that the human and murine Bcl2-A1 promoter is physiologically regulated via NF-κB transcription factor in T cells (Edelstein et al., 2003; Grumont et al., 1999).

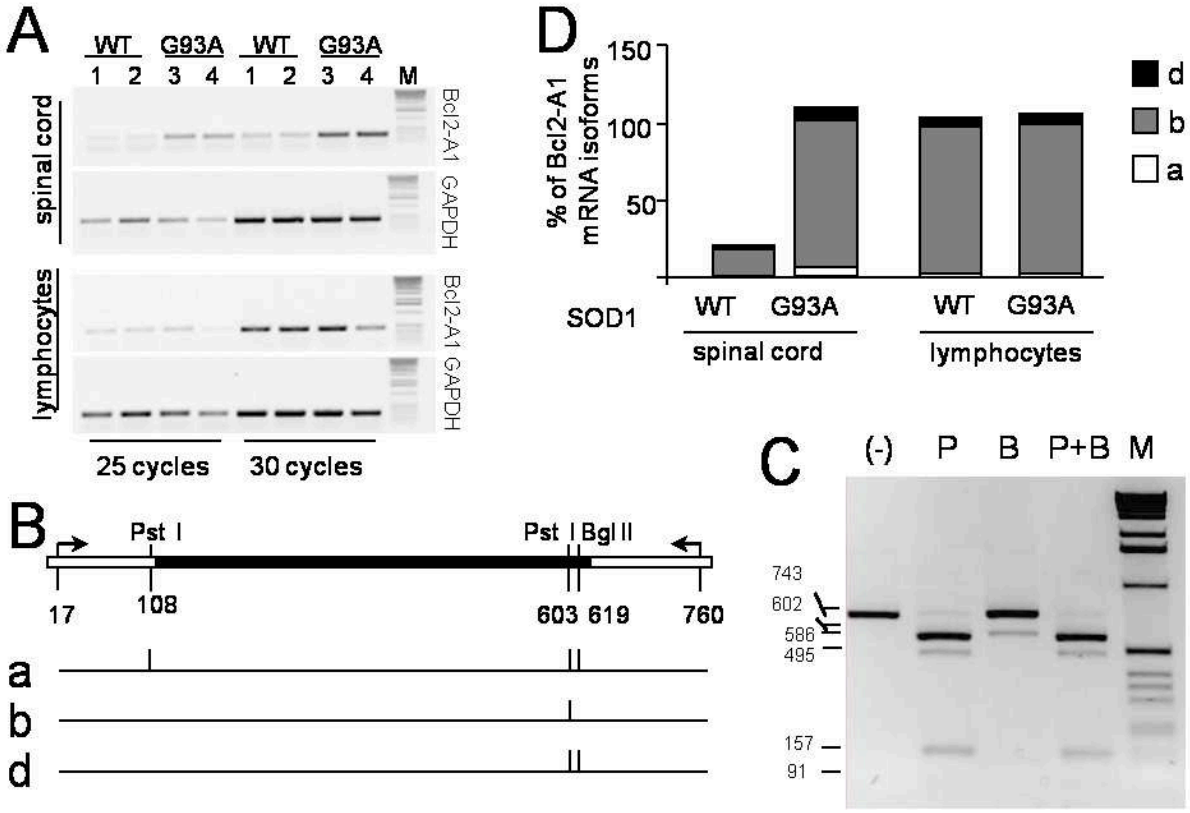

Fig. 1. Relative expression level of each Bcl2-A1 subtype in spinal cord of SOD1^{G93A} mice. A: Semiquantitative RT-PCR on 1 µg of total RNA extracted from spinal cord and lymphocytes of two mice, expressing human either wild type (WT, mice 1 and 2) or mutant (G93A, mice 3 and 4) SOD1. PCR was performed using oligos indicated by arrows in panel B to amplify all the Bcl2-A1 mRNA isoforms; amplification of GAPDH was used as positive control; M=GeneRuler™DNA Ladder Mix (Fermentas). B: Schematic representation of murine Bcl2-A1 mRNA isoforms. Arrows indicate the position of oligos utilized for PCR, while vertical lines point at PstI and BglII restriction sites. C: Representative experiment showing the digestion product of RT-PCR amplicons obtained from SOD1^{G93A} spinal cord RNA; PCR product undigested (−), digested with restriction enzymes PstI (lane P) and BglII (lane B) or both of them (lanes P+B). Major fragments were as follows: 743 bp fragments, A1b (lane B); 602 bp fragments, A1a or A1d (lanes B and P/B); 586 bp fragments, A1b or A1d (lane P) and A1-d (lanes P and P/B); 495 bpfragments,A1a (lanes P and P/B). RNA(1 µg) isolated from lymphocytes or spinal cord of SOD1^{G93A} mice was reverse transcribed and amplified. RT-PCR products were digested by restriction enzymes as indicated above, electrophoresed on 1.3% agarose gels and D: the relative amount of each mRNA as evaluated by densitometric analysis.

Moreover, the assembly of an enhanceosome-like complex, in which cooperative protein–protein and protein–DNA interactions involving NF-κB and AP1 binding sites

concur to the efficient formation of the transcriptional complex, has been observed on the human Bcl2-A1 promoter (Edelstein et al., 2003). Using a bioinformatics approach (Cartharius et al., 2005), I was able to identify a potential AP1 site on murine Bcl2-A1b promoter, located upstream to NF-κB binding site, in a position (nucleotide from −522 to −512) compatible with the formation of an enhanceosome-like complex. I therefore cloned murine Bcl2-A1b promoter in a wild type form or with either a mutagenized NFκB or a mutagenized putative AP1 binding site upstream a luciferase reporter gene (Fig. 2A). These plasmids were used to transfect motor neuronal NSC-34 cells and, as expected, mutations of NF-κB, but also on the putative AP1 binding sites on murine Bcl2-A1b promoter impair induction upon TNFα stimulation (Fig. 2B). In contrast, induction of Bcl2-A1b upon mutant SOD1 expression is AP1-dependent and NF-κB-independent (Fig. 2C). The above experiments show a direct link between mutant SOD1 expression and Bcl2-A1 induction in motor neurons and that this induction is dependent on the activation of transcription factor AP1.

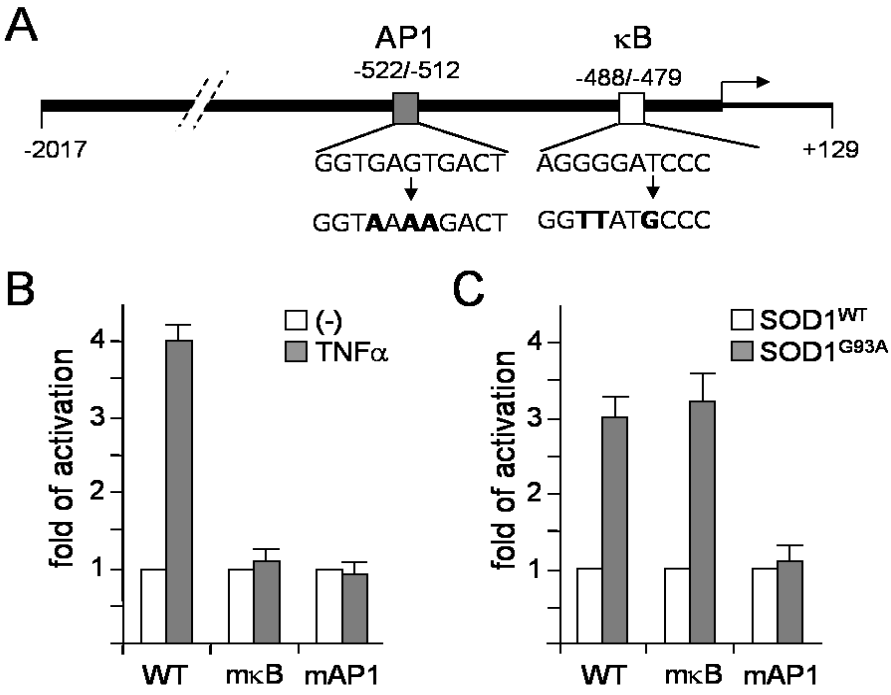

Fig. 2. SOD1^{G93A} induces Bcl2-A1b expression via AP1 transcription factor. A: Schematic diagram of the Bcl2-A1b 5′ flanking region (GenBank accession no. 515003) cloned into the luciferase reporter plasmid pGL2-Basic. The white open box represents the NF-κB-binding site (5′-AGGGGATCCC-3′: −488 to −479) in the promoter or the mutated motif (5′-AGGTCATAAC-3′) generated by PCR; the gray open box represents the putative AP1-binding site (5′-GGTGAGTGACT-3′: −512 to −522) or the mutated motif (5′-GGTAAAAGACT-3′). The arrow denotes the transcription initiation site. B: NSC-34 motoneuronal cells transfected with the indicated plasmids were harvested 24 h post-transfection and analyzed for luciferase activities. Mutagenesis of both AP1 and NF-κB binding sites impairs TNFα induction of Bcl2-A1b. Luciferase values obtained in basal condition (−) were arbitrarily assigned a value of 1.0 and activation

represents the relative normalized luciferase activities obtained upon treatment with TNFα (10 ng/ml for 8 h), (n-fold). C: $SOD1^{G93A}$-mediated induction of Bcl2-A1b requires AP1, but not NF-κB binding site; NSC-34 cells were transfected as in B; luciferase values obtained by co-transfection with pCMV-$SOD1^{WT}$ were arbitrarily assigned a value of 1.0 and activation represents the relative normalized luciferase activities obtained upon co-transfection with pCMV-$SOD1^{G93A}$ plasmids (n-fold). The data are rapresentative of three independent experiments.

2. Bcl2-A1 interacts with pro-caspase-3

In order to get insight on Bcl2-A1 molecular mechanism of action, I looked for molecular interactors of Bcl2-A1 in motor neurons, using an approach of GST-pull down coupled to mass spectrometry. We cloned the mouse Bcl2-A1 (b isoform) coding sequence at the C-terminal of GST sequence in the prokaryotic pGEX-3 expression vector and used this plasmid to transform E. coli. Induction with IPTG leads to a significant expression of GST-Bcl2-A1 fusion protein (Fig. 3A). The fusion protein, isolated under native conditions by a single step of purification using a Glutathione Sepharose Fast Flow column, has been used in GST-pull down experiments using total protein extracts from spinal cord of $SOD1^{G93A}$ mice. The proteins associated with GST-Bcl2-A1 were separated by SDS-PAGE (Fig. 3B) and identified by MALDI-MS. The analysis of MS spectra led to the identification of pro-caspase-3 as a candidate protein (pb0.05). To confirm the Bcl2-A1/pro-caspase-3 interaction in vitro I performed a GST-pulldown experiment followed by Western blot using a specific antibody against caspase-3. As shown in Fig. 3C, GST-Bcl2-A1 is able to pulldown specifically pro-caspase-3, since no interaction is detected using GST alone.

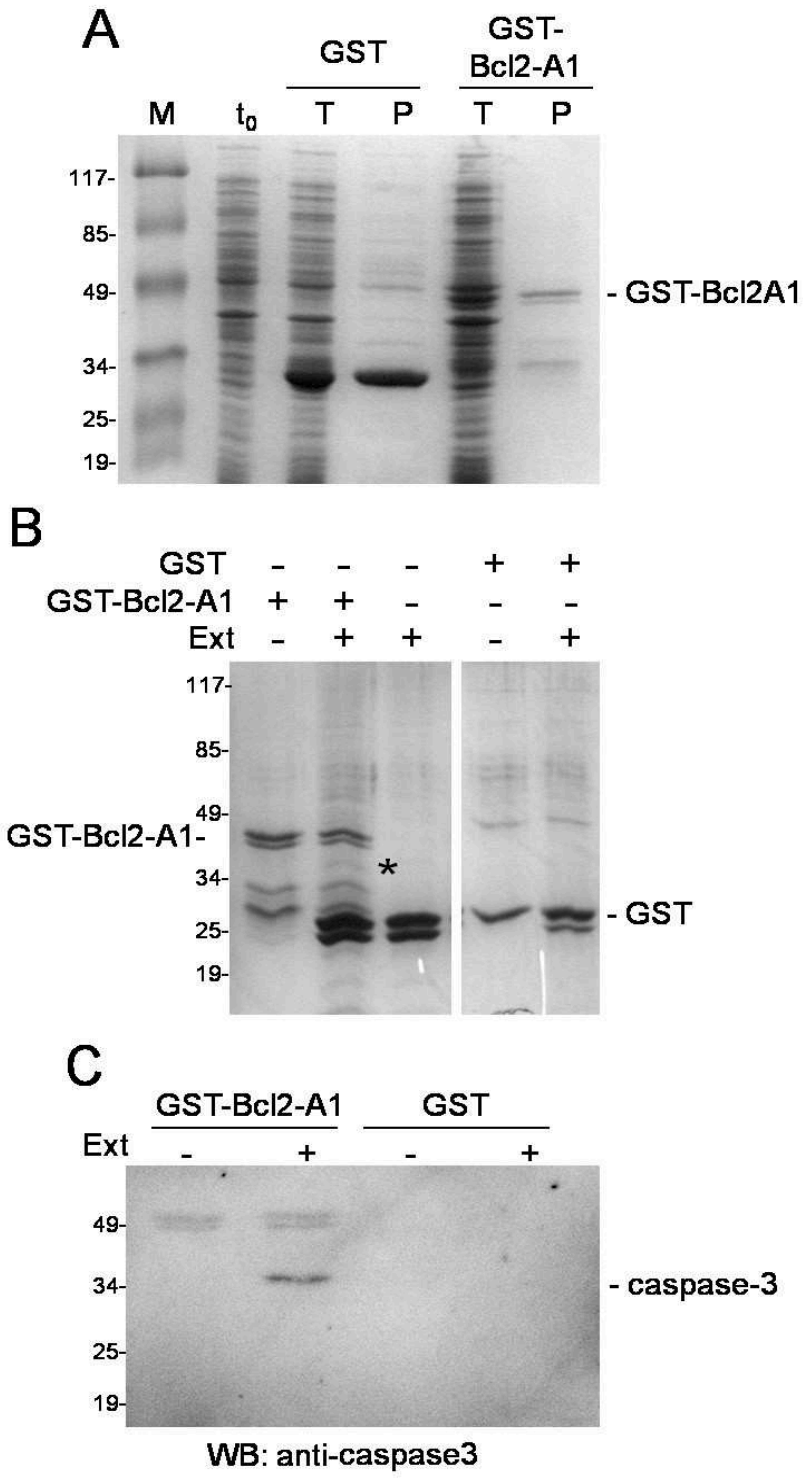

Fig. 3. Identification of pro-caspase-3 as Bcl2-A1 interactor. A: Expression and purification of GST-Bcl2-A1 and GST from E. coli BL21 cells. M = molecular marker expressed in kD (Prestained Protein Molecular Marker. Fermentas); t0 = total protein extract before induction; T = total protein after 2 h induction with IPTG 0.5 mM; P = purified recombinant protein. B: 500 ng of GST-Bcl2-A1 or GST alone were bound to glutathione sepharose and then incubated with 2 mg of proteins from $SOD1^{G93A}$ spinal cord (indicated as Ext). Proteins bound to GST-Bcl2-A1 or GST alone were isolated by SDS-PAGE. The gel was stained with high sensitive colloidal Coomassie and the protein precipitated by GST-Bcl2-A1 (indicated with an asterisk) was identified by mass spectrometry. C: The presence of pro-caspase-3 in the bound fraction was verified by immunoblotting.

In order to evaluate whether I could detect a direct interaction between Bcl2-A1 and pro-caspase-3 also in vivo, I performed a series of co-immunoprecipitation experiments. I cloned murine pro-caspase-3 downstream to 3xFlag epitope and I observed that, when transfected in HEK293 cells, the Flag-tagged protein can be normally processed and activated upon induction of apoptosis by staurosporine (Fig. 4A). Then I co-transfected HEK293 cells with plasmids coding for myc-Bcl2-A1 and Flag-pro-caspase-3. Co-immunoprecipitation experiments demonstrated that using specific antibodies for each of the two proteins we can immunoprecipitate the other one (Fig. 4B). The observed interaction of murine Bcl2-A1 with murine pro-caspase-3 was confirmed also for their human counterparts in both HEK293 and NSC-34 cells (Fig. 4C).

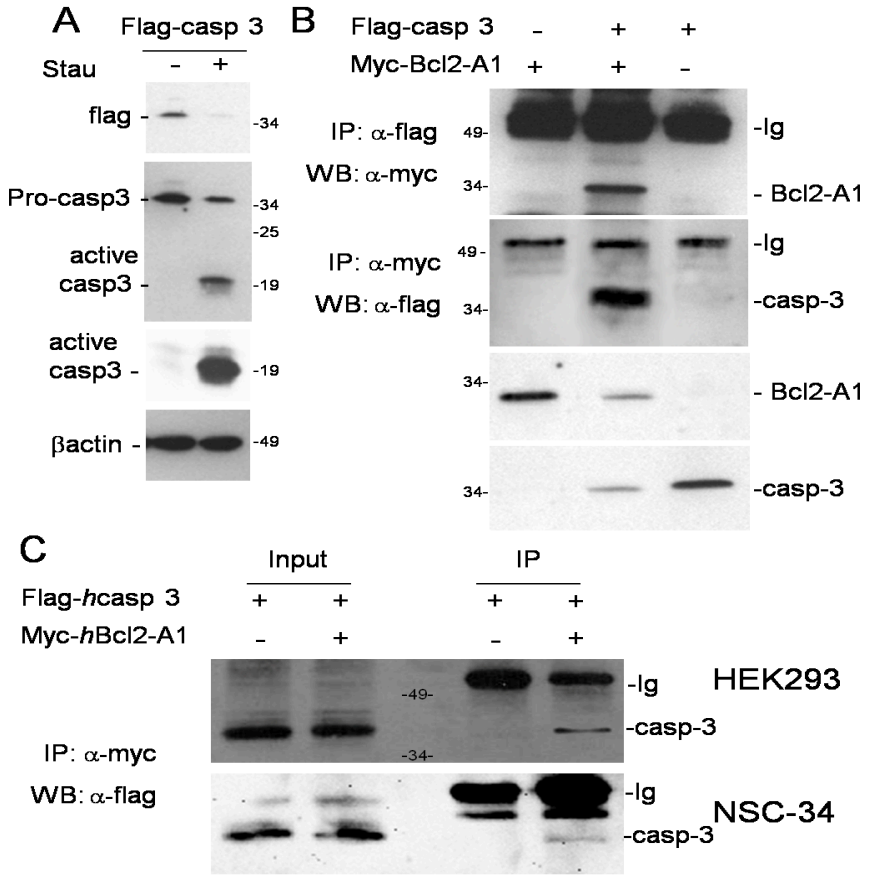

Fig. 4. Bcl2-A1 binds to pro-caspase-3. A: N-terminal fusion of 3xFlag repeats to pro-caspase-3 does not impair its normal processing. HEK293 cells were transfected with 3xFlag-procaspase-3 and 24 h post-transfection treated or not (−) with 10 μM staurosporine for additional 5 h. Protein extracts were analyzed by Western blot with antibodies against Flag, caspase-3, active caspase-3 and β−actin. B: HEK293 cells were transiently transfected with the indicated constructs. Two days later the cells were lysed in NP-40 buffer. Lysates were immunoprecipitated with an anti-Flag antibody or anti-Myc antiserum. Precipitates (IP) were analyzed by Western blot with anti-Myc or anti-Flag antibody, respectively. The levels of transfected proteins were visualized by Western blot on cell lysates used for the co-immunoprecipitation. C: plasmids coding for the Homo sapiens homologues of Bcl2-A1 and pro-caspase-3 were transfected in HEK293 or NSC-34 cells and the samples were processed as in B.

3. Bcl2-A1 interacts with pro-caspase-3 via its C-terminal helix α9

Bcl2-A1 has a helical structure typical of that seen in other Bcl-2 proteins (Brien et al., 2009; Smits et al., 2008). Different lines of evidence indicate that Bcl2-A1 may coexist in two distinct conformational states and that the amphipathic helix α9 at the C-terminal of the protein is required both for the anchorage to mitochondria and to regulate the anti-apoptotic function (Brien et al., 2009; Duriez et al., 2000; Ko et al., 2007, 2011; Smits et al., 2008). To investigate the contribution of the different Bcl2-A1 sub-regions to the binding with pro-caspase-3, I generated four different deletion mutants (indicated as Δα1, Δα1–3, Δα7–9 and Δα9, Fig. 4A), in fusion with the myc epitopes and expressed in HEK293 cells. Co-immunoprecipitation experiments on total extracts from these cells demonstrate that the helix α9 is required for the interaction with pro-caspase-3. Moreover, the lack of helix α1–3 strongly increases the binding to pro-caspase-3, probably because the deletion encompasses the BH3-binding cleft in which helix α9 can shift in and out (Brien et al., 2009) (Fig. 5B). Since helix α9 of Bcl2-A1 is required for both caspase-3 and mitochondria binding, I analyzed the distribution of wild-type or Δα9 Bcl2-A1 in the cytoplasmic and mitochondrial compartments. Immunofluorescence analysis on NSC-34 transfected cells shows that wild type Bcl2-A1 is distributed both free in the cytoplasm and anchored to associate with mitochondria membrane (Fig. 5C). This distribution is further confirmed by Western blot on purified cytoplasmic and mitochondrial protein fractions (Fig. 5D). In agreement with published data (Brien et al., 2009; Duriez et al., 2000), my experiments indicate that Bcl2-A1 is in equilibrium between the cytoplasmic and mitochondrial fractions although mainly anchored to the mitochondrial membrane and that the deletion α9 helix moves this equilibrium towards the soluble cytoplasmic fraction.

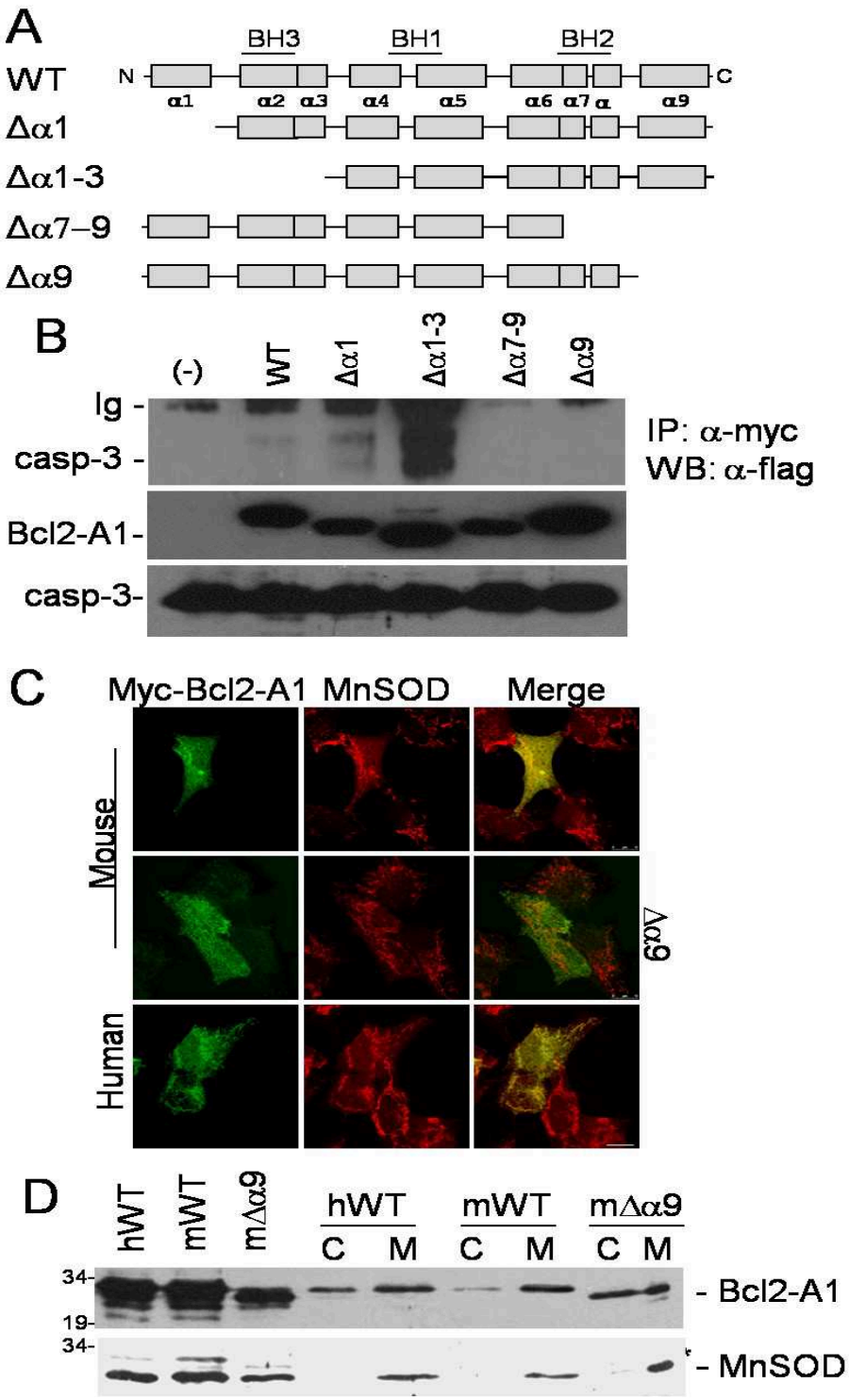

Fig. 5. Bcl2-A1 interacts with pro-caspase-3 via helices α9. A: Schematic representation of Bcl2-A1 deletion mutants. B: Co-immunoprecipitation was performed as described in Fig. 4B. C: Confocal microscopy analysis of NSC-34 cells transfected with human or mouse Bcl2-A1 or mouse Bcl2A1-Δα9. Antibodies against MnSOD were used for mitochondria staining. The yellow color shows the co-localization of the indicated Bcl2-A1 protein variant with mitochondria. D: Cytosolic (C) or mitochondrial (M) protein extracts were prepared from transiently transfected HEK293 as in panel C. The presence of Bcl2-A1 protein was assessed by Western blot on 20 µg of protein samples using antimyc antibody. MnSOD is a marker of mitochondrial fractions.

4. Bcl2-A1 inhibits pro-caspase-3 activation in vitro and in vivo

To further explore the functional relevance of Bcl2-A1/procaspase-3 interaction I used an in vitro approach, evaluating the effect of Bcl2-A1 on pro-caspase-3 processing in the presence of recombinant caspase-8. Incubation of recombinant caspase-8 and protein extracts containing caspase-3 leads the caspase-3 proteolitic processing that is readily detected by a specific antibody against the active form of caspase-3 (compare lanes 1 and 2 of Fig. 6A and relative quantification in Fig. 6B). Addition of Bcl2-A1, immunoprecipitated from transfected eukaryotic cells, to the reaction mixture inhibits procaspase- 3 activation in a dose-dependent manner (Fig. 6A), suggesting a novel Bcl2-A1-dependent anti-apoptotic mechanism of action. In order to investigate the anti-apoptotic contribution of helix α9 against $SOD1^{G93A}$ induced toxicity, I co-transfected NSC-34 motoneuronal cells with Flag-pro-caspase-3 in the presence of WT or mutant Bcl2-A1 and in presence or absence of $SOD1^{G93A}$. In agreement with my previous results, Bcl2-A1 is protective against $SOD1^{G93A}$ induced toxicity, as indicated by the impairment of Flag-caspase-3 decrease (compare lanes 5 and 6 in Fig. 6C and relative quantification in Fig. 6D). This anti-apoptotic effect relies both on presence of helix α9 and helix α1-3 (Figs. 6C and D). The loss of anti-apoptotic activity of Δα1-3 is not surprising since although this protein binds more tightly to pro-caspase-3 (Fig. 5B), the missing domains are also involved in vivo in the maintenance of the pro-apoptotic protein Bax in an inactive state (Simmons et al., 2008). Finally I show that caspase-3 cleavage parallels with an increase in its activity by analyzing PARP cleavage (Fig. 6E) and by counting apoptotic nuclei (Fig. 6F).

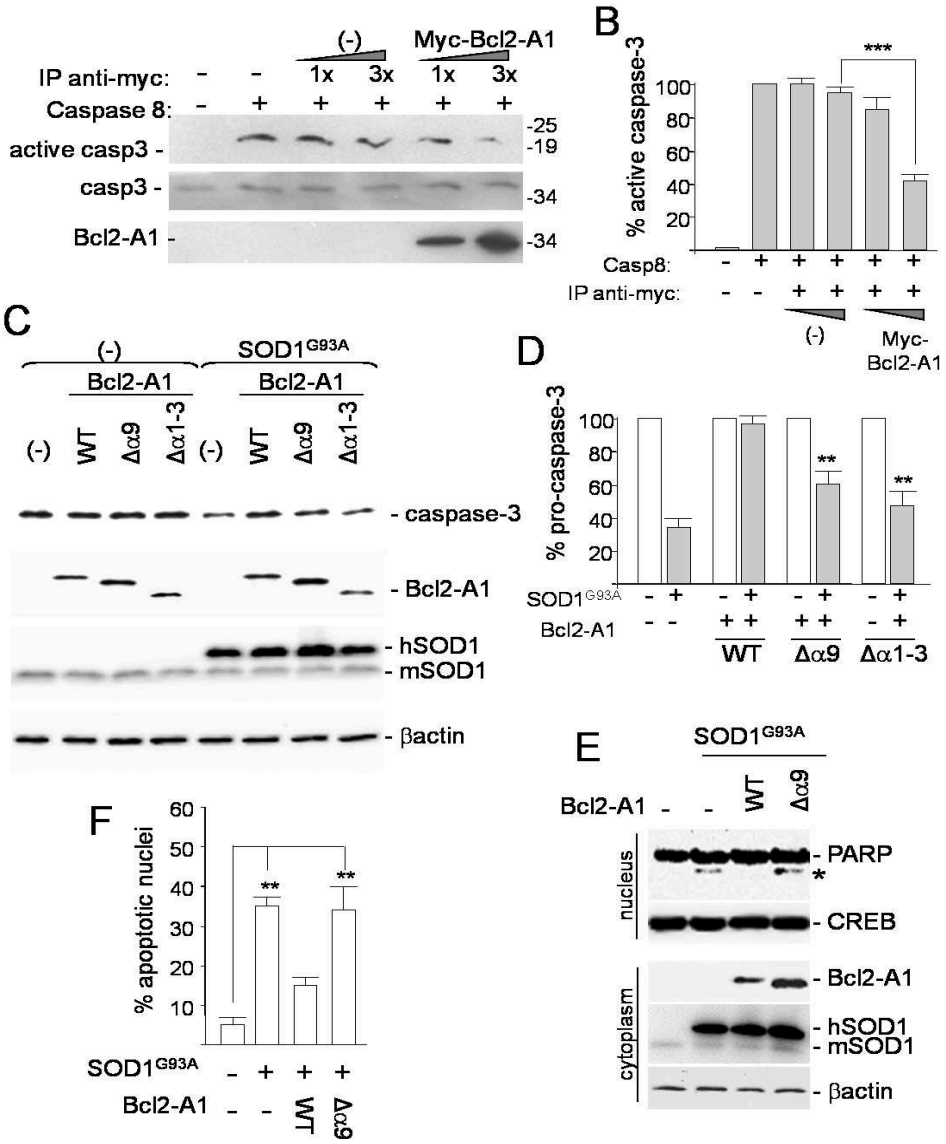

Fig. 6. Effect of Bcl2-A1 binding on pro-caspase-3 maturation in vitro and in vivo. A: Bcl2-A1 impairs in vitro pro-caspase-3 activation by caspase-8. Aliquots of 2 µg of cell extracts from HEK293 transfected with Flag-pro-caspase-3 were incubated with increasing concentrations of immunoprecipitates with anti-myc antibody from HEK293 either transfected with Myc-Bcl2-A1 or untransfected, in presence or absence of recombinant caspase-8. Note that immunoprecipitated Myc-Bcl2-A1 is in the nmolar range. The caspase-3 activation was analyzed by Western blot with a specific antibody that recognizes only the active form. Antibodies against Flag and Myc were used as control for total caspase-3 and Bcl2-A1 presence. B: Quantification of the experiments in (A) by densitometric assay. Results obtained from samples containing only caspase-8 were defined as 100%. Results are expressed as the mean±SEM of three independent experiments. ***=pb0.001. C: Deletion of α9 helix of Bcl2-A1 impairs its anti-apoptotic properties. Flag-pro-caspase-3 and the indicated Bcl2-A1 constructs were transfected in NSC-34 cells in a ratio 1:5, in absence (−) or presence of $SOD1^{G93A}$. 48 h after transfection cell lysates were subjected to SDS–PAGE and analyzed by Western blot with the indicated antibodies. D: Quantification of the experiments in (C) by densitometric assay. Results obtained from sample not transfected with $SOD1^{G93A}$ were defined as 100%. Results are expressed as the means±SEM of three independent experiments. **=pb0.01. E: Evaluation of PARP activation in absence (−) or presence of $SOD1^{G93A}$. Deletion of α9 helix of Bcl2-A1 results in PARP activation, compared to WT Bcl2-A1, in the presence of $SOD1^{G93A}$. 48 h after transfection in NSC-34, cell lysates were subjected to SDS–PAGE and analyzed by Western blot with the indicated antibodies. * indicates cleaved PARP. F: Cells as in E were stained with Hoechst 33342 to assess cell death. Quantitative analysis of apoptotic nuclei is shown as mean±SEM of n=3 independent experiments.

Discussion

This study demonstrates that mutant SOD1 induces the expression of Bcl2-A1, which plays an important role in the modulation of caspase-3 activity, in a cell-specific manner via AP1 transcription factor (Fig. 7).

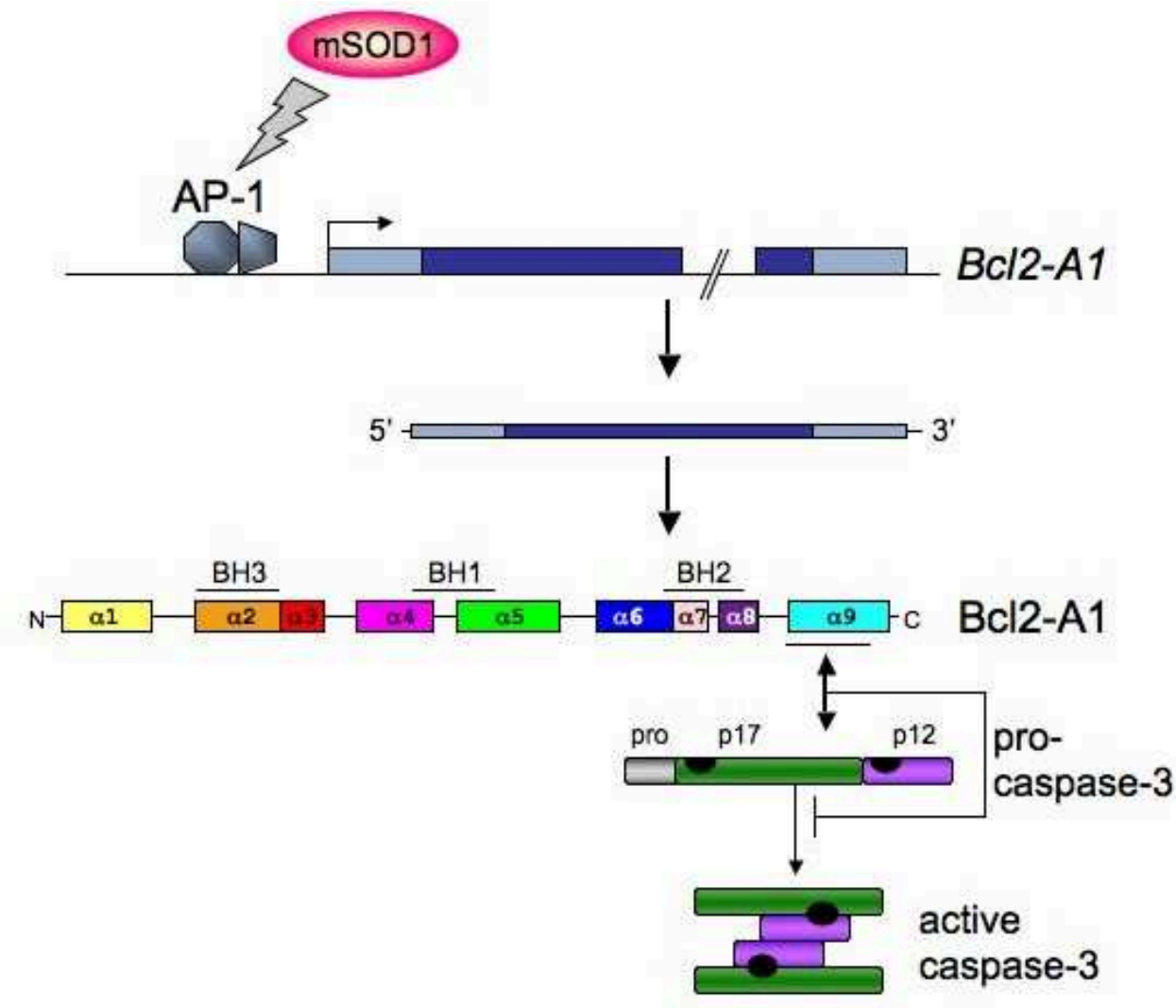

Fig.7. Up-regulation of Bcl2-A1 by mutant SOD1 is mediated by activation of the redox sensitive transcription factor AP1 and that Bcl2-A1 interacts with pro-caspase-3 via its C-terminal helix α9. Furthermore, Bcl2-A1 inhibits pro-caspase-3 activation in immortalized motor neurons expressing mutant SOD1 and thus induction of Bcl2-A1 in ALS mice represents a pro-survival strategy aimed at counteracting the toxic effects of mutant SOD1.

Bcl2-A1 is a member of the Bcl2 family, the key regulators of the mitochondria-dependent apoptotic pathway and of outer mitochondrial membrane integrity (Chipuk et

al., 2010). Different lines of evidence link Bcl2-A1 overexpression to ALS, indicating that injured motor neurons may counteract damage by overexpressing an anti-apoptotic protein such as Bcl2-A1 (Crosio et al., 2006; Pun et al., 2006). Bcl2-A1 over-expression in ALS mice model is limited to spinal cord and it is directly linked to mutant SOD1 expression (Figs. 1 and 2), with a pattern that mirrors the tissue specificity of the disease. Although Bcl2-A1 is mainly expressed in lymphocytes, the present study indicates that constitutive mutant SOD1 over-expression does not modify either the expression level or the relative isoform abundance in this cell type. Moreover, in immortalized motoneurons Bcl2-A1 is transcriptionally regulated by the redox sensitive transcription factor AP1, most likely contributing to lineage- and stimulus-dependent cell specificity of Bcl2-A1 transcription. In fact, it was previously demonstrated that Bcl2-A1 is transcriptionally regulated by NFκB in lymphocytes through B- or T-cell receptor activation (Grumont et al., 1999; Zong et al., 1999), by NFAT in mast cells activated through FcεRI crosslinking (Ulleras et al., 2008) and by PU.1 during neutrophil differentiation (Jenal et al., 2010). The AP1 binding site, already characterized in the human Bcl2-A1 promoter, was demonstrated to be relevant for the assembly of an enhanceosome-like complex in PMA ionomycin-treated Jurkat T cells (Edelstein et al., 2003).

The involvement of AP1 in motor neuron degeneration in ALS is not surprising considering that different proteins belonging to the c-Fos, c-Jun and ATF families are activated in this disease: (i) ATF3 and phospho-c-Jun have been detected in spinal cord and brainstem neurons in SOD1^{G93A} mice, and they can be considered effective markers to identify motor neurons in an early phase of their degeneration (Vlug et al., 2005; Jaarsma et al., 1996); (ii) CSF from ALS patients seems to stimulate Fos expression in certain populations of spinal neurons via the NMDA receptors (Manabe et al., 1999); (iii) c-Jun activation has been identified in post-mortem ALS spinal cord specimens (Virgo and de Belleroche, 1995). Interestingly, using a GST-pull down approach combined to mass spectrometry we were able to identify pro-caspase 3 as a binding partner for Bcl2-A1. This interaction is highly specific both in vivo and in vitro and it depends on Bcl2-A1 helix α9 (Figs. 5 and 6). This amphipathic carboxy-terminal helix was shown to regulate the localization and the pro-survival function of both murine (Smits et al., 2008) and human (Brien et al., 2009) Bcl2-A1. Molecular modeling of Bcl2-A1 indicates that helix α9 may adopt two distinct conformational states. In one of these

states, helix α9 is located in the hydrophobic binding groove and gives rise to a compact molecule: in this conformation helix α9 may play a regulatory role by limiting the access to the hydrophobic BH3-binding cleft. In a second conformation, the molecule is more extended, with helix α9 protruding from the globular core of the protein and therefore potentially mediating interactions with membranes and pro-apoptotic proteins such as Bak (Brien et al., 2009; Smits et al., 2008). According to this model, we have shown that both murine and human Bcl2-A1 are partially localized in mitochondria via helix α9 (Fig. 5), although the anchorage is not fully dependent on this region. In fact, deletion of helix α9 increases the percentage cytoplasmatic Bcl2-A1, but does not fully prevent binding to mitochondria, indicating that Bcl2-A1 subcellular localization relies on multiple factors. Bcl2-A1 seems to be a highly versatile protein, displaying different biological effects according to the cellular models and toxic insult. Wild-type Bcl2-A1 shows anti-apoptotic effects in many different experimental systems, including haematopoietic, tumor and neuronal cell lines, independently from the toxic stimulus and from the fusion partner (Brien et al., 2009; Crosio et al., 2006; D'Sa-Eipper and Chinnadurai, 1998; Ko et al., 2007; Kucharczak et al., 2005; Simmons et al., 2008). Deletion of the C-terminal domain corresponding to helix α9, on the contrary, seems to have a dual effect increasing (Kucharczak et al., 2005) or decreasing/impairing (Herold et al., 2006; Ko et al., 2007; Simmons et al., 2008) Bcl2-A1 anti-apoptotic activity according to cell type and stimulus. This contradictory experimental data can be explained considering that Bcl2-A1 can be regulated at multiple levels: (i) at transcriptional level; as described above, Bcl2-A1 is regulated by many different transcription factors (NFκB, NFTA, AP1, PU.1) enabling different cell types to quickly respond to apoptotic insults (Edelstein et al., 2003; Jenal et al., 2010; Kim et al., 2004; Ulleras et al., 2008;Wang et al., 1999; Zong et al., 1999); (ii) post-transcriptionally, via alternative splicing to produce in human cells a shorter form (Ko et al., 2003); (iii) post-translationally by ubiquitin mediated proteasomal degradation in human haematopoietic cells and tumors (Fan et al., 2010; Herold et al., 2006; Kucharczak et al., 2005); (iv) via interaction with multidomain and BH3-only pro-apoptotic proteins (Chen et al., 2005; Herman et al., 2008; Simmons et al., 2008; Smits et al., 2008;Werner et al., 2002). Here we also provide evidence of a new anti-apoptotic Bcl2-A1 mechanism of action. Bcl2-A1 can physically interact in vitro and in vivo, via helix α9, with pro-caspase-3, preventing its activation. To our knowledge, Bcl2-A1 is the only protein inhibitor of caspase-3 able to bind the zymogen precursor and to prevent its

caspase-8 mediated activation, since both viral (serpin CrmA and p35) and cellular (IAP, inhibitor of apoptosis protein) inhibitors bind the activated formof this caspase (Fuentes-Prior and Salvesen, 2004). For instance XIAP (X-linked inhibitor of apoptosis protein) is able to bind and inhibit the activated form of caspase-3 while not impairing the caspase-8 mediated activation (Deveraux et al., 1997). On the whole, our results contribute to the knowledge of molecular mechanisms of action and functional role of Bcl2-A1 that have important implications in ALS, where prevention of motor neuronal cell death is one of the major therapeutic aims.

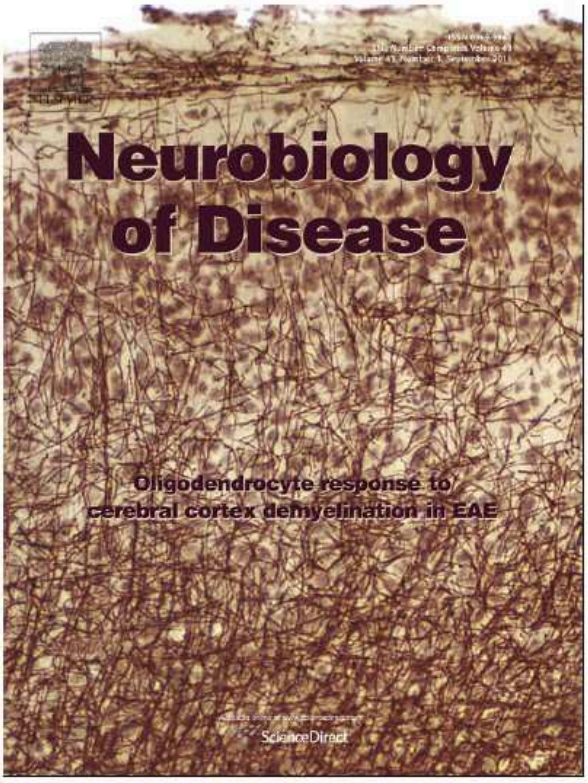

Neurobiology of Disease 43 (2011) 642–650

Contents lists available at ScienceDirect

Neurobiology of Disease

journal homepage: www.elsevier.com/locate/ynbdi

Bcl2-A1 interacts with pro-caspase-3: Implications for amyotrophic lateral sclerosis

Ciro Iaccarino [a,b,*,1], Maria Elena Mura [a,1], Sonia Esposito [a], Franco Carta [c], Giovanna Sanna [a], Franco Turrini [c,d], Maria Teresa Carrì [b,e], Claudia Crosio [a,b,*]

[a] Dept. of Physiological, Biochemical and Cell Science, University of Sassari, Via Muroni 25, 07100 Sassari, Italy
[b] Fondazione Santa Lucia IRCCS, c/o CERC, Via del Fosso di Fiorano 64, 00143 Rome, Italy
[c] Nurex, S.r.l, Sassari, Italy
[d] Dept. of Genetics, Biology and Biochemistry, University of Turin, via Santena 5 bis, 10126 Turin, Italy
[e] Dept. of Biology, University of Rome "Tor Vergata", Via della Ricerca Scientifica, 00133 Rome, Italy

ARTICLE INFO

Article history:
Received 27 January 2011
Revised 23 April 2011
Accepted 14 May 2011
Available online 25 May 2011

Keywords:
ALS, amyotrophic lateral sclerosis
Apoptosis
Pro-caspase-3
Bcl2-A1
Mutant SOD1
NSC34 cells

ABSTRACT

Expression of mutant SOD1 typical of familial amyotrophic lateral sclerosis (ALS) induces the expression of Bcl2-A1, a member of the Bcl2 family of proteins, specifically in motor neurons of transgenic mice.
In this work, we have used immortalized motor neurons (NSC-34) and transgenic mice expressing mutant SOD1 to unravel the molecular mechanisms and the biological meaning of this up-regulation.
We report that up-regulation of Bcl2-A1 by mutant SOD1 is mediated by activation of the redox sensitive transcription factor AP1 and that Bcl2-A1 interacts with pro-caspase-3 via its C-terminal helix α9. Furthermore, Bcl2-A1 inhibits pro-caspase-3 activation in immortalized motor neurons expressing mutant SOD1 and thus induction of Bcl2-A1 in ALS mice represents a pro-survival strategy aimed at counteracting the toxic effects of mutant SOD1.
These data provide significant new insights on how molecular signaling, driven by expression of the ALS-causative gene SOD1, affects regulation of apoptosis in motor neurons and thus may have implications for ALS therapy, where prevention of motor neuronal cell death is one of the major aims.

Introduction

Amyotrophic Lateral sclerosis (ALS) is the most common motor neuron disease and it is invariably fatal since no effective therapy is available (Carrì et al., 2006). Most ALS cases are sporadic, but 5–10% of cases are familial and among these 20% of cases show mutations within the SOD1 gene (OMIM #105400). Notably SOD1 is also responsible of 1.5% of sALS, suggesting a possible role of this protein in both forms of the disease (Pasinelli and Brown, 2006; Rothstein, 2009). Recently mutations in other genes, including TDP-43 and FUS/TLS, have been associated to ALS, but they are present at lower percentages (Lagier-Tourenne et al., 2010; Mackenzie et al., 2010). Current hypotheses for the biology underlying both sporadic and familiar ALS forms outline a model in which non-competing mechanisms are likely to converge in various unfortunate patterns to mediate selective motor neuron degeneration. The proposed mechanisms include oxidative stress, mitochondrial impairment, protein aggregation, glutamate cytotoxicity, transcription dysfunction, alterations in RNA processing, inflammation and apoptotic cell death. Moreover the assessment of the different cell types implicated in the development of ALS and their interactions with motor neurons has led to the identification of several additional pathogenic mechanisms (Boillee et al., 2006; Rothstein, 2009). These significant progresses in understanding the cellular mechanisms of motor neuron degeneration in ALS have not been matched with an effective disease-modifying pharmacotherapy, mostly because the molecular basis of selective vulnerability of motor neurons upon mutant SOD1 expression is still debated. A crucial step in filling this gap is the identification of genes whose expression is altered by mutant SOD1 in motor neurons. We previously demonstrated that motor neuronal death prompted by the expression of mutant SOD1 induces specific up-regulation of the Bcl2 family member Bcl2-A1 gene (Crosio et al., 2006). Bcl2-A1 (also known as Bcl2-related protein A1, BFL1; A1; Bfl-1/A1) is the only member of Bcl2 family to be up-regulated selectively in spinal motor neurons of mice transgenic for G93A–SOD1 already at the asymptomatic stage. Bcl2-A1 is protective against death of neuronal cells induced by expression of G93A–SOD1, but is detrimental upon stimulation of those cells with TNFα (Crosio et al., 2006). Although Bcl2-A1 is the unique example of apoptotic protein specifically over-expressed in motor neurons of mouse model of ALS, the molecular mechanisms of Bcl2-A1 pro/anti-apoptotic action

Abbreviations: ALS, amyotrophic lateral sclerosis; Bcl2-A1, B-cell leukemia/lymphoma 2 related protein A1; PBS, phosphate-buffered saline; SDS, sodium dodecyl sulfate; SOD1, superoxide dismutase 1; NF-κB, nuclear factor kappa-light-chain-enhancer of activated B cells; AP-1, activator protein 1; GST, glutathione S-transferase.

* Corresponding authors at: Dept. of Physiological, Biochemical and Cell Science, University of Sassari, Via Muroni 25, 07100 Sassari, Italy.
E-mail addresses: ciaccarino@uniss.it (C. Iaccarino), ccrosio@uniss.it (C. Crosio).
[1] C.I. and M.E.M. contributed equally to this work.
Available online on ScienceDirect (www.sciencedirect.com).

0969-9961/$ – see front matter © 2011 Elsevier Inc. All rights reserved.
doi:10.1016/j.nbd.2011.05.013

is still unclear. The pro- and anti-apoptotic behavior of Bcl2-A1 seems to be mediated by two independent pathways (Kucharczak et al., 2005). Both in man and mouse Bcl2-A1 has a helical structure typical of other pro-survival Bcl-2 proteins, with a C-terminal tail-anchor domain corresponding to helix α9, needed for its association with mitochondria and for the prosurvival activity (Brien et al., 2009; Fan et al., 2010; Ko et al., 2007, 2011; Kucharczak et al., 2005; Smits et al., 2008). In B lymphocytes stimulated with TNFα, the Bcl2-A1 anti-apoptotic mechanism seems to be mediated by cytoplasmic protein partners, while the pro-apoptotic function seems to be regulated by post-translational modifications, including proteolytic cleavage and phosphorylation, that can alter Bcl2-A1 localization or its ability to interact with other factors (Kucharczak et al., 2005).

In this context, we have investigated the molecular pathways leading to Bcl2-A1 transcriptional activation upon mutant SOD1 expression and the molecular mechanisms underlying the anti-apoptotic action of Bcl2-A1 in ALS cellular models.

Material and methods

Animals and tissue dissection

We used SOD1^{G93A} transgenic mice (strain B6.Cg-Tg(SOD1–G93A)-1Gur from The Jackson Laboratory, 99.99% C57BL/6 genetic background, 50% survive at 157.1 ± 9.3 days, http://jaxmice.jax.org/strain/004435.html). Non-transgenic littermates were used as control. All animal procedures have been performed according to the European Guidelines for the use of animals in research (86/609/CEE) and the requirements of Italian laws (D.L. 116/92).

At early symptomatic stage of the disease (120 days), mice were anesthetized with chloral hydrate 500 mg/kg, sacrificed and tissue dissected. Spinal cord was manually dissected and stored dried at −80 °C. Lymphocytes were isolated from 1 ml heparinated blood samples by standard centrifugation on a Ficoll gradient. All efforts were made to minimize suffering. All animals have been raised and crossed in the indoor animal house in a 12 h light/dark cycle in a virus/antigen-free facility with controlled temperature and humidity and have been provided with water and food *ad libitum*.

Plasmid construction

A fragment corresponding to mouse Bcl2-A1b gene promoter (ch NCBIM37:9: 89093447:89103264:1), spanning from −2017 to +129 was cloned in pGL2-basic (Promega). Mutations of NF-κB (5′-CTTGCTGCTGTTTCAGGTCATAACAGGTTTCGTCTCAGCG-3′) and AP1 (5′-TTAAGGACTAGAGAGGTAAAAGACTCAGGAATTAAG-3′) binding site were generated in the Bcl2-A1b promoter using the Quickchange site-directed mutagenesis kit (Stratagene). The GST-Bd2-A1 construct was obtained by cloning a PCR fragment corresponding to mouse Bcl2-A1b coding sequence (NM_007534.3), into *BamH*I and *Sma*I restriction sites of the pGEX-3 vector (GE healthcare). Coding sequences corresponding to mouse (NM_009810) and human (NM_004346.3) pro-caspase 3 were isolated by RT-PCR and cloned downstream to 3xFlag repeats (p3xFlag-CMV-10 vector, Sigma-Aldrich). Plasmids coding for SOD1^{WT}, SOD1^{G93A}, mouse 5xMyc-Bcl2-A1b (mBcl2-A1b), human 5xMyc-Bcl2-A1 (hBcl2-A1) were described elsewhere (Crosio et al., 2006; Ferri et al., 2006). Bcl2-A1 deletion mutants Δα1 (Δ aa 4–34), Δα1–3 (Δ aa 4–64), Δα7–9 (Δ aa 130–168), Δα9 (Δ aa 150–168), were obtained by mutagenesis, using the Quickchange site-directed mutagenesis kit (Stratagene), starting from 5xMyc-mBcl2-A1b plasmid described above.

Detection of Bcl2-A1 subtype mRNA by RT-PCR

Bcl2-A1a, Bcl2-A1b, Bcl2-A1d were amplified from mouse cDNA, obtained by retro-transcription of spinal cord and lymphocyte total RNA from SOD1^{G93A} transgenic mouse and control mice. Specific primers for all the three mRNAs were used for the amplification (5′ACTCCCTGGCTGAGCACTA3′; 5′AGTTTCCAGTTTTGTGGCA3′) and the product was analyzed by single and double digestion with *Pst*I and *Bgl* II.

Cell cultures

HEK293 human embryonic kidney cells were cultured as recommended by the American Type Culture Collection (Rockville, Md.). Motoneuronal NSC-34 cells (Durham et al., 1993) were grown in DMEM-F12 + 10% Fetal Calf Serum (FCS, Invitrogen) at 37 °C. Transient expression of each plasmid (1.5 μg DNA/5–7 × 10^5 cells) was obtained in transfecting cells with LipofectAMINE Plus reagent (Invitrogen) according to the manufacturer's instructions. After 3 hour incubation with transfection reagents, cells were cultured in normal growth medium for additional 24–48 h.

Luciferase assay

Transfected NSC-34 cells were lysed in Lysis Reagent (25 mM Tris-phosphate pH 7.8, 2 mM DTT, 2 mM 1,2-diaminocyclohexane-N,N,N′,N′-tetraacetic acid, 10% glycerol, 1% Triton X-100). Equal amount of protein extracts were incubated with 100 μl of Luciferase Assay Reagent (Promega) and luminescence determined using the Victor 5 Wallace workstation (PerkinElmer) according to manufacturer's instruction.

GST pull-down assay

The GST-Bd2-A1 fusion protein was expressed in *E. coli* BL21. After induction with 0.5 mM IPTG for 3 h at 30 °C, bacteria were collected, washed twice in PBS 1X and lysed in *lysis buffer* (50 mM Tris HCl pH 8.0, 1 mM EDTA, 150 mM NaCl, 1% Triton X100, 1 mM PMSF, protease inhibitor cocktail 1X, 200 μg/ml lysozime). Bacterial cell lysates were kept 30′ on ice and then sonicated for 5″ at 100 W for 3 times. GST-proteins were purified on glutathione–Sepharose 4 fast flow resin (GE Healthcare). Aliquots (500 ng) of GST-Bcl2-A1 or GST alone were incubated with 2 mg of total spinal cord protein extracts from SOD1^{G93A} transgenic mice, obtained by homogenization in *lysis buffer* (50 mM Tris–HCl [pH 8.0], 150 mM NaCl, 1% NP-40, 1 mM PMSF, protease inhibitor cocktail 1X). After an overnight incubation at 4 °C, GST-Bcl2-A1 or GST alone were collected by adding to the mixture 10 μl of glutathione-Sepharose 4 fast flow resin for 2 h at 4 °C. After five washes in *lysis buffer*, the beads were resuspended in Laemmli Buffer 1X and loaded on SDS/PAGE acrylamide gel. SDS/PAGE loaded with GST-pulldown samples were stained with Mass Compatible Super Blue Stain Kit (Nurex srl, Sassari) or analyzed by Western blot as described below.

In-gel digestion and matrix-assisted laser desorption/ionization (MALDI) mass spectrometry (MS) analysis

Proteins of interest were excised with a sterile scalpel and destained with 100 μl of 5 mM NH_4HCO_3/50% acetonitril and the mass spectrometry analysis was performed as decsribed in Lepedda et al. (2009). The MS spectra acquired were submitted to MASCOT (Matrix Science, London UK).

Western blot analyses

Protein extracts were resolved by standard SDS-polyacrylamide gel electrophoresis (PAGE) and were analyzed by Western blot as previously described (Crosio et al., 2006), using the following antibodies: anti-Flag M2 monoclonal antibody (Sigma-Aldrich), anti-myc monoclonal antibody 9E10 (Sigma-Aldrich), anti-β-actin monoclonal antibody AC-15 (Sigma-Aldrich), rabbit polyclonal anti-Cu-ZnSOD antibody (Stressgen), rabbit polyclonal anti-human

Maria Elena Mura
Molecular mechanisms involved in Amyotrophic Lateral Sclerosis:
role of Bcl2-A1 and TDP-43 genes in motor neuron degeneration
Tesi di dottorato in Scienze Biomolecolari e Biotecnologiche
Università degli studi di Sassari

MnSOD antibody (Stressgen), rabbit anti-cleaved caspase-3 (Cell signaling), rabbit anti-caspase-3 (Cell signaling), rabbit anti-PARP (Cell signaling), rabbit anti-CREB (Cell signaling). Secondary antibodies (peroxidase-conjugated) were obtained from Invitrogen. Densitometric analyses were performed using Quantity One software program (Bio-Rad Laboratories) and normalized against the signal obtained by re-probing the membranes with an antibody against mouse β-actin. Student's *t* test was used for data analysis and differences were considered statistically significant if $p<0.05$. All statistical computations were performed using GraphPad Prism 4.0 (GraphPad Software).

Immunoprecipitations

At 48 h after transfection, HEK293 cells were lysed in 1 ml of *lysis buffer*. After centrifugation at 12,000 g for 10 min at 4 °C, the supernatants were precleared at 4 °C for 1 h with protein A-Sepharose. The anti-Myc or the anti–Flag antibodies were added at 1:1000 dilution, and after an overnight incubation at 4 °C, the immunoprecipitates were collected by adding 20 µl of protein A-Sepharose. The beads were washed five times in *lysis buffer*, resuspended in Laemmli Buffer 1X and analyzed by Western blotting.

Subcellular fractioning

5×10^6 HEK293 were transfected with plasmids coding for WT or the deletion mutant Δα9 of murine Bcl2-A1 and the human Bcl2-A1. 48 h after transfection cells were harvested, washed in 1 ml of ice-cold PBS with 1 mM EDTA and centrifuged at 600 ×g for 5′ at 4 °C. The pellet was solubilized in 1 ml of mitochondrial buffer (210 mM mannitol, 70 mM sucrose, 1 mM EDTA, 10 mM Hepes-KOH pH 7.5) containing protease inhibitors cocktail (Sigma-Aldrich). 50 µl of the solubilized (total) fraction was stored and the remaining was homogenized in a glass-teflon potter homogenizer (10–15 strokes) and centrifuged at 600 ×g for 5′ at 4 °C. The supernatant was harvested and again centrifuged in the same conditions. Following an additional centrifugation at 10,000 ×g for 10′ at 4 °C, the supernatant (cytosolic fraction) was collected and the mithocondrial pellet was washed in 1 ml of mitochondrial buffer and centrifuged at 10,000 ×g for 10′ at 4 °C. The pellet was carefully resuspended in 100 µl of lysis buffer (50 mM Tris–HCl pH 8.0, 150 mM NaCl, 1% NP-40) and protease inhibitors, incubated for 10′ on ice and centrifuged at 10,000 ×g for 10′ at 4 °C; the supernatant (mitochondrial fraction) was stored at −20 °C. Protein concentration was evaluated using Coomassie Protein Assay Reagent (Fluka Analytical) and 10 µg of each fraction was loaded on SDS/PAGE followed by Western Blot analysis.

Immunofluorescence

1×10^5 NSC-34 cells, grown on a cover-glass, were washed twice with PBS 1X and then fixed with 1 ml of 4% paraformaldehyde/PBS 1X for 10 min. Cells were permeabilized with 0.1% Triton X-100 in PBS and non-specific binding was blocked with 5% bovine serum albumin, 0.1% Triton X-100 diluted in PBS for 1 h at room temperature. Cells were incubated with primary antibodies (mouse anti-myc diluted 1:1000, Sigma-Aldrich, rabbit anti-MnSOD diluted 1:2000, Stressgene) diluted in blocking solution, overnight at 4 °C and then with secondary antibodies Alexa594- and Alexa488-conjugated (Molecular Probe, Invitrogen) diluted 1:1000 in blocking solution for 1 h at room temperature. Cells were analyzed with a Leica TCS SP5 confocal microscopy with LAS lite 170 image software.

In vitro assay for caspase-3 activation

To test caspase-3 activation *in vitro* we used a protocol modified from (Deveraux et al., 1997). Aliquots of 2 µg of HEK293 cells transfected with

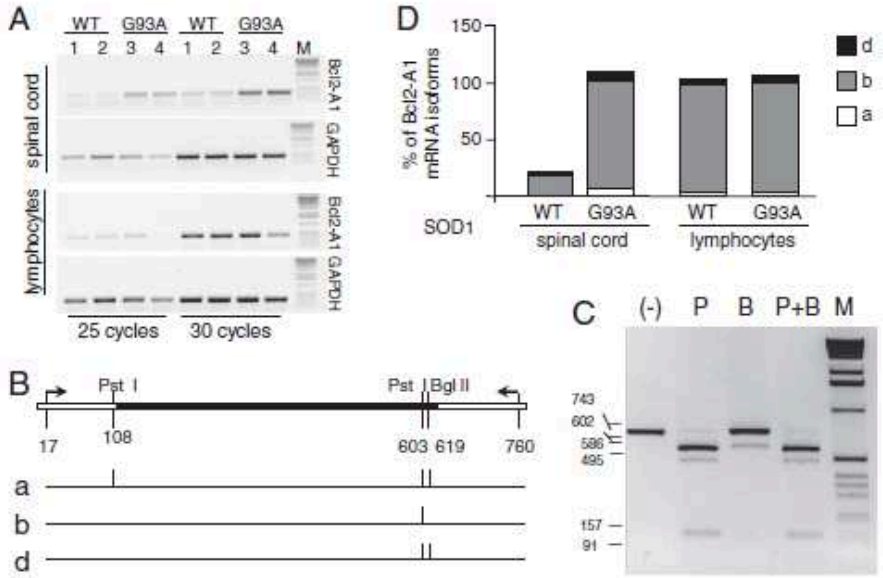

Fig. 1. Relative expression level of each Bcl2-A1 subtype in spinal cord of SOD1^{G93A} mice. A: Semiquantitative RT-PCR on 1 µg of total RNA extracted from spinal cord and lymphocytes of two mice, expressing human either wild type (WT, mice 1 and 2) or mutant (G93A, mice 3 and 4) SOD1. PCR was performed using oligos indicated by arrows in panel B to amplify all the Bcl2-A1 mRNA isoforms; amplification of GAPDH was used as positive control; M = GeneRuler™ DNA Ladder Mix (Fermentas). B: Schematic representation of murine Bcl2-A1 mRNA isoforms. Arrows indicate the position of oligos utilized for PCR, while vertical lines point at PstI and BglII restriction sites. C: Representative experiment showing the digestion product of RT-PCR amplicons obtained from SOD1^{G93A} spinal cord RNA; PCR product undigested (−), digested with restriction enzymes PstI (lane P) and BglII (lane B) or both of them (lanes P + B). Major fragments were as follows: 743 bp fragments, A1b (lane B); 602 bp fragments, A1a or A1d (lanes B and P/B); 586 bp fragments, A1b or A1d (lane P) and A1-d (lanes P and P/B); 495 bp fragments, A1a (lanes P and P/B). RNA (1 µg) isolated from lymphocytes or spinal cord of SOD1^{G93A} mice was reverse transcribed and amplified. RT-PCR products were digested by restriction enzymes as indicated above, electrophoresed on 1.3% agarose gels and D: the relative amount of each mRNA as evaluated by densitometric analysis.

Maria Elena Mura
Molecular mechanisms involved in Amyotrophic Lateral Sclerosis:
role of Bcl2-A1 and TDP-43 genes in motor neuron degeneration
Tesi di dottorato in Scienze Biomolecolari e Biotecnologiche
Università degli studi di Sassari

Flag-pro-caspase-3 were incubated with scalar quantity of myc-immunoprecipitates from HEK293 cells transfected or not (−) with 5xmyc-Bcl2A1 at 30 °C for 30′ in a final volume of 20 µl. 50 ng of recombinant active caspase-8 (Sigma-Aldrich) was added and the reaction was incubated for additional 15′ at 30 °C. The reactions were then stopped by adding 6 µl of Laemmli Buffer 5X. The samples were finally analyzed by Western Blot.

Assessment of cell death

Quantification of apoptotic cells was obtained by direct visual counting after nuclear staining of 4% paraformaldehyde-fixed cells with the fluorescent probe Hoechst 33342 (1 µg/ml, Sigma). One hundred cells were analyzed in each examined field at 20× magnification, and eight randomly chosen fields for each experimental condition were counted. Only the cells containing clearly picnotic or fragmented nuclei were considered apoptotic.

Results

Mutant SOD1 induces Bcl2-A1 expression via AP1

We have previously shown that Bcl2-A1 is specifically induced in motor neurons of SOD1^{G93A} mice (Crosio et al., 2006). Since mice have multiple Bcl2-A1 genes (the isoforms -a, -b and -d consist of two exons and encode a full length protein, while isoform -c lacks putative exon 2 and it is most likely a pseudogene), in a preliminary experiment we carried out the classification and relative quantification of Bcl2-A1a, -A1b and -A1d mRNA subtypes in spinal cord and lymphocytes of mice expressing wild-type (WT) or mutant (G93A) SOD1. Semiquantitative RT-PCR shows that Bcl2-A1 is induced only in the spinal cord of SOD1^{G93A} mice, since lymphocytes of both genotypes have comparable levels of Bcl2-A1 mRNA (Fig. 1A). The amplicons were subjected to digestion with restriction enzymes that allow discrimination of Bcl2-A1 isoforms, as reported by Hatakeyama et al. (1998) (Fig. 1B). In the spinal cord, all three isoforms are induced, although isoform A1b is clearly the most abundant (Figs. 1C and D).

Previous reports have demonstrated that the human and murine Bcl2-A1 promoter is physiologically regulated via NFκB transcription factor in T cells (Edelstein et al., 2003; Grumont et al., 1999). Moreover, the assembly of an enhanceosome-like complex, in which cooperative protein–protein and protein–DNA interactions involving NFκB and AP-1 binding sites concur to the efficient formation of the

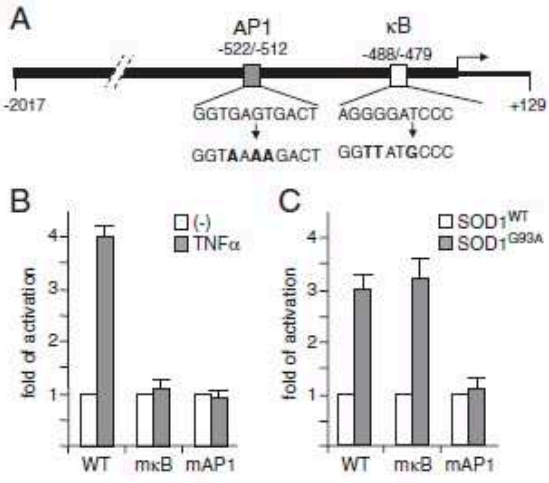

Fig. 2. SOD1^{G93A} induces Bcl2-A1b expression via AP1 transcription factor. A: Schematic diagram of the Bcl2-A1b 5′ flanking region (GenBank accession no. 515003) cloned into the luciferase reporter plasmid pGL3. The white open box represents the NFκB-binding site (5′-AGGGGATCCC-3′: −488 to −479) in the promoter or the mutated motif (5′-AGGTCATAAC-3′) generated by PCR; the gray open box represents the putative AP1-binding site (5′-GGTGAGTGACT-3′: −512 to −522) or the mutated motif (5′-GGTAAAAGACT-3′). The arrow denotes the transcription initiation site. B: NSC-34 motoneuronal cells transfected with the indicated plasmids were harvested 24 h post-transfection and analyzed for luciferase activities. Mutagenesis of both AP1 and NFκB binding sites impairs TNFα induction of Bcl2-A1b. Luciferase values obtained in basal condition (−) were arbitrarily assigned a value of 1.0 and activation represents the relative normalized luciferase activities obtained upon treatment with TNFα (10 ng/ml for 8 h), (*n*-fold). C: SOD1^{G93A}-mediated induction of Bcl2-A1b requires AP1, but not NFκB binding site; NSC-34 cells were transfected as in B); luciferase values obtained by cotransfection with pCMV-SOD1^{WT} were arbitrarily assigned a value of 1.0 and activation represents the relative normalized luciferase activities obtained upon cotransfection with pCMV-SOD1^{G93A} plasmids (*n*-fold). The data are representative of three independent experiments.

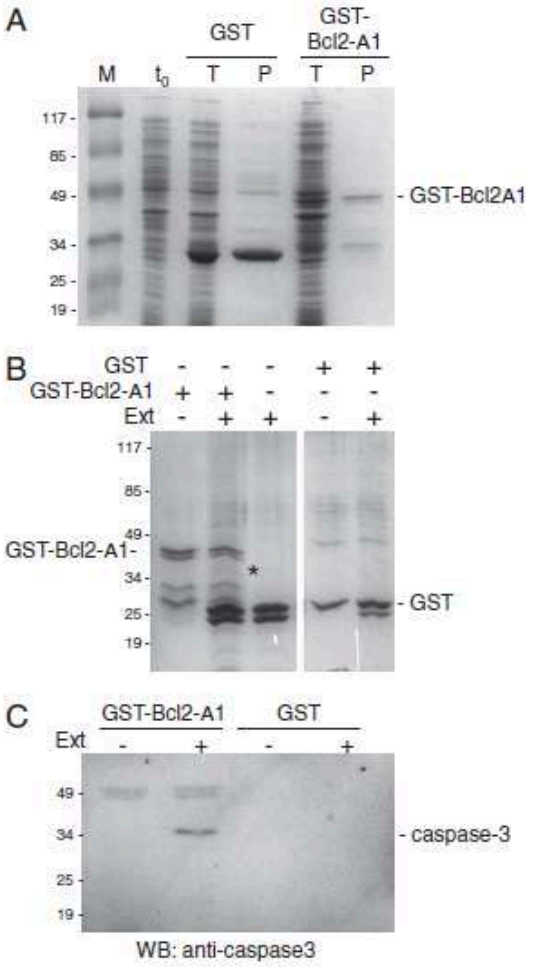

Fig. 3. Identification of pro-caspase-3 as Bcl2-A1 interactor. A: Expression and purification of GST-Bcl2-A1 and GST from *E. coli* BL21 cells. M = molecular marker expressed in kD (Prestained Protein Molecular Marker, Fermentas); t_0 = total protein extract before induction; T = total protein after 2 h induction with IPTG 0.5 mM; P = purified recombinant protein. B: 500 ng of GST-Bcl2-A1 or GST alone were bound to glutathione sepharose and then incubated with 2 mg of proteins from SOD1^{G93A} spinal cord (indicated as Ext). Proteins bound to GST-Bcl2-A1 or GST alone were isolated by SDS-PAGE. The gel was stained with high sensitive colloidal Coomassie and the protein precipitated by GST-Bcl2-A1 (indicated with an asterisk) was identified by mass spectrometry. C: The presence of pro-caspase-3 in the bound fraction was verified by immunoblotting.

Maria Elena Mura
Molecular mechanisms involved in Amyotrophic Lateral Sclerosis:
role of Bcl2-A1 and TDP-43 genes in motor neuron degeneration
Tesi di dottorato in Scienze Biomolecolari e Biotecnologiche
Università degli studi di Sassari

transcriptional complex, has been observed on the human Bcl2-A1 promoter (Edelstein et al., 2003). Using a bioinformatics approach (Cartharius et al., 2005), we were able to identify a potential AP1 binding site on murine Bcl2-A1b promoter, located upstream to NF-κB binding site, in a position (nucleotide from −522 to −512) compatible with the formation of an enhanceosome-like complex. We therefore cloned murine Bcl2-A1b promoter in a wild type form or with either a mutagenized NFκB or a mutagenized putative AP1 binding site upstream a luciferase reporter gene (Fig. 2A). These plasmids were used to transfect motor neuronal NSC-34 cells and, as expected, mutations of NFκB, but also on the putative AP1 binding sites on murine Bcl2-A1b promoter impair induction upon TNFα stimulation (Fig. 2B). In contrast, induction of Bd2-A1b upon mutant SOD1 expression is AP1-dependent and NFκB-independent (Fig. 2C). The above experiments show a direct link between mutant SOD1 expression and Bcl2-A1 induction in motor neurons and that this induction is dependent on the activation of transcription factor AP1.

Bcl2-A1 interacts with pro-caspase-3

In order to get insight on Bcl2-A1 molecular mechanism of action, we looked for molecular interactors of Bcl2-A1 in motor neurons, using an approach of GST-pull down coupled to mass spectrometry. We cloned the mouse Bcl2-A1 (b isoform) coding sequence at the C-terminal of GST sequence in the prokaryotic pGEX-3 expression vector and used this plasmid to transform *E. coli*. Induction with IPTG leads to a significant expression of GST-Bd2-A1 fusion protein (Fig. 3A). The fusion protein, isolated under native conditions by a single step of purification using a Glutathione Sepharose Fast Flow column, has been used in GST-pull down experiments using total protein extracts from spinal cord of SOD1^{G93A} mice. The proteins associated with GST-Bcl2-A1 were separated by SDS-PAGE (Fig. 3B) and identified by MALDI-MS. The analysis of MS spectra led to the identification of pro-caspase-3 as a candidate protein ($p<0.05$). To confirm the Bcl2-A1/pro-caspase-3 interaction *in vitro* we performed a GST-pulldown experiment followed by Western blot using a specific antibody against caspase-3. As shown in Fig. 3C, GST-Bd2-A1 is able to pulldown specifically pro-caspase-3, since no interaction is detected using GST alone.

In order to evaluate whether we could detect a direct interaction between Bd2-A1 and pro-caspase-3 also *in vivo*, we performed a series of co-immunoprecipitation experiments. We cloned murine pro-caspase-3 downstream to 3xFlag epitope and we observed that, when transfected in HEK293 cells, the Flag-tagged protein can be normally processed and activated upon induction of apoptosis by staurosporine (Fig. 4A).

Then we co-transfected HEK293 cells with plasmids coding for myc-Bcl2-A1 and Flag-pro-caspase-3. Co-immunoprecipitation

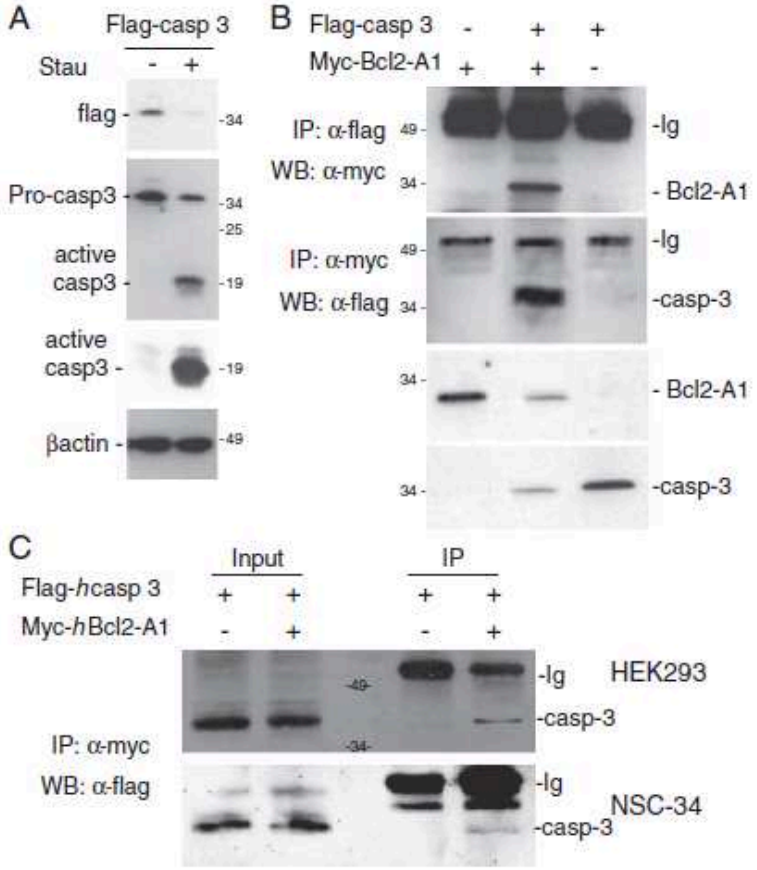

Fig. 4. Bcl2-A1 binds to pro-caspase-3. A: N-terminal fusion of 3xFlag repeats to pro-caspase-3 does not impair its normal processing. HEK293 cells were transfected with 3xFlag-pro-caspase-3 and 24 h post-transfection treated or not (−) with 10 μM staurosporine for additional 5 h. Protein extracts were analyzed by Western blot with antibodies against Flag, caspase-3, active caspase-3 and β−actin. B: HEK293 cells were transiently transfected with the indicated constructs. Two days later the cells were lysed in NP-40 buffer. Lysates were subjected to immunoprecipitation with an anti-Flag antibody or anti-Myc antiserum. Precipitates (IP) were analyzed by Western blot with anti-Myc or anti-Flag antibody, respectively. The levels of transfected proteins were visualized by Western blot on cell lysates used for the co-immunoprecipitation. C: plasmids coding for the *Homo sapiens* homologues of Bcl2-A1 and pro-caspase-3 were transfected in HEK293 or NSC-34 cells and the samples were processed as in B.

Maria Elena Mura
Molecular mechanisms involved in Amyotrophic Lateral Sclerosis:
role of Bcl2-A1 and TDP-43 genes in motor neuron degeneration
Tesi di dottorato in Scienze Biomolecolari e Biotecnologiche
Università degli studi di Sassari

experiments demonstrated that using specific antibodies for each of the two proteins we can immunoprecipitate the other one (Fig. 4B). The observed interaction of murine Bcl2-A1 with murine pro-caspase-3 was confirmed also for their human counterparts in both HEK293 and NSC-34 cells (Fig. 4C).

Bcl2-A1 interacts with pro-caspase-3 via its C-terminal helix α9

Bcl2-A1 has a helical structure typical of that seen in other Bcl-2 proteins (Brien et al., 2009; Smits et al., 2008). Different lines of evidence indicate that Bcl2-A1 may coexist in two distinct conformational states and that the amphipathic helix α9 at the C-terminal of the protein is required both for the anchorage to mitochondria and to regulate the anti-apoptotic function (Brien et al., 2009; Duriez et al., 2000; Ko et al., 2007, 2011; Smits et al., 2008). To investigate the contribution of the different Bcl2-A1 sub-regions to the binding with pro-caspase-3, we generated four different deletion mutants (indicated as Δα1, Δα1–3, Δα7–9 and Δα9, Fig. 4A), in fusion with the myc epitopes and expressed in HEK293 cells. Co-immunoprecipitation experiments on total extracts from these cells demonstrate that the helix α9 is required for the interaction with pro-caspase-3. Moreover, the lack of helix α1–3 strongly increases the binding to pro-caspase-3, probably because the deletion encompasses the BH3-binding cleft in which helix α9 can shift in and out (Brien et al., 2009) (Fig. 5B).

Since helix α9 of Bcl2-A1 is required for both caspase-3 and mitochondria binding, we analyzed the distribution of wild-type or Δα9 Bcl2-A1 in the cytoplasmic and mitochondrial compartments. Immunofluorescence analysis on NSC-34 transfected cells shows that wild type Bcl2-A1 is distributed both free in the cytoplasm and anchored to associate with mitochondria membrane (Fig. 5C). This distribution is further confirmed by Western blot on purified cytoplasmic and mitochondrial protein fractions (Fig. 5D). In agreement with published data (Brien et al., 2009; Duriez et al., 2000), our experiments indicate that Bcl2-A1 is in equilibrium between the cytoplasmic and mitochondrial fractions although mainly anchored to the mitochondrial membrane and that the deletion α9 helix moves this equilibrium towards the soluble cytoplasmic fraction.

Bcl2-A1 inhibits pro-caspase-3 activation in vitro and in vivo

To further explore the functional relevance of Bcl2-A1/pro-caspase-3 interaction we used an *in vitro* approach, evaluating the effect of Bcl2-A1 on pro-caspase-3 processing in the presence of recombinant caspase-8. Incubation of recombinant caspase-8 and protein extracts containing caspase-3 leads the caspase-3 proteolitic processing that is readily detected by a specific antibody against the active form of caspase-3 (compare lanes 1 and 2 of Fig. 6A and relative quantification in Fig. 6B). Addition of Bcl2-A1, immunoprecipitated from transfected eukaryotic cells, to the reaction mixture inhibits pro-caspase-3 activation in a dose-dependent manner (Fig. 6A), suggesting a novel Bcl2-A1-dependent anti-apoptotic mechanism of action.

In order to investigate the anti-apoptotic contribution of helix α9 against $SOD1^{G28A}$ induced toxicity, we co-transfected NSC-34 motoneuronal cells with Flag-pro-caspase-3 in the presence of WT or mutant Bcl2-A1 and in presence or absence of $SOD1^{G93A}$. In agreement with our previous results, Bcl2-A1 is protective against $SOD1^{G93A}$ induced toxicity, as indicated by the impairment of Flag-caspase-3 decrease (compare lanes 5 and 6 in Fig. 6C and relative quantification in Fig. 6D). This anti-apoptotic effect relies both on presence of helix α9 and helix α1-3 (Figs. 6C and D). The loss of anti-apoptotic activity of Δα1-3 is not surprising since although this protein binds more tightly to pro-caspase-3 (Fig. 5B), the missing domains are also involved *in vivo* in the maintenance of the pro-apoptotic protein Bax in an inactive state (Simmons et al., 2008). Finally we show that caspase-3 cleavage parallels with an increase in its activity by analyzing PARP cleavage (Fig. 6E) and by counting apoptotic nuclei (Fig. 6F).

Discussion

This study demonstrates that mutant SOD1 induces the expression of Bcl2-A1, which plays an important role in the modulation of caspase-3 activity, in a cell-specific manner via AP1 transcription factor. Bcl2-A1 is a member of the Bcl2 family, the key regulators of the mitochondria-dependent apoptotic pathway and of outer mitochondrial membrane integrity (Chipuk et al.,

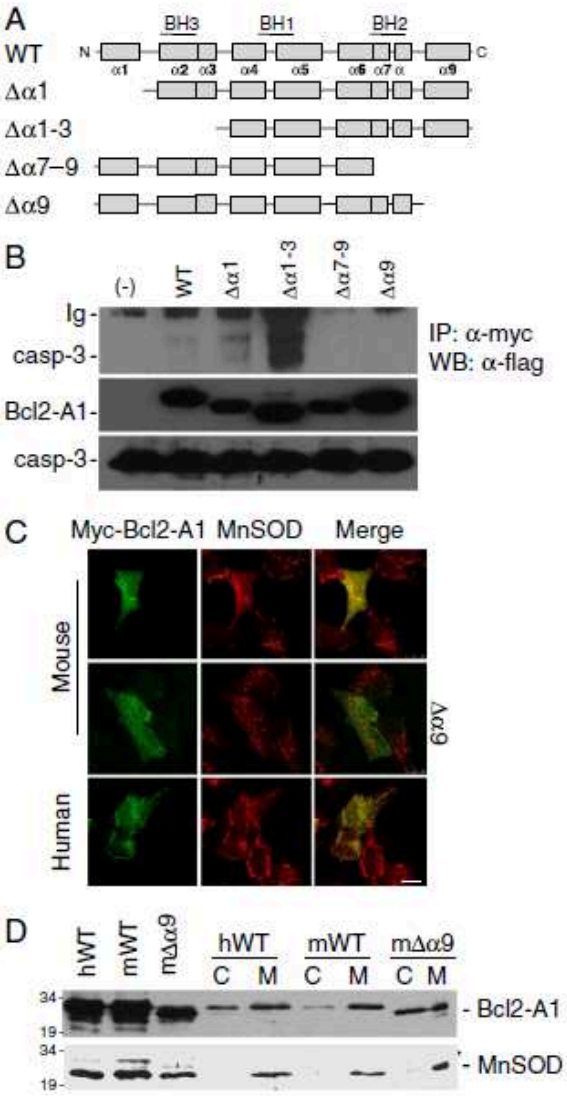

Fig. 5. Bcl2-A1 interacts with pro-caspase-3 via helices α9. A: Schematic representation of Bcl2-A1 deletion mutants. B: Co-immunoprecipitation was performed as described in Fig. 4B. C: Confocal microscopy analysis of NSC-34 cells transfected with human or mouse Bcl2-A1 or mouse Bcl2A1-Δα9. Antibodies against MnSOD were used for mitochondria staining. The yellow color shows the co-localization of the indicated Bcl2-A1 protein variant with mitochondria. D: Cytosolic (C) or mitochondrial (M) protein extracts were prepared from transiently transfected HEK293 as in panel C. The presence of Bcl2-A1 protein was assessed by Western blot on 20 μg of protein samples using anti-myc antibody. MnSOD is a marker of mitochondrial fractions.

Maria Elena Mura
Molecular mechanisms involved in Amyotrophic Lateral Sclerosis:
role of Bcl2-A1 and TDP-43 genes in motor neuron degeneration
Tesi di dottorato in Scienze Biomolecolari e Biotecnologiche
Università degli studi di Sassari

2010). Different lines of evidence link Bcl2-A1 overexpression to ALS, indicating that injured motor neurons may counteract damage by overexpressing an anti-apoptotic protein such as Bcl2-A1 (Crosio et al., 2006; Pun et al., 2006).

Bcl2-A1 over-expression in ALS mice model is limited to spinal cord and it is directly linked to mutant SOD1 expression (Figs. 1 and 2), with a pattern that mirrors the tissue specificity of the disease. Although Bcl2-A1 is mainly expressed in lymphocytes, the present study indicates that constitutive mutant SOD1 over-expression does not modify either the expression level or the relative isoform abundance in this cell type. Moreover, in immortalized motoneurons Bcl2-A1 is transcriptionally regulated by the redox sensitive transcription factor AP1, most likely contributing to lineage- and stimulus-dependent cell specificity of Bcl2-A1 transcription. In fact, it was previously demonstrated that Bcl2-A1 is transcriptionally regulated by NFκB in lymphocytes through B- or T-cell receptor activation (Grumont et al., 1999; Zong et al., 1999), by NFAT in mast cells activated through FcεRI crosslinking (Ulleras et al., 2008) and by PU.1 during neutrophil differentiation (Jenal et al., 2010). The AP1 binding site, already characterized in the human Bcl2-A1 promoter, was demonstrated to be relevant for the assembly of an enhanceosome-like complex in PMA ionomycin-treated Jurkat T cells (Edelstein et al., 2003). The involvement of AP1 in motor neuron degeneration in ALS is

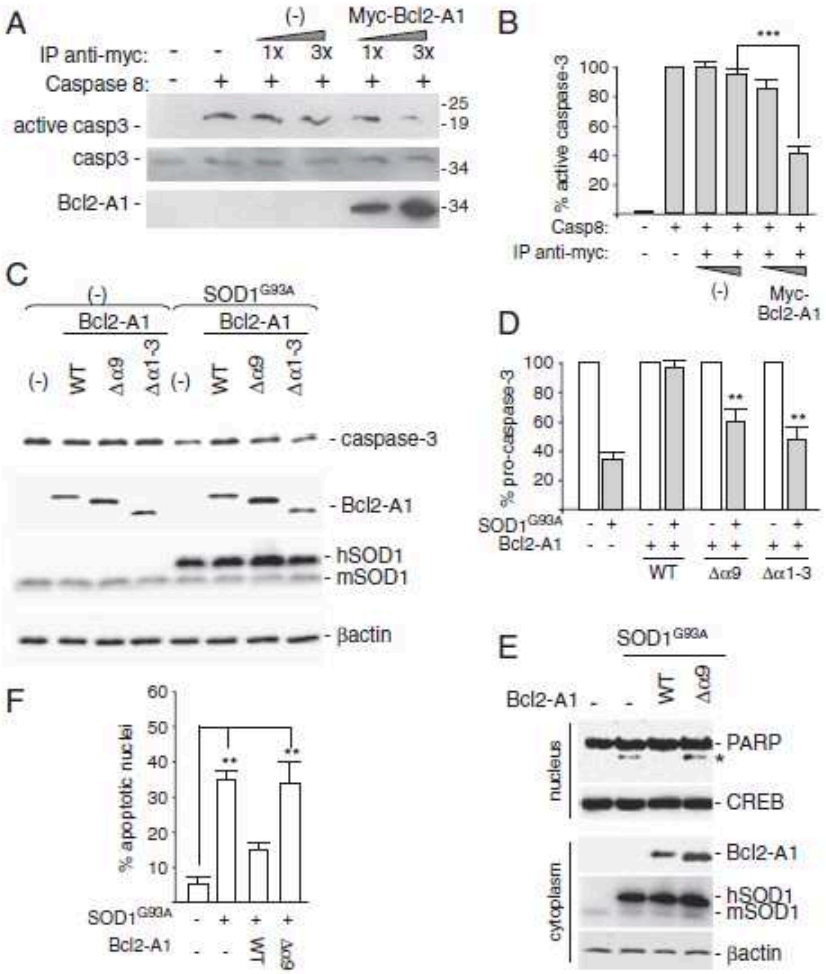

Fig. 6. Effect of Bcl2-A1 binding on pro-caspase-3 maturation *in vitro* and *in vivo*. A: Bcl2-A1 impairs *in vitro* pro-caspase-3 activation by caspase-8. Aliquots of 2 μg of cell extracts from HEK293 transfected with Flag-pro-caspase-3 were incubated with increasing concentrations of immunoprecipitates with anti-myc antibody from HEK293 either transfected with Myc-Bcl2-A1 or untransfected, in presence or absence of recombinant caspase-8. Note that immunoprecipitated Myc-Bcl2-A1 is in the nmolar range. The caspase-3 activation was analyzed by Western blot with a specific antibody that recognizes only the active form. Antibodies against Flag and Myc were used as control for total caspase-3 and Bcl2-A1 presence. B: Quantification of the experiments in (A) by densitometric assay. Results obtained from samples containing only caspase-8 were defined as 100%. Results are expressed as the mean ± SEM of three independent experiments. *** = $p<0.001$. C: Deletion of α9 helix of Bcl2-A1 impairs its anti-apoptotic properties. Flag-pro-caspase-3 and the indicated Bcl2-A1 constructs were transfected in NSC-34 cells in a ratio 1:5, in absence (−) or presence of $SOD1^{G93A}$. 48 h after transfection cell lysates were subjected to SDS–PAGE and analyzed by Western blot with the indicated antibodies. D: Quantification of the experiments in (C) by densitometric assay. Results obtained from sample not transfected with $SOD1^{G93A}$ were defined as 100%. Results are expressed as the means ± SEM of three independent experiments. ** = $p<0.01$. E: Evaluation of PARP activation in absence (−) or presence of $SOD1^{G93A}$. Deletion of α9 helix of Bcl2-A1 results in PARP activation, compared to WT Bcl2-A1, in the presence of $SOD1^{G93A}$. 48 h after transfection in NSC-34, cell lysates were subjected to SDS–PAGE and analyzed by Western blot with the indicated antibodies. * indicates cleaved PARP. F: Cells as in E were stained with Hoechst 33342 to assess cell death. Quantitative analysis of apoptotic nuclei is shown as mean ± SEM of n = 3 independent experiments.

not surprising considering that different proteins belonging to the c-Fos, c-Jun and ATF families are activated in this disease: (i) ATF3 and phospho-c-Jun have been detected in spinal cord and brainstem neurons in $SOD1^{G93A}$ mice, and they can be considered effective markers to identify motor neurons in an early phase of their degeneration (Vlug et al., 2005; Jaarsma et al., 1996); (ii) CSF from ALS patients seems to stimulate Fos expression in certain populations of spinal neurons via the NMDA receptors (Manabe et al., 1999); (iii) c-Jun activation has been identified in post-mortem ALS spinal cord specimens (Virgo and de Belleroche, 1995).

Interestingly, using a GST-pull down approach combined to mass spectrometry we were able to identify pro-caspase 3 as a binding partner for Bcl2-A1. This interaction is highly specific both *in vivo* and *in vitro* and it depends on Bcl2-A1 helix α9 (Figs. 5 and 6). This amphipathic carboxy-terminal helix was shown to regulate the localization and the pro-survival function of both murine (Smits et al., 2008) and human (Brien et al., 2009) Bd2-A1. Molecular modeling of Bd2-A1 indicates that helix α9 may adopt two distinct conformational states. In one of these states, helix α9 is located in the hydrophobic binding groove and gives rise to a compact molecule: in this conformation helix α9 may play a regulatory role by limiting the access to the hydrophobic BH3-binding cleft. In a second conformation, the molecule is more extended, with helix α9 protruding from the globular core of the protein and therefore potentially mediating interactions with membranes and pro-apoptotic proteins such as Bak (Brien et al., 2009; Smits et al., 2008). According to this model, we have shown that both murine and human Bcl2-A1 are partially localized in mitochondria via helix α9 (Fig. 5), although the anchorage is not fully dependent on this region. In fact, deletion of helix α9 increases the percentage cytoplasmatic Bcl2-A1, but does not fully prevent binding to mitochondria, indicating that Bcl2-A1 subcellular localization relies on multiple factors.

Bcl2-A1 seems to be a highly versatile protein, displaying different biological effects according to the cellular models and toxic insult. Wild-type Bcl2-A1 shows anti-apoptotic effects in many different experimental systems, including haematopoietic, tumor and neuronal cell lines, independently from the toxic stimulus and from the fusion partner (Brien et al., 2009; Crosio et al., 2006; D'Sa-Eipper and Chinnadurai, 1998; Ko et al., 2007; Kucharczak et al., 2005; Simmons et al., 2008). Deletion of the C-terminal domain corresponding to helix α9, on the contrary, seems to have a dual effect increasing (Kucharczak et al., 2005) or decreasing/impairing (Herold et al., 2006; Ko et al., 2007; Simmons et al., 2008) Bd2-A1 anti-apoptotic activity according to cell type and stimulus. This contradictory experimental data can be explained considering that Bcl2-A1 can be regulated at multiple levels: (i) at transcriptional level; as described above, Bd2-A1 is regulated by many different transcription factors (NFκB, NFTA, AP1, PU.1) enabling different cell types to quickly respond to apoptotic insults (Edelstein et al., 2003; Jenal et al., 2010; Kim et al., 2004; Ulleras et al., 2008; Wang et al., 1999; Zong et al., 1999); (ii) post-transcriptionally, via alternative splicing to produce in human cells a shorter form (Ko et al., 2003); (iii) post-translationally by ubiquitin mediated proteasomal degradation in human haematopoietic cells and tumors (Fan et al., 2010; Herold et al., 2006; Kucharczak et al., 2005); (iv) via interaction with multidomain and BH3-only pro-apoptotic proteins (Chen et al., 2005; Herman et al., 2008; Simmons et al., 2008; Smits et al., 2008; Werner et al., 2002).

Here we also provide evidence of a new anti-apoptotic Bd2-A1 mechanism of action. Bcl2-A1 can physically interact *in vitro* and *in vivo*, via helix α9, with pro-caspase-3, preventing its activation. To our knowledge, Bcl2-A1 is the only protein inhibitor of caspase-3 able to bind the zymogen precursor and to prevent its caspase-8 mediated activation, since both viral (serpin CrmA and p35) and cellular (IAP, inhibitor of apoptosis protein) inhibitors bind the activated form of this caspase (Fuentes-Prior and Salvesen, 2004). For instance XIAP (X-linked inhibitor of apoptosis protein) is able to bind and inhibit the activated form of caspase-3 while not impairing the caspase-8 mediated activation (Deveraux et al., 1997).

On the whole, our results contribute to the knowledge of molecular mechanisms of action and functional role of Bd2-A1 that have important implications in ALS, where prevention of motor neuronal cell death is one of the major therapeutic aims.

Acknowledgments

This work was supported by "Fondazione Banco di Sardegna" and PRIN 2008 (Grant no 20083R593R_002) to C.C. and by Ministero della Salute to M.T.C.

We wish to thank Manuela Galioto for invaluable technical support and Cristiana Valle, Alberto Ferri and Mauro Cozzolino for constant support and critical reading of the manuscript.

References

Boillee, S., et al., 2006. ALS: a disease of motor neurons and their nonneuronal neighbors. Neuron 52, 39–59.
Brien, G., et al., 2009. C-terminal residues regulate localization and function of the antiapoptotic protein Bfl-1. J. Biol. Chem. 284, 30257–30263.
Carri, M.T., et al., 2006. Targets in ALS: designing multidrug therapies. Trends Pharmacol. Sci. 27, 267–273.
Cartharius, K., et al., 2005. MatInspector and beyond: promoter analysis based on transcription factor binding sites. Bioinformatics 21, 2933–2942.
Chen, L., et al., 2005. Differential targeting of prosurvival Bcl-2 proteins by their BH3-only ligands allows complementary apoptotic function. Mol. Cell 17, 393–403.
Chipuk, J.E., et al., 2010. The BCL-2 family reunion. Mol. Cell 37, 299–310.
Crosio, C., et al., 2006. Bcl2a1 serves as a switch in death of motor neurons in amyotrophic lateral sclerosis. Cell Death Differ. 13, 2150–2153.
Deveraux, Q.L., et al., 1997. X-linked IAP is a direct inhibitor of cell-death proteases. Nature 388, 300–304.
D'Sa-Eipper, C., Chinnadurai, G., 1998. Functional dissection of Bfl-1, a Bcl-2 homolog: anti-apoptosis, oncogene-cooperation and cell proliferation activities. Oncogene 16, 3105–3114.
Durham, H.D., et al., 1993. Evaluation of the spinal cord neuron X neuroblastoma hybrid cell line NSC-34 as a model for neurotoxicity testing. Neurotoxicology 14, 387–395.
Duriez, P.J., et al., 2000. A1 functions at the mitochondria to delay endothelial apoptosis in response to tumor necrosis factor. J. Biol. Chem. 275, 18099–18107.
Edelstein, L.C., et al., 2003. NF-kappa B-dependent assembly of an enhanceosome-like complex on the promoter region of apoptosis inhibitor Bfl-1/A1. Mol. Cell. Biol. 23, 2749–2761.
Fan, G., et al., 2010. Defective ubiquitin-mediated degradation of antiapoptotic Bfl-1 predisposes to lymphoma. Blood 115, 3559–3569.
Ferri, A., et al., 2006. Familial ALS-superoxide dismutases associate with mitochondria and shift their redox potentials. Proc. Natl. Acad. Sci. U. S. A. 103, 13860–13865.
Fuentes-Prior, P., Salvesen, G.S., 2004. The protein structures that shape caspase activity, specificity, activation and inhibition. Biochem. J. 384, 201–232.
Grumont, R.J., et al., 1999. Rel-dependent induction of A1 transcription is required to protect B cells from antigen receptor ligation-induced apoptosis. Genes Dev. 13, 400–411.
Hatakeyama, S., et al., 1998. Multiple gene duplication and expression of mouse bcl-2-related genes, A1. Int. Immunol. 10, 631–637.
Herman, M.D., et al., 2008. Completing the family portrait of the anti-apoptotic Bcl-2 proteins: crystal structure of human Bfl-1 in complex with Bim. FEBS Lett. 582, 3590–3594.
Herold, M.J., et al., 2006. The stability and anti-apoptotic function of A1 are controlled by its C terminus. J. Biol. Chem. 281, 13663–13671.
Jaarsma, D., et al., 1996. Induction of c-Jun immunoreactivity in spinal cord and brainstem neurons in a transgenic mouse model for amyotrophic lateral sclerosis. Neurosci. Lett. 219, 179–182.
Jenal, M., et al., 2010. The anti-apoptotic gene BCL2A1 is a novel transcriptional target of PU.1. Leukemia 24, 1073–1076.
Kim, J.K., et al., 2004. Up-regulation of Bfl-1/A1 via NF-kappaB activation in cisplatin-resistant human bladder cancer cell line. Cancer Lett. 212, 61–70.
Ko, J.K., et al., 2003. Bfl-1S, a novel alternative splice variant of Bfl-1, localizes in the nucleus via its C-terminus and prevents cell death. Oncogene 22, 2457–2465.
Ko, J.K., et al., 2007. The tail-anchoring domain of Bfl1 and HCCS1 targets mitochondrial membrane permeability to induce apoptosis. J. Cell Sci. 120, 2912–2923.
Ko, J.K., et al., 2011. Amphipathic tail-anchoring peptide and Bcl-2 homology domain-3 (BH3) peptides from Bcl-2 family proteins induce apoptosis through different mechanisms. J. Biol. Chem. 286, 9038–9048.
Kucharczak, J.F., et al., 2005. Constitutive proteasome-mediated turnover of Bfl-1/A1 and its processing in response to TNF receptor activation in FL5.12 pro-B cells convert it into a prodeath factor. Cell Death Differ. 12, 1225–1239.
Lagier-Tourenne, C., et al., 2010. TDP-43 and FUS/TLS: emerging roles in RNA processing and neurodegeneration. Hum. Mol. Genet. 19, R46–R64.
Lepedda, A.J., et al., 2009. A proteomic approach to differentiate histologically classified stable and unstable plaques from human carotid arteries. Atherosclerosis 203, 112–118.
Mackenzie, I.R., et al., 2010. TDP-43 and FUS in amyotrophic lateral sclerosis and frontotemporal dementia. Lancet Neurol. 9, 995–1007.

Manabe, Y., et al., 1999. Enhanced Fos expression in rat lumbar spinal cord cultured with cerebrospinal fluid from patients with amyotrophic lateral sclerosis. Neurol. Res. 21, 309–312.
Pasinelli, P., Brown, R.H., 2006. Molecular biology of amyotrophic lateral sclerosis: insights from genetics. Nat. Rev. Neurosci. 7, 710–723.
Pun, S., et al., 2006. Selective vulnerability and pruning of phasic motoneuron axons in motoneuron disease alleviated by CNTF. Nat. Neurosci. 9, 408–419.
Rothstein, J.D., 2009. Current hypotheses for the underlying biology of amyotrophic lateral sclerosis. Ann. Neurol. 65 (Suppl 1), S3–S9.
Simmons, M.J., et al., 2008. Bfl-1/A1 functions, similar to Mcl-1, as a selective tBid and Bak antagonist. Oncogene 27, 1421–1428.
Smits, C., et al., 2008. Structural plasticity underpins promiscuous binding of the prosurvival protein A1. Structure 16, 818–829.
Ulleras, E., et al., 2008. NFAT but not NF-kappaB is critical for transcriptional induction of the prosurvival gene A1 after IgE receptor activation in mast cells. Blood 111, 3081–3089.
Virgo, L., de Belleroche, J., 1995. Induction of the immediate early gene c-jun in human spinal cord in amyotrophic lateral sclerosis with concomitant loss of NMDA receptor NR-1 and glycine transporter mRNA. Brain Res. 676, 196–204.
Vlug, A.S., et al., 2005. ATF3 expression precedes death of spinal motoneurons in amyotrophic lateral sclerosis-SOD1 transgenic mice and correlates with c-Jun phosphorylation, CHOP expression, somato-dendritic ubiquitination and Golgi fragmentation. Eur. J. Neurosci. 22, 1881–1894.
Wang, C.Y., et al., 1999. NF-kappaB induces expression of the Bcl-2 homologue A1/Bfl-1 to preferentially suppress chemotherapy-induced apoptosis. Mol. Cell. Biol. 19, 5923–5929.
Werner, A.B., et al., 2002. Bcl-2 family member Bfl-1/A1 sequesters truncated bid to inhibit is collaboration with pro-apoptotic Bak or Bax. J. Biol. Chem. 277, 22781–22788.
Zong, W.X., et al., 1999. The prosurvival Bcl-2 homolog Bfl-1/A1 is a direct transcriptional target of NF-kappaB that blocks TNFalpha-induced apoptosis. Genes Dev. 13, 382–387.

Theme 2: Biological effects of TDP-43 mutants in neuronal cells: implication for ALS

Accumulations of aggregated proteins are a key feature of the pathology of all of the major neurodegenerative diseases. Amyotrophic lateral sclerosis was brought into this fold quite recently with the discovery of TDP-43 (TAR DNA binding protein, 43 kDa) inclusions in nearly all ALS cases. The identification of TDP-43 mutations in rare familial forms of ALS confirmed that altered TDP-43 function can be a primary cause of the disease. However, the simple concept that TDP-43 is an aggregation-protein that forms toxic inclusions capable of promoting neurodegeneration has not been upheld by initial investigations. The aim of this work is the understanding of the relationship between TDP-43 aggregation and neurodegeneration, and in particular the relationship between aggregates and TDP-43 mutations. Preliminary results, obtained by biochemical purification and immunofluorescence, demonstrate that there is not a link between aggregates formation and mutants available in my laboratory, or that the formation of these aggregates does not depend exclusively by gene mutations.

1. Biochemical properties of TDP-43^{A382T} missense mutation

It has been demonstrated that purified TDP-43 synthesized in bacteria is highly prone to aggregation and rapidly falls out of solution over time, supporting that the protein is intrinsically aggregation prone (Johnson et al., 2009). The C-terminal region was required for this aggregation tendency, as a fragment of the N-terminus containing only the RNA recognition motif (RRM) domains remained soluble. TDP-43 was cleaved into C-terminal fragments in the disease state, and became phosphorylated. Electron microscopy showed that purified full-length TDP-43 or C-terminal fragments formed amorphous aggregates and did not have properties of amyloid. This is akin to the properties of inclusions in ALS patient tissues, which likewise appear amorphous and non-amyloid. A second study of purified protein supported that the C-terminus of TDP-43 is critical for aggregation, and found that one particularly aggregation-prone subregion could also form amyloid fibrils (Chen et al., 2010). Finally, TDP-43 point mutations linked to ALS increased the propensity of purified TDP-43 to aggregate, supporting that increased tendency to aggregate may be an important property of ALS

associated TDP-43 mutations (Johnson et al., 2009). As reported in the Introduction the TDP-43^{A382T} missense mutation accounts for approximately one-third of all ALS cases in the Sardinian population (Orrù et al., 2011; Chiò et al., 2010). To gain some information about the physiopathological mechanisms of this ALS caused by TDP43 mutation, I cloned TDP-43 gene in a wild type form, isolated from SH-SY5Y RNA by RT-PCR, into pCS2-MTK and then mutagenized to obtain pCS2-MTK-TDP-43^{Q331K}, -TDP-43^{M337V}, -TDP-43^{A382T}, in fusion with myc epitopes.

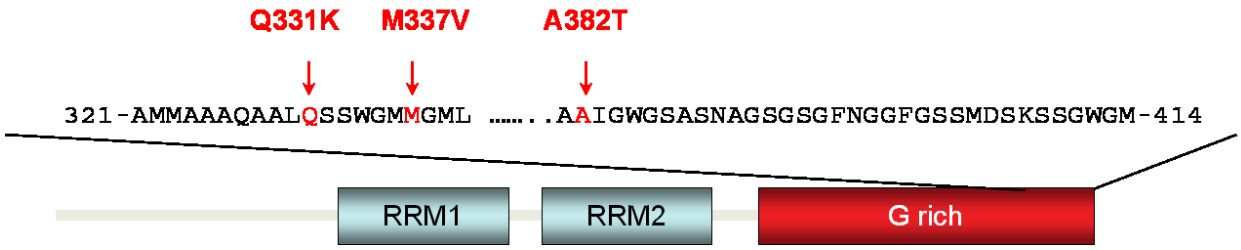

Fig. 1 Schematic diagram of the TARDBP gene with three of five functional domains : RRM1 and RRM2, the two RNA recognition motifs, a glycine-rich C-terminal region with three mutations (Q331K, M337V, A382T).

In order to investigate the subcellular distribution of TDP-43^{A382T} I perform an immunofluorescence analysis on SH-SY5Y transfected cells. Figure 2 shows that wild type TDP-43 is was largely restricted to the nucleus. In some cells, however, TDP43^{A382T} was distributed throughout the cytoplasm and the nucleus, with a distribution overlapping with the one described for the others TDP-43 mutants (Barmada et al., 2010).

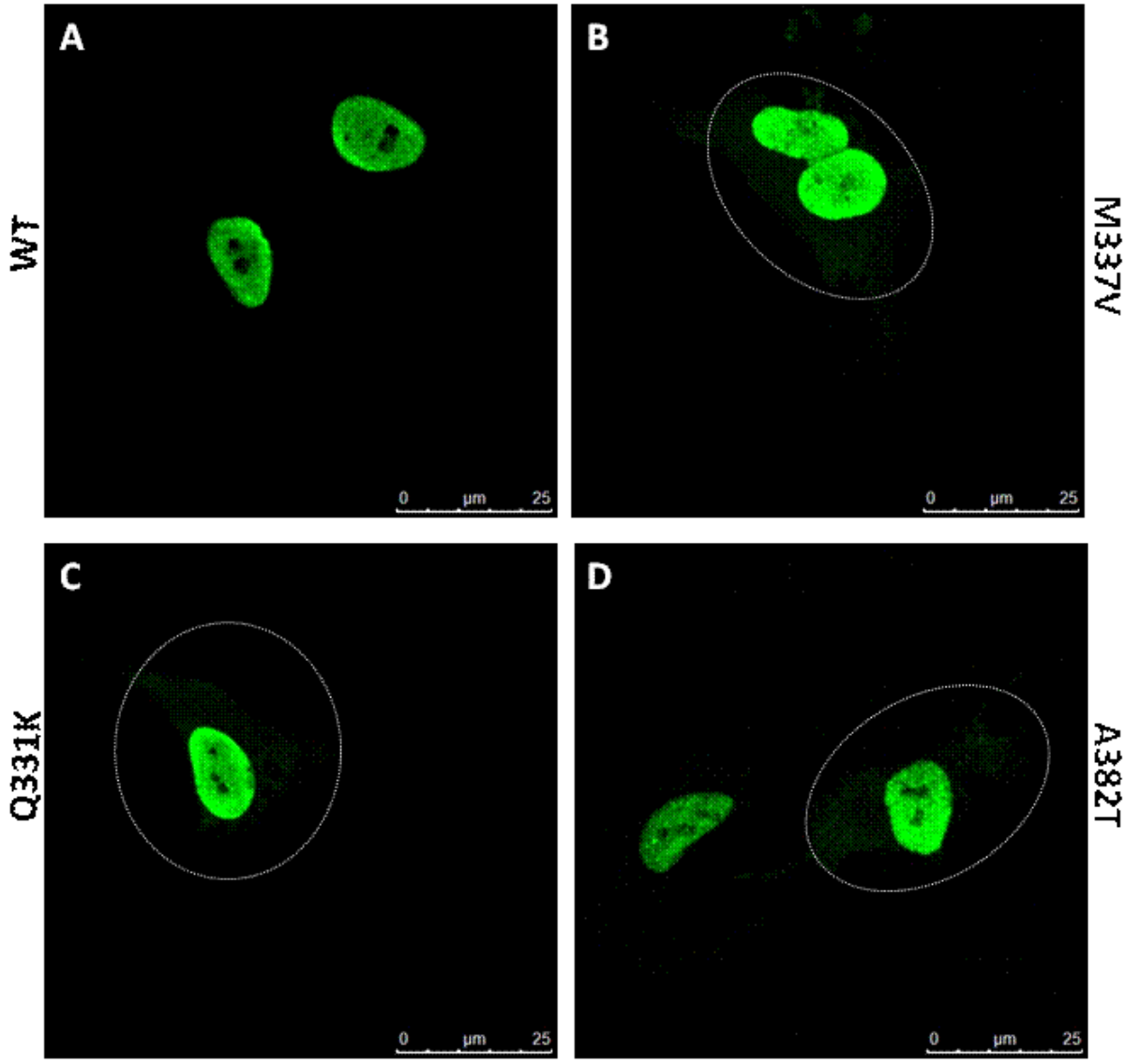

Fig. 2. Confocal microscopy analysis of SH-SY5Y cells transfected with (A) human TDP-43 wild type or (B) human TDP-43^{Q331K}, (C) TDP-43^{M337V}, (D) TDP-43^{A382T}.The immunofluorescence was performed after 48 h of transient transfection. Antibody anti-myc was used to show the localization of the TDP-43 protein. Inside the white circles is showed the partial cytoplasmic redistribution of mutant TDP-43 (Fig. 2B,C,D) compared to the wild type protein (Fig. 2A).

The effect of the A382T mutation on protein localization was also evaluated by subcellular fractionation (Fig. 3), showing that cells expressing TDP43^{A382T} displayed approximately as much cytoplasmic protein as those expressing TDP43^{WT}, TDP43^{Q331K}, TDP43^{M337V}.

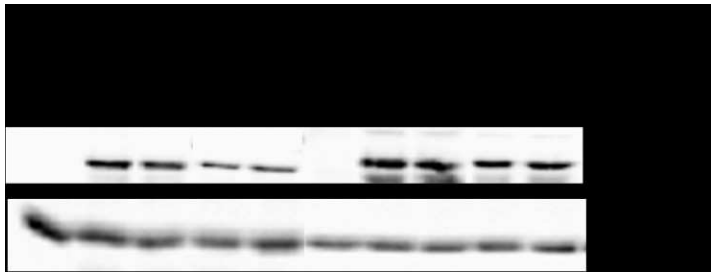

Fig. 3. Cytosolic and nuclear protein extracts were prepared after 48 h of transient transfection of SH-SY5Y. The presence of TDP-43 protein was assessed by Western blot using anti-myc antibody. is a marker of mitochondrial fractions. β-actina was used as a control of protein concentration

I further extend my analysis, by testing the aggregation properties of A382T mutant, using a biochemical approach. SH-SY5Y cells were transfected, with the indicated plasmid, and the extracted proteins were separated according to their solubility. As shown in figure 4 I did not observe any difference between TDP-43^{WT} and all the three mutants analysed.

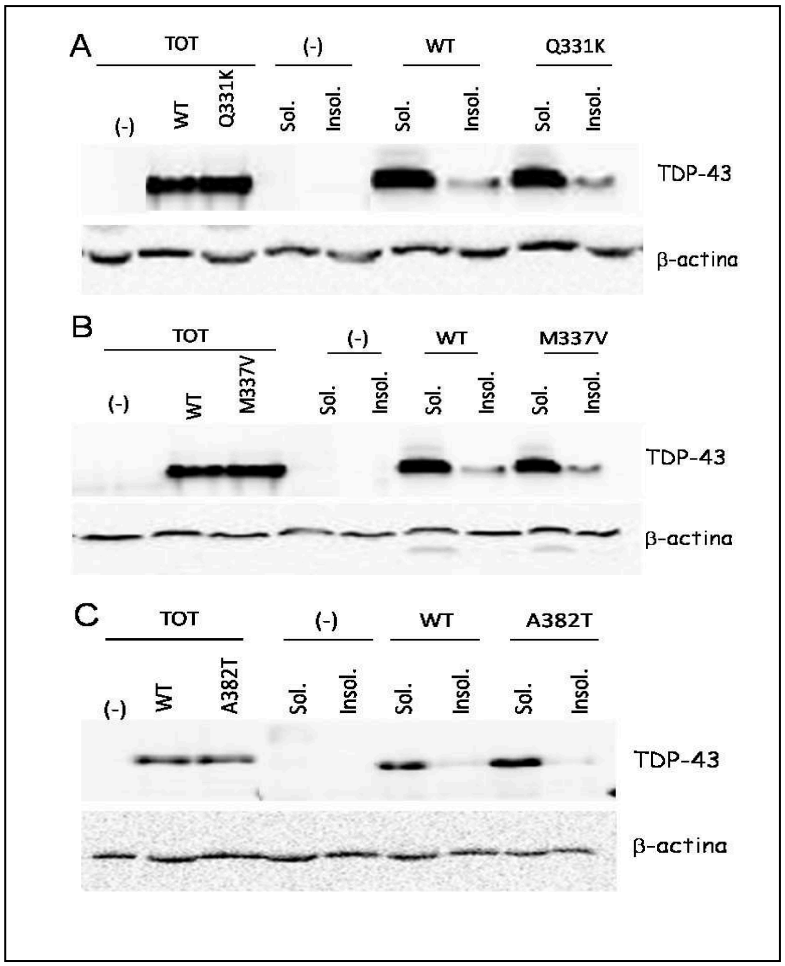

Fig. 4. Total (TOT), Soluble (Sol.) and insoluble (Insol.) protein extracts were prepared after 72 h of transient transfection of SH-SY5Y cells. The presence of Bcl2-A1 protein was assessed by Western blot using anti-myc antibody. β-actina was used as a control of protein concentration.

Lanes 6 and 7, 8 and 9 of every Western blot (Fig. 3A,B,C) show that the protein signal is very strong in the soluble fraction of wild type and mutant TDP-43, compared to the respective insoluble fraction, to indicate that there is not misaccumulation of the protein in the insoluble fraction of the wild type protein and in the mutant proteins neither.
This kind of experiments were performed also in immortalized motor neuron cells (NSC-34) and the results were comparable to results obtained in SH-SY5Y cells (data not shown).

Discussion

Within a few years since the discovery of TDP-43 inclusions in ALS, our knowledge has expanded rapidly. I have learned that TDP-43 aggregation is observed in a diverse set of neurodegenerative and myodegenerative diseases, not just ALS. Furthermore the importance of the C-terminal domain, the location of the majority of the ALS-associated mutations, for promoting self-aggregation in addition to mediating protein–protein interactions has come to light. Recent studies have pointed to the possibility that TDP-43 inclusion pathology may reflect an exaggeration of normal accumulation of TDP-43 into cytoplasmic granules. Finally, while detergent-insoluble inclusions were the key feature leading to the connection between TDP-43 and neurodegeneration, existing animal models clearly demonstrate that TDP-43 toxicity (at least in the context of overexpression) can occur without the formation of TDP-43 inclusions. While somewhat disconcerting, the same ambiguous relationship between inclusion formation and neurodegeneration is familiar to many other fields. In Alzheimer's disease models, increased amyloid-β production promotes amyloid plaque formation and synaptic dysfunction, but not neurodegeneration (Ashe et al., 2010). By contrast, in polyglutamine diseases (including spinocerebellar ataxias and Huntington's disease) toxicity and neurodegeneration do not require inclusion formation, analogous to what is observed in TDP-43 model systems (Klement et al., 1998; Saudou et al., 1998)

Many studies analyze the link between mutations and TDP-43 aggregation, in the same way I have started to study this phenomenon, in particular in this study, the role of three new TARDBP mutations (Q331K, M337V and A382T) was investigated using SH-SY5Y cell line. The data validate that these mutations determine a partial redistribution of the protein, compared to the wild type protein, but in neuroblastoma cell line and in immortalized motor neuron cells (NSC-34) the expression of mutant TDP-43 did not induce toxicity and aggregation was not observed. The molecular mechanism through which mutant TDP-43 leads motor neurons to the disease is still not understood and a better understanding of the molecular partners of TDP-43 as well as its function in motor neurons is required. Therefore, it appears that we are just at the beginning of our understanding of the relationship between TDP-43 aggregation, inclusion formation and neurodegeneration. Though a challenging topic, an improved understanding of this

relationship will be necessary as I consider ways to modulate TDP-43 aggregation for potential therapeutic benefit in ALS.

References

Adams J.M., Cory S. The bcl-2 protein family: arbiters of cell survival. Science 281: 1322-6 (1998).

Adlam M. and Siu G. Immunity, Volume 18, Issue 2: 173-184 (2003).

Aggarwal S.P., et al.. Safety and efficacy of lithium in combination with riluzole for treatment of amyotrophic lateral sclerosis: a randomised, double-blind, placebo-controlled trial. Lancet Neurol 9: 481–88 (2010).

Al-Chalabi A., et al.. Recessive amyotrophic lateral sclerosis families with the D90A SOD1 mutation share a common founder: evidence for a linked protective factor. Hum Mol Genet.7(13): 2045-50 (1998).

Alexianu M.E., et al.. Immune reactivity in a mouse model of familial ALS correlates with disease progression. Neurology 57: 1282–9 (2001).

Al-Kateb H., et al.. Multiple Superoxide Dismutase 1/Splicing Factor Serine Alanine15 Variants Are Associated With the Development and Progression of Diabetic Nephropathy: The Diabetes Control and Complications Trial/Epidemiology of Diabetes Interventions and Complications Genetics Study. Diabetes 57(1): 218–228 (2008).

Allen S., et al.. Analysis of the Cytosolic Proteome in a Cell Culture Model of Familial Amyotrophic Lateral Sclerosis Reveals Alterations to the Proteasome, Antioxidant Defenses, and Nitric Oxide Synthetic Pathways. The Journal Of Biological Chemistry Vol. 278 No. 8: 6371–6383 (2003).

Andersen P.M. and Al-Chalabi A.. Clinical genetics of amyotrophic lateral sclerosis: what do we really know? Nat. Rev. Neurol. 7: 603–615 (2011).

Andersen P.M., et al.. Amyotrophic lateral sclerosis associated with homozygosity for an Asp90Ala mutation in Cu/Zn superoxide dismutase. Nat Genet. 10: 61-66 (1995).

Andersen P.M., et al.. Amyotrophic lateral sclerosis associated with mutations in the CuZn superoxide dismutase gene. Curr. Neurol. Neurosci. Rep. 6: 37–46 (2006).

Anderson P. and Kedersha N. RNA granules: post-transcriptional and epigenetic modulators of gene expression. Nat. Rev. Mol. Cell. Biol. 10: 430–436 (2009).

Andersson M.K., et al.. The multifunctional FUS, EWS and TAF15 proto-oncoproteins show cell type-specific expression patterns and involvement in cell spreading and stress response. BMC Cell. Biol. 9: 37 (2008).

Andersson S., et al.. Cloning, structure, and expression of the mitochondrial cytochrome P-450 sterol 26-hydroxylase, a bile acid biosynthetic enzyme. J. Biol. Chem. 264: 8222-8229 (1989).

Andreassen O.A., et al.. Partial deficiency of manganese superoxide dismutase exacerbates a transgenic mouse model of amyotrophic lateral sclerosis. Ann Neurol 47: 447–55 (2000).

Antonsson B., Martinou J.C.. The Bcl-2 protein family. Exp Cell Res 256: 50-7 (2000).

Arai T., et al.. TDP-43 is a component of ubiquitin-positive tau-negative inclusions in frontotemporal lobar degeneration and amyotrophic lateral sclerosis. Biochem. Biophys. Res. Commun. 351: 602–611 (2006).

Arnesano F., et al.. The Unusually Stable Quaternary Structure of Human Cu,Zn-Superoxide Dismutase 1 Is Controlled by Both Metal Occupancy and Disulfide Status. The Journal Of Biological Chemistry Vol. 279, No. 46: 47998–48003 (2004).

Ashe K.H. and Zahs K.R. Probing the biology of Alzheimer's disease in mice. Neuron 66: 631–645 (2010).

Ayala Y.M., et al.. Human, Drosophila, and C. elegans TDP43: nucleic acid binding properties and splicing regulatory function. J. Mol. Biol., 348, 575–588 (2005).

Ayala Y.M., et al.. TDP-43 regulates retinoblastoma protein phosphorylation through the repression of cyclin-dependent kinase 6 expression. Proc. Natl Acad. Sci. USA 105: 3785–3789 (2008).

Banci L., et al.. Fully Metallated S134N Cu,Zn-Superoxide Dismutase Displays Abnormal Mobility and Intermolecular Contacts in Solution. The journal of biological chemistry. Vol. 280 No. 43: 35821-35821 (2005).

Banci L., et al.. SOD1 and Amyotrophic Lateral Sclerosis: Mutations and Oligomerization. Plos one 3(2): 1677 (2008).

Banks G.T., et al.. TDP-43 is a culprit in human neurodegeneration, and not just an innocent bystander. Mamm. Genome 19: 299–305 (2008).

Banner S.J., et al.. The expression of the glutamate re-uptake transporter excitatory amino acid transporter 1 (EAAT1) in the normal human CNS and in motor neurone disease: an immunohistochemical study. Neuroscience 109(1): 27-44 (2002).

Baralle F.E. and Buratti E.. TDP-43: Overview of the series. FEBS Journal 278: 3529 (2011).

Barber S.C., et al.. Oxidative stress in ALS: A mechanism of neurodegeneration and a therapeutic target Biochimica et Biophysica Acta 1762: 1051–1067 (2006).

Barmada S.J., et al.. Cytoplasmic mislocalization of TDP-43 is toxic to neurons and enhanced by a mutation associated with familial amyotrophic lateral sclerosis. J. Neurosci. 30: 639–649 (2010).

Beckman J.S., et al.. ALS, SOD and peroxynitrite, Nature 364: 584 (1993).

Bendotti C. and Carrì M.T.. Lessons from models of SOD1-linked familial ALS. Trends in Molecular Medicine 8: 393-400 (2004).

Bendotti C., et al.. Transgenic SOD1 G93A mice develop reduced GLT-1 in spinal cord without alterations in cerebrospinal fluid glutamate levels. Journal of Neurochemistry 79: 737-746 (2001).

Bensimon G., et al.. A controlled trial of riluzole in amyotrophic lateral sclerosis. ALS/Riluzole Study Group. N Engl. J. Med 330: 585–591 (1994).

Beretta S., et al.. The sinister side of Italian soccer. THE LANCET Neurology Vol 2 (2003).

Bernadette H., et al.. Disruption of Dynein/Dynactin Inhibits Axonal Transport in Motor Neurons Causing Late-Onset Progressive Degeneration. Neuron Vol. 34: 715–727 (2002).

Biedler J.L., et al.. Multiple neurotransmitter synthesis by human neuroblastoma cell lines and clones. Cancer Res. 38: 3751-3757 (1978).

Boillee S., et al.. ALS: a disease of motor neurons and their nonneuronal neighbors. Neuron 52: 39–59 (2006).

Borner C, et al.. Dissection of functional domains in Bcl-2 alpha by site-directed mutagenesis. Biochem Cell Biol 72: 463-9 (1994).

Borthwick G.M., et al.. Mitochondrial enzyme activity in amyotrophic lateral sclerosis: implications for the role of mitochondria in neuronal cell death. Ann Neurol 46: 787–90 (1999).

Brien G., et al.. C-terminal Residues Regulate Localization and Function of the Antiapoptotic Protein Bfl-1. The Journal Of Biological Chemistry Vol. 284 No. 44: 30257–30263 (2009).

Brooks B.R., et al. Natural history of amyotrophic lateral sclerosis. Quantification of symptoms, signs, strength, and function. Adv Neurol 68:163–84 (1995).

Bruening W., et al.. Up-Regulation of Protein Chaperones Preserves Viability of Cells Expressing Toxic Cu/Zn-Superoxide Dismutase Mutants Associated with Amyotrophic Lateral Sclerosis. J. Neurochem. Vol. 72 No. 2 (1999).

Bruijn L.I., et al.. Aggregation and motor neuron toxicity of an ALS linked SOD1 mutant independent from wild-type SOD1. Science 281: 1851-1854 (1998).

Bruijn, L.I. et al.. Unraveling the mechanisms involved in motor neuron degeneration in ALS. Annu. Rev. Neurosci. 27, 723–749 (2004).

Buchan J.R. & Parker R. Eukaryotic stress granules: the ins and outs of translation. Mol Cell 36: 932–941 (2009).

Buratti E. and Baralle F.E. Multiple roles of TDP-43 in gene expression, splicing regulation, and human disease. Front Biosci. 13: 867–878 (2008).

Buratti E. and Baralle F.E.. The multiple roles of TDP-43 in pre-mRNA processing and gene expression regulation. RNA Biology 7:4: 420-429 (2010).

Buratti E., et al.. TDP-43 binds heterogeneous nuclear ribonucleoprotein A/B through its C-terminal tail: an important region for the inhibition of cystic fibrosis transmembrane conductance regulator exon 9 splicing. J. Biol. Chem. 280: 37572–37584 (2005).

Caccamo A., et al.. Rapamycin rescues TDP-43 mislocalization and the associated low molecular mass neurofilament instability. J. Biol. Chem. 284: 27416–27424 (2009).

Cai J., et al.. Mitochondrial control of apoptosis: the role of cytochrome c. Biochim Biophys Acta 1366: 139-49 (1998).

Cairns N.J., et al.. TDP-43 proteinopathy in familial motor neurone disease with TARDBP A315T mutation: a case report. Neuropathology and Applied Neurobiology 36: 673–679 (2010).

Carrì M.T., Cozzolino M.. SOD1 and mitochondria in ALS: a dangerous liaison. J Bioenerg Biomembr (2011).

Carrı M.T., et al.. Targets in ALS: designing multidrug Terapie. TRENDS in Pharmacological Sciences Vol. 27 No.5 (2006).

Carriedo S.G., et al.. AMPA exposures induce mitochondrial Ca(2+) overload and ROS generation in spinal motor neurons in vitro, J. Neurosci. 20: 240–250 (2000).

Carriedo S.G., et al.. Motor neurons are selectively vulnerable to AMPA/kainate receptor-mediated injury in vitro. J. Neurosci. 16, 4069–4079 (1996).

Cartharius K., et al... MatInspector and beyond: promoter analysis based on transcription factor binding sites. Bioinformatics 21 No. 13: 2933–2942 (2005).

Caughey B. and Lansbury P.T.. Protofibrils, pores, fibrils, and neurodegeneration: separating the responsible protein aggregates from the innocent bystanders. Annu. Rev. Neurosci. 26: 267–298 (2003).

Chang Y., et al.. Messenger RNA oxidation occurs early in disease pathogenesis and promotes motor neuron degeneration in ALS. PLoS ONE 3 (2008).

Chaudhury A., et al.. Heterogeneous nuclear ribonucleoproteins (hnRNPs) in cellular processes: focus on hnRNP E1's multifunctional regulatory roles. RNA 16: 1449–1462 (2010).

Chen A.K., et al.. Induction of amyloid fibrils by the C-terminal fragments of TDP-43 in amyotrophic lateral sclerosis. J Am Chem Soc 132, 1186–1187 (2010).

Chen C.Y., et al.. AU binding proteins recruit the exosome to degrade ARE-containing mRNAs. Cell 107: 451–464 (2001).

Chen H., et al.. Head injury and amyotrophic lateral sclerosis. Am J Epidemiol 166(7): 810-6 (2007).

Chen L., et al.. Differential Targeting of Prosurvival Bcl-2 Proteins by Their BH3-Only Ligands Allows Complementary Apoptotic Function. Molecular Cell Vol. 17: 393–403 (2005).

Chen Y.Z, et al.. DNA/RNA Helicase Gene Mutations in a Form of Juvenile Amyotrophic Lateral Sclerosis (ALS4). Am. J. Hum. Genet. 74: 1128–1135 (2004).

Chiba M. & Masironi R.. Toxic and trace elements in tobacco and tobacco smoke. Bulletin of the World Health Organization 70 (2): 269-275 (1992).

Chiò A., et al.. Large proportion of amyotrophic lateral sclerosis cases in Sardinia due to a single founder mutation of the TARDBP gene. Italian Amyotrophic Lateral Sclerosis Genetic (ITALSGEN) Consortium. Arch Neurol 68(5): 594-8 2011.

Chiò A., et al.. Severely increased risk of amyotrophic lateral sclerosis among Italian professional football players. Brain 128(Pt 3): 472-6 (2005).

Chipuk J.E., et al.. The BCL-2 family reunion. Mol. Cell 37: 299–310 (2010).

Chiu A.Y., et al.. Age-dependent penetrance of disease in a transgenic mouse model of familial amyotrophic lateral sclerosis. Mol. Cell. Neurosci. 6: 349-362 (1995).

Choi S.S., et al.. A novel Bcl-2 related gene, Bfl-1, is overexpressed in stomach cancer and preferentially expressed in bone marrow.Oncogene 11: 1693-1698 (1995).

Cleary M.L., et al.. Cloning and structural analysis of cDNAs for bcl-2 and a hybrid bcl-2/immunoglobulin transcript resulting from the t(14;18) translocation. Cell 47: 19-28 (1986).

Clement A.M., et al.. Wild-Type Non neuronal Cells Extend Survival of SOD1 Mutant Motor Neurons in ALS Mice. SCIENCE Vol. 302 (2003).

Colombrita C., et al.. TDP-43 is recruited to stress granules in conditions of oxidative insult. J. Neurochem. 111: 1051–1061 (2009).

Comi G.P., et al..Cytochrome c oxidase subunit I microdeletion in a patient with motor neuron disease. Ann Neurol 43: 110–16 (1998).

Corrado L., et al.. High Frequency of TARDBP Gene Mutations in Italian Patients With Amyotrophic Lateral Sclerosis. Human Mutation Vol. 30 No. 4: 688–694 (2009).

Cory S., et al.. Insights from Bcl-2 and Myc: malignancy involves abrogation of apoptosis as well as sustained proliferation. Cancer Res 59(suppl): 1685S-92S (1999).

Couillard-Despre´S S., et al.. Protective effect of neurofilament heavy gene overexpression in motor neuron disease induced by mutant superoxide dismutase. Neurobiology Vol. 95: 9626–9630(1998).

Cozzolino M., et al.. Apoptosome inactivation rescues proneural and neural cells from neurodegeneration. Cell Death Differ. 11(11): 1179-91 (2004).

Crosio C., et al.. Bcl2a1 serves as a switch in death of motor neurons in amyotrophic lateral sclerosis. Cell Death and Differentiation 13: 2150–2153 (2006).

Crow J.P., et al.. Decreased zinc affinity of amyotrophic lateral sclerosis-associated superoxide dismutase mutants leads to enhanced catalysis of tyrosine nitration by peroxynitrite. J. Neurochem. 69: 1936–1944 (1997).

Cruz D.C., et al.. Physical trauma and family history of neurodegenerative diseases in amyotrophic lateral sclerosis: a population-based case-control study. Neuroepidemiology 18(2): 101-10 (1999).

Cudkowicz M.E., et al.. Epidemiology of mutations in superoxide dismutase in amyotrophic in amyotrophic lateral sclerosis. Ann. Neurol. 41: 210–221 (1997).

Culotta V.C., et al.. Activation of superoxide dismutases: Putting the metal to the Pedal. Biochim Biophys Acta 1763(7): 747–758 (2006).

D'Sa-Eipper C., et al.. Bfl-1, a bcl-2 homologue, suppresses p53-induced apoptosis and exhibits potent cooperative transforming activity. Cancer Res.56: 3879–3882 (1996).

Da Cruz S. and Cleveland D.W. Understanding the role of TDP-43 and FUS/TLS in ALS and beyond. Current Opinion in Neurobiology 21: 1–16 (2011).

D'Ambrosi N., et al.. The proinflammatory action of microglial P2 receptors is enhanced in SOD1 models for amyotrophic lateral sclerosis. J Immunol. 183(7): 4648-56 (2009).

Daoud H., et al.. Contribution of TARDBP mutations to sporadic amyotrophic lateral sclerosis. J. Med. Genet. 46: 112–114 (2009).

Davidson Y., et al.. Ubiquitinated pathological lesions in frontotemporal lobar degeneration contain the TAR DNA-binding protein, TDP-43. Acta Neuropathol. 113: 521–533 (2007).

de Jong D., et al..Subcellular localization of the bcl-2 protein in malignant and normal lymphoid cells. Cancer Res 54: 256-60 (1994).

Deng H.X., et al.. Amyotrophic lateral sclerosis and structural defects in Cu,Zn superoxide dismutase. Science 261: 1047–1051 (1993).

Deveraux Q.L., et al.. X-linked IAP is a direct inhibitor of cell-death proteases. Nature 388: 300–304 (1997).

Dhaliwal G.K., Grewal R.P.. Mitochondrial DNA deletion mutation levels are elevated in ALS brains, NeuroReport 11 2507–2509 (2000).

Dickson D.W., et al.. TDP-43 in differential diagnosis of motor neuron disorders. Acta Neuropathol. 114: 71–79 (2007).

Dion P.A., et al.. Genetics of motor neuron disorders: new insights into pathogenic mechanisms. NATURe RevIewS Genetics Vol. 10: 769 (2009).

Doble A. The pharmacology and mechanism of action of riluzole. Neurology 47 (6 Suppl 4): S233–S241 (1996).

Dormann D., et al.. ALS-associated fused in sarcoma (FUS) mutations disrupt transportin-mediated nuclear import. EMBO J. 29: 2841–2857 (2010).

Dormann D., et al.. Proteolytic processing of TAR DNA binding protein-43 by caspases produces C-terminal fragments with disease defining properties independent of progranulin. J. Neurochem. 110: 1082–1094 (2009).

D'Sa-Eipper C. and Chinnadurai G.. Functional dissection of Bfl-1, a Bcl-2 homolog: anti-apoptosis, oncogene-cooperation and cell proliferation activities. Oncogene 16: 3105-3114 (1998).

D'Sa-Eipper C., et al.. Bfl-1, a bcl-2 homologue, suppresses p53-induced apoptosis and exhibits potent cooperative transforming activity. Cancer Res. 56(17): 3879-82 (1996).

Duan W., et al.. Mutant TAR DNA-binding protein 43 induces oxidative injury in motor neuron-like cell. Neuroscience 169, 1621–1629 (2010).

Durham H.D., et al.. Aggregation of mutant Cu/Zn superoxide dismutase proteins in a culture model of ALS. J Neuropathol Exp Neurol.: 56(5): 523-30 (1997).

Durham H.D., et al.. Evaluation of the spinal cord neuron X neuroblastoma hybrid cell line NSC-34 as a model for neurotoxicity testing. Neurotoxicology 14: 387–395 (1993).

Duriez P.J., et al.. A1 Functions at the Mitochondria to Delay Endothelial Apoptosis in Response to Tumor Necrosis Factor. The Journal Of Biological Chemistry Vol. 275 No. 24: 18099–18107 (2000).

Edelstein L.C., et al.. NF-kappa B-dependent assembly of an enhanceosome-like complex on the promoter region of apoptosis inhibitor Bfl-1/A1. Mol. Cell. Biol. 23: 2749–2761 (2003).

Elvira G., et al.. Characterization of an RNA granule from developing brain. Mol. Cell. Proteomics 5: 635–651 (2006).

Estevez A.G., et al.. Induction of Nitric Oxide-Dependent Apoptosis in Motor Neurons by Zinc-Deficient Superoxide Dismutase. Science Vol. 286 (1999).

Fan G., et al.. Defective ubiquitin-mediated degradation of antiapoptotic Bfl-1 predisposes to lymphoma. Blood 115(17): 3559–3569 (2010).

Ferraiuolo L., et al.. Microarray analysis of the cellular pathways involved in the adaptation to and progression of motor neuron injury in the SOD1 G93A mouse model of familial ALS. J. Neurosci. 27: 9201–9219 (2007).

Ferri A., et al.. Familial ALS-superoxide dismutases associate with mitochondria and shift their redox potentials. Proc. Natl. Acad. Sci. U. S. A. 103: 13860–13865 (2006).

Ferri A., et al.. Glutaredoxin 2 prevents aggregation of mutant SOD1 in mitochondria and abolishes its toxicity. Human Molecular Genetics Vol. 19 No. 22: 4529–4542 (2010).

Fields M.L., et al.. Fas/Fas ligand deficiency results in altered localization of anti–double-stranded DNA B cells and dendritic cells. J Immunol 167: 2370-8 (2001).

Fiesel F.C. & Kahle P.J. TDP-43 and FUS/TLS: cellular functions and implications for neurodegeneration. FEBS J 278: 3550–3568 (2011).

Fiesel F.C., et al.. Knockdown of transactive response DNA-binding protein (TDP-43) downregulates histone deacetylase 6. Embo J. 29: 209–221 (2010).

Figlewicz D.A., et al.. Variants of the heavy neurofilament subunit are associated with the development of amyotrophic lateral sclerosis. Hum Mol Genet 3: 1757–61 (1994).

Fikrig E., et al.. Protection of mice against the Lyme disease agent by immunizing with recombinant OspA. Science 250: 553 (1990).

Fray A.E., et al.. The expression of the glial glutamate transporter protein EAAT2 in motor neuron disease: an immunohistochemical study. Eur. J. Neurosci. 10: 2481±2489 (1998).

Freibaum B.D., et al.. Global analysis of TDP-43 interacting proteins reveals strong association with RNA splicing and translation machinery. J. Proteome Res. 9: 1104–1120 (2010).

Freibaum B.D., et al.. Global analysis of TDP-43 interacting proteins reveals strong association with RNA splicing and translation machinery. J Proteome Res 9: 1104–1120 (2010).

Friedlander R.M., et al.. Inhibition of ICE slows ALS in mice. Nature 388(6637): 31 (1997).

Fuentes-Prior P.and Salvesen G. S.. The protein structures that shape caspase activity, specificity, activation and inhibition. Biochem. J. 384: 201–232 (2004).

Ge W.W, et al.. Neuronal tissue-specific ribonucleoprotein complex formation on SOD1 mRNA: Alterations by ALS SOD1 mutations. Neurobiology of Disease 23: 342–350 (2006).

Geser F., et al.. Evidence of multisystem disorder in whole-brain map of pathological TDP-43 in amyotrophic lateral sclerosis. Arch. Neurol. 65: 636–641 (2008).

Ghadge G.D., et al.. Glutamate carboxypeptidase II inhibition protects motor neurons from death in familial amyotrophic lateral sclerosis models. PNAS Vol. 100 No. 16: 9554–9559 (2003).

Ghadge G.D., et al.. Truncated wild-type SOD1 and FALS-linked mutant SOD1 cause neural cell death in the chick embryo spinal cord. Neurobiol. Dis. 21: 194–205 (2006).

Giordana M.T., et al.. TDP-43 redistribution is an early event in sporadic amyotrophic lateral sclerosis. Brain Pathol. 20, 351–360 (2010).

Gitcho M.A., et al.. TARDBP 3′-UTR variant in autopsy-confirmed frontotemporal lobar degeneration with TDP-43 proteinopathy. Acta Neuropathol. 118: 633–645 (2009).

Goldberg G.S., Lau A.F.. Transfection of mammalian cells with PEG-purified plasmid DNA. Biotechniques 14:548-550 (1993).

Gonzalez-Scarano F., Baltuch G.. Microglia as mediators of inflammatory and degenerative diseases. Annu Rev Neurosci 22: 219–40 (1999).

Graham F.L. et al.. Characteristics of a human cell line transformed by DNA from human adenovirus type 5. J. Gen Virol 36(1): 59-74 (1977).

Green D.G., Beere H.M.. Killers or clean-up crew. How central are the central mechanisms of apoptosis. Humana Press: 157-74 (1999).

Greenlund L.J., et al.. Role of BCL-2 in the survival and function of developing and mature sympathetic neurons. Neuron. 15(3): 649-61 (1995).

Greenway M.J., et al.. ANG mutations segregate with familial and ‘sporadic’ amyotrophic lateral sclerosis. Nat. Genet. 38: 411–3 (2006).

Gregory R.I., et al.. The Microprocessor complex mediates the genesis of microRNAs. Nature 432: 235–240 (2004).

Gregory R.I., et al.. The microprocessor complex mediates the genesis of microRNAs. Nature 432: 235–240 (2004).

Groen E.J., et al.. FUS mutations in familial amyotrophic lateral sclerosis in the Netherlands. Arch. Neurol. 67: 224–230 (2010).

Gros-Louis F., et al.. Intracerebroventricular infusion of monoclonal antibody or its derived Fab fragment against misfolded forms of SOD1 mutant delays mortality in a mouse model of ALS. J Neurochem 113(5): 1188-99 (2010).

Grumont R.J., et al.. Rel-dependent induction of A1 transcription is required to protect B cells from antigen receptor ligation-induced apoptosis. Genes Dev. 13: 400–411 (1999).

Guegan C., et al.. Recruitment of the Mitochondrial-Dependent Apoptotic Pathway in Amyotrophic Lateral Sclerosis. The Journal of Neuroscience 21(17): 6569–6576 (2001).

Guégan C., Przedborski S.. Programmed cell death in amyotrophic lateral sclerosis. J Clin Invest.: 111(2): 153-61 (2003).

Gurmeet K., et al.. Mitochondrial DNA deletion mutation levels are elevated in ALS brains. NEUROREPORT Vol. 11 No. 11 (2000).

Gurney M.E., et al.. Motor neuron degeneration in mice that express a human Cu,Zn superoxide dismutase mutation. Science 264: 1772–1775 (1994).

Hafezparast M., et al.. Mutations in dynein link motor neuron degeneration to defects in retrograde transport. Science Vol. 300: 808–12 (2003).

Hand C.K. and Rouleau G.A.. Familial Amyotrophic Lateral Sclerosis. Muscle Nerve 25: 135–159 (2002).

Hand C.K., et al.. Compound heterozygous D90A and D96N SOD1 mutations in a recessive amyotrophic lateral sclerosis family. Ann. Neurol. 49: 267–271 (2001).

Hasegawa M., et al.. Phosphorylated TDP-43 in frontotemporal lobar degeneration and amyotrophic lateral sclerosis. Ann. Neurol. 64: 60–70 (2008).

Hatakeyama S., et al.. Multiple gene duplication and expression of mouse bcl-2-related genes, A1. International Immunology Vol. 10 No. 5: 631–637 (1998).

Hayward C., et al.. Homozygosity for Asn86Ser mutation in the CuZn-superoxide dismutase gene produces a severe clinical phenotype in a juvenile onset case of familial amyotrophic lateral sclerosis. Med Genet 35: 174-176 (1998).

Hengartner M., et al.. C. elegans gene ced-9 protects cells from programmed cell death. Nature (London): 356: 494-9 (1992).

Hensley K., et al.. Temporal patterns of cytokine and apoptosis-related gene expression in spinal cords of the G93A-SOD1 mouse model of amyotrophic lateral sclerosis. Journal of Neurochemistry 82: 365–374 (2002).

Herman M.D., et al.. Completing the family portrait of the anti-apoptotic Bcl-2 proteins: crystal structure of human Bfl-1 in complex with Bim. FEBS Lett. 582: 3590–3594 (2008).

Herold M.J., et al.. The Stability and Anti-apoptotic Function of A1 Are Controlled by Its C Terminus. The Journal Of Biological Chemistry Vol. 281 No. 19: 13663–13671 (2006).

Hewitt C., et al. Novel FUS/TLS mutations and pathology in familial and sporadic amyotrophic lateral sclerosis. Arch. Neurol. 67: 455–461 (2010).

Higgins C.M., et al.. Mutant Cu, Zn superoxide dismutase that causes motoneuron degeneration is present in mitochondria in the CNS. J. Neurosci. 22 RC215 (2002).

Highley J.R., et al.. TARDBP mutations, amyotrophic lateral sclerosis and alternative splicing in human fibroblasts. Brain Pathol. 20 (Suppl. 1): 32 (2010).

Houseley J., et al.. RNA-quality control by the exosome. Nat Rev Mol Cell Biol 7: 529–539 (2006).

Jung-Ha H., et al.. Expression of Bfl-1 in normal and tumor tissues: Bfl-1 overexpression in cancer is attributable to its preferential expression in infiltrating inflammatory cells. Hum Pathol. 29(7): 723-8 (1998).

Igaz L.M., et al.. Enrichment of C-terminal fragments in TAR DNA-binding protein-43 cytoplasmic inclusions in brain but not in spinal cord of frontotemporal lobar degeneration and amyotrophic lateral sclerosis. Am. J. Pathol 173: 182–194 (2008).

Igaz L.M., et al.. Expression of TDP-43 C-terminal fragments in vitro recapitulates pathological features of TDP-43 proteinopathies. J. Biol. Chem. 284: 8516–8524 (2009).

Iko Y., et al. Domain architectures and characterization of an RNA-binding protein, TLS. J Biol Chem 279: 44834–44840 (2004).

Inukai Y., et al.. Abnormal phosphorylation of Ser409/410 of TDP-43 in FTLD-U and ALS. FEBS Lett. 582: 2899–2904 (2008).

Ito D., et al.. Nuclear transport impairment of amyotrophic lateral sclerosis-linked mutations in FUS/TLS. Ann. Neurol. 69: 152–162 (2010).

Iwai K., et al.. Anticipation in familial amyotrophic lateral sclerosis with SOD1-G93S mutation. J. Neurol. Neurosurg. Psychiatry 72: 819–820 (2002).

Jaarsma D., et al.. CuZn superoxide dismutase (SOD1) accumulates in vacuolated mitochondria in transgenic mice expressing amyotrophic lateral sclerosis-linked SOD1 mutations. Acta Neuropathol 102: 293–305 (2001).

Jaarsma D., et al.. Induction of c-Jun immunoreactivity in spinal cord and brainstem neurons in a transgenic mouse model for amyotrophic lateral sclerosis. Neurosci. Lett. 219: 179–182 (1996).

Jabri E.. P-bodies take a RISC. Nat Struct Mol Biol 12: 564 (2005).

Jenal M., et al.. The anti-apoptotic gene BCL2A1 is a novel transcriptional target of PU.1. Leukemia 24: 1073–1076 (2010).

Johnson B.S., et al.. TDP-43 is intrinsically aggregationprone, and amyotrophic lateral sclerosis-linked mutations accelerate aggregation and increase toxicity. J Biol Chem 284: 20329–20339 (2009).

Johnson F.O., Atchison W.D.. The role of environmental mercury, lead and pesticide exposure in development of amyotrophic lateral sclerosis. Neurotoxicology 30(5): 761-5 (2009).

Johnson K. S., et al.. Vaccination against ovine cysticercosis using a defined recombinant antigen. Nature 338: 585 (1989).

Johnston J.A., et al.. Formation of high molecular weight complexes of mutant Cu,Zn-superoxide dismutase in a mouse model for familial amyotrophic lateral sclerosis. PNAS vol. 97 no. 23: 12571–12576 (2000).

Julien J.P.. ALS: astrocytes move in as deadly neighbors. NATURE NEUROSCIENCE Vol. 10 No. 5 (2007).

Kabashi E., et al.. Gain and loss of function of ALS-related mutations of TARDBP (TDP-43) cause motor deficits in vivo. Human Molecular Genetics Vol. 19 No. 4: 671–683 (2010).

Kabashi E., et al.. TARDBP mutations in individuals with sporadic and familial amyotrophic lateral sclerosis. NATURE GENETICS Vol. 40 No. 5 (2008).

Kamel F., et al.. Lead exposure and amyotrophic lateral sclerosis. Epidemiology. 13(3):311-9 (2002).

Karsan A, et al.. Cloning of human Bcl-2 homologue: inflammatory cytokines induce human A1 in cultured endothelial cells. Blood 87(8):3089-96 (1996).

Karsan A., et al.. Endothelial cell death induced by tumor necrosis factor-alpha is inhibited by the Bcl-2 family member, A1. J Biol Chem.: 271(44): 27201-4 (1996).

Kaufmann P., et al.. Phase II trial of CoQ10 for ALS finds insufficient evidence to justify Phase III. Ann Neurol 66(2): 235–244 (2009).

Kawahara Y., et al.. Glutamate receptors: RNA editing and death of motor neurons. Nature 427: 801 (2004).

Kawamata T., et al.. Immunologic reactions in amyotrophic lateral sclerosis brain and spinal cord tissue. Am J Pathol Vol. 140 No. 3: 691–707 (1992).

Kelekar A., Thompson C.B.. Bcl-2 family proteins: the role of the BH3 domain in apoptosis. Trends Cell Biol 8: 324-30 (1998).

Kieran D., et al.. Control of motoneuron survival by angiogenin. J. Neurosci. 28: 14056–14061 (2008).

Kiernan M.C, et al.. Amyotrophic lateral sclerosis. Lancet 377: 942–55 (2011).

Kim J.K., et al.. Up-regulation of Bfl-1/A1 via NF-kappaB activation in cisplatinresistant human bladder cancer cell line. Cancer Lett. 212: 61–70 (2004).

Kim S.H., et al.. Potentiation of amyotrophic lateralmsclerosis (ALS)-associated TDP-43 aggregation by the proteasome-targeting factor, ubiquilin 1. J. Biol. Chem. 284: 8083–8092 (2009).

Kirby J., et al. Mutant SOD1 alters the motor neuronal transcriptome: implications for familial ALS. Brain 128: 1686–1706 (2005).

Klement I.A., et al.. Ataxin-1 nuclear localization and aggregation: role in polyglutamine-induced disease in SCA1 transgenic mice. Cell 95: 41–53 (1998).

Ko J.K., et al.. Amphipathic tail-anchoring peptide and Bcl-2 homology domain-3 (BH3) peptides from Bcl-2 family proteins induce apoptosis through different mechanisms. J. Biol. Chem. 286: 9038–9048 (2011).

Ko J.K., et al.. Bfl-1S, a novel alternative splice variant of Bfl-1, localizes in the nucleus via its C-terminus and prevents cell death. Oncogene 22: 2457–2465 (2003).

Ko J.K., et al.. Conversion of Bfl-1, an anti-apoptotic Bcl-2 family protein, to a potent pro-apoptotic protein by fusion with green fluorescent protein (GFP). FEBS Lett. 551: 29–36 (2003).

Ko J.K., et al.. The tail-anchoring domain of Bfl1 and HCCS1 targets mitochondrial membrane permeability to induce apoptosis. J. Cell Sci. 120, 2912–2923 (2007).

Korsmeyer S.J.. Bcl-2 gene family and the regulation of programmed cell death. Cancer Res 59(suppl): 1693S-700S (1999).

Kostic V., et al.. Midbrain dopaminergic neuronal degeneration in a transgenic mouse model of familial amyotrophic lateral sclerosis. Ann Neurol.: 41(4): 497-504 (1997).

Kruman I.I., et al.. ALS-Linked Cu/Zn–SOD Mutation Increases Vulnerability of Motor Neurons to Excitotoxicity by a Mechanism Involving Increased Oxidative Stress and Perturbed Calcium Homeostasis. Experimental Neurology 160: 28–39 (1999).

Kucharczak J.F., et al.. Constitutive proteasome-mediated turnover of Bfl-1/A1 and its processing in response to TNF receptor activation in FL5.12 pro-B cells convert it into a prodeath factor. Cell Death Differ. 12: 1225–1239 (2005).

Kuo P.H., et al.. Structural insights into TDP-43 in nucleic-acid binding and domain interactions. Nucleic Acids Res. 37: 1799–1808 (2009).

Kwiatkowski T.J. Jr., et al.. Mutations in the FUS/TLS Gene on Chromosome 16 Cause Familial Amyotrophic Lateral Sclerosis. SCIENCE VOL 323 (2009).

Lacomblez L., et al.: A confirmatory dose-ranging study of riluzole in ALS. ALS/Riluzole Study Group-II. Neurology 47: S242–50 (1996).

Lagier-Tourenne C., et al.. TDP-43 and FUS/TLS: emerging roles in RNA processing and neurodegeneration. Human Molecular Genetics Vol. 19 Review Issue 1: R46–R64 (2010).

Lagier-Tourenne C.and Cleveland D.W.. Rethinking ALS: the FUS about TDP-43. Cell 136(6): 1001–1004 (2009).

LaMonte BH, et al.. Disruption of dynein/dynactin inhibits axonal transport in motor neurons causing late-onset progressive degeneration. Neuron 34: 715–27 (2002).

Lariviere R.C., et al.. Peripherin is not a contributing factor to motor neuron disease in a mouse model of amyotrophic lateral sclerosis caused by mutant superoxide dismutase. Neurobiol Dis 13: 158–66 (2003).

Law W.J., et al.. TLS, EWS and TAF15: a model for transcriptional integration of gene expression. Brief Funct. Genomic. Proteomic. 5: 8–14 (2006).

Lee M.K., et al.. A mutant neurofilament subunit causes massive, selective motor neuron death: implications for the pathogenesis of human motor neuron disease. Neuron 13: 975–88 (1994).

Lepedda A.J., et al.. A proteomic approach to differentiate histologically classified stable and unstable plaques fromhuman carotid arteries. Atherosclerosis 203: 112–118 (2009).

Levine B. and Kroemer G.. Autophagy in the pathogenesis of disease. Cell 132: 27–42 (2008).

Li H., et al.. Cleavage of BID by caspase 8 mediates the mitochondrial damage in the Fas pathway of apoptosis. Cell 94: 491-501 (1998).

Li H.Y., et al.. Hyperphosphorylation as a Defense Mechanism to Reduce TDP-43 Aggregation. PLoS ONE Vol. 6 (2011).

Li S., et al.. Angiogenin inhibits nuclear translocation of apoptosis inducing factor in a Bcl-2-dependent manner. J. Cell Physiol. (2011).

Li Y., et al.. A Drosophila model for TDP-43 proteinopathy. Proc. Natl Acad. Sci. USA 107: 3169–3174 (2010).

Li Y.Y., et al.. Myocardial extracellular matrix remodeling in transgenic mice overexpressing tumor necrosis factor alpha can be modulated by anti-tumor necrosis factor alpha therapy. Proc Natl Acad Sci U S A.: 97(23): 12746-51 (2000).

Licatalosi D.D., et al.. HITS-CLIP yields genome-wide insights into brain alternative RNA processing. Nature 456: 464–469 (2008).

Lin C.L., et al.. Aberrant RNA processing in a neurodegenerative disease: the cause for absent EAAT2, a glutamate transporter, in amyotrophic lateral sclerosis. Neuron 20: 589–602 (1998).

Lino M.M, et al.. Accumulation of SOD1 Mutants in Postnatal Motoneurons Does Not Cause Motoneuron Pathology or Motoneuron Disease. The Journal of Neuroscience 22 (12): 4825–4832 (2002).

Liu J., et al.. Toxicity of familial ALS-Linked SOD1 mutants from selective recruitment to spinal mitochondria, Neuron 43: 5–17 (2004).

Liu R. et al.. Increased mitochondrial antioxidative activity or decreased oxygen free radical propagation prevent mutant SOD1- mediated motor neuron cell death and increase amyotrophic lateral sclerosis-like transgenic mouse survival. J. Neurochem. 80: 488–500 (2002).

Liu X., et al.. MicroRNAs: biogenesis and molecular functions. Brain Pathol 18: 113–121 (2008).

Longstreth W.T., et al.. Risk of amyotrophic lateral sclerosis and history of physical activity: a population-based case-control study. Arch Neurol 55(2): 201-6 (1998).

Los M., et al.. Caspases: more than just killers? Trends Immunol 22: 31-4 (2001).

Loschi M., et al.. Dynein and kinesin regulate stress-granule and P-body dynamics. J Cell Sci 122: 3973–3982 (2009).

Luquin N., et al.. Genetic variants in the promoter of TARDBP in sporadic amyotrophic lateral sclerosis. Neuromuscul. Disord. 19: 696–700 (2009).

Lyons T.J., et al.. Metal Ions Biol. Syst. 36: 125–177 (1999).

Macfarlane L.A. & Murphy P.R.. MicroRNA: biogenesis, function and role in cancer. Curr Genomics 11: 537–561 (2010).

Mackenzie I.R., et al.. TDP-43 and FUS in amyotrophic lateral sclerosis and frontotemporal dementia. Lancet Neurol. 9: 995–1007 (2010).

Manabe Y., et al.. Enhanced Fos expression in rat lumbar spinal cord cultured with cerebrospinal fluid from patients with amyotrophic lateral sclerosis. Neurol. Res. 21: 309–312 (1999).

Matsumoto A.O. and Fridovich I.. Subcellular Distribution of Superoxide Dismutases (SOD) in Rat Liver. Vol. 276 No. 42: 38388–38393 (2001).

Mattiazzi M., et al.. Mutated Human SOD1 Causes Dysfunction of Oxidative Phosphorylation in Mitochondria of Transgenic Mice. The Journal Of Biological Chemistry Vol. 277 No. 33: 29626–29633 (2002).

McDonnell J.M., et al.. Solution structure of the pro-apoptotic molecule Bid: A structural basis for apoptotic agonists and antagonists. Cell 96:625-34 (1999).

McGuire V., et al.. Occupational exposures and amyotrophic lateral sclerosis. A population-based case-control study. Am J Epidemiol 145(12): 1076-88 (1997).

Mello C.C. & Conte D. Jr.. Revealing the world of RNA interference. NATURE Vol. 431 (2004).

Michael D., et al.. “True” Sporadic ALS Associated with a Novel SOD-1 Mutation. Ann Neurol 52: 680–683 (2002).

Miller R.G., et al.: Riluzole for amyotrophic lateral sclerosis (ALS)/motor neuron disease (MND). Cochrane Database Syst Rev: CD001447 (2007).

Moisse K., et al.. Divergent patterns of cytosolic TDP-43 and neuronal progranulin expression following axotomy: implications for TDP-43 in the physiological response to neuronal injury. Brain Res. 1249: 202–211 (2009).

Monaghan P., et al.. Ultrastructural localization of bcl-2 protein. J Histochem Cytochem 40: 1819-25 (1992).

Mori F., et al.. Maturation process of TDP-43-positive neuronal cytoplasmic inclusions in amyotrophic lateral sclerosis with and without dementia. Acta Neuropathol. 116: 193–203 (2008).

Mukherjee D., et al.. The mammalian exosome mediates the efficient degradation of mRNAs that contain AU-rich elements. EMBO J 21: 165–174 (2002).

Nagai M., et al.. Rats Expressing Human Cytosolic Copper–Zinc Superoxide Dismutase Transgenes with Amyotrophic Lateral Sclerosis: Associated Mutations Develop Motor Neuron Disease. The Journal of Neuroscience 21(23): 9246–9254 (2001).

Naganska E., Matyja E.. Amyotrophic lateral sclerosis – looking for pathogenesis and effective therapy. Folia Neuropathol 49 (1): 1-13 (2011).

Nelson P.T., et al.. MicroRNAs (miRNAs) in neurodegenerative diseases. Brain Pathol 18: 130–138 (2008).

Neumann M., et al.. Ubiquitinated TDP-43 in frontotemporal lobar degeneration and amyotrophic lateral sclerosis. Science 314: 130–133 (2006).

Newbery H.J., and Abbott C.M.. Of mice, men and motor neurons. TRENDS in Molecular Medicine Vol.8 No.2 (2002).

Nirmalananthana N., and Greensmith L.. Amyotrophic lateral sclerosis: recent advances and future terapie. Current Opinion in Neurology 18: 712–719 (2005).

Nishimoto Y., et al.. Characterization of alternative isoforms and inclusion body of the TAR DNA-binding protein-43. J. Biol. Chem. 285: 608–619 (2010).

Nishimura A.L., et al.. A Mutation in the Vesicle-Trafficking Protein VAPB Causes Late-Onset Spinal Muscular Atrophy and Amyotrophic Lateral Sclerosis. Am. J. Hum. Genet. 75: 822–831 (2004).

Nonaka T., et al.. Truncation and pathogenic mutations facilitate the formation of intracellular aggregates of TDP-43. Hum. Mol. Genet. 18: 3353–3364 (2009).

Oltvai Z.N., et al.. Bcl-2 heterodimerizes in vivo with a conserved homologue, Bax, that accelerates programmed cell death. Cell 74: 609-19 (1993).

Orom U.A., et al.. MicroRNA-10a binds the 5'UTR of ribosomal protein mRNAs and enhances their translation. Mol Cell 30: 460–471 (2008).

Orrù S, et al.. High frequency of the TARDBP p.Ala382Thr mutation in Sardinian patients with amyotrophic lateral sclerosis. Clin Genet: 1399-0004 (2011).

Ou S.H., et al.. Cloning and characterization of a novel cellular protein, TDP-43, that binds to human immunodeficiency virus type 1 TAR DNA sequence motifs. J. Virol. 69: 3584–3596 (1995).

Pamphlett R., et al.. TDP-43 neuropathology is similar in sporadic amyotrophic lateral sclerosis with or without TDP-43 mutations. Neuropathol. Appl. Neurobiol.,35: 222–225 (2009).

Pardo C.A., et al.. Superoxide dismutase is an abundant component in cell bodies, dendrites, and axons of motor neurons and in a subset of other neurons. Neurobiology Vol. 92: 954-958 (1995).

Park S.K., et al.. A strong promoter activity of pre-B cell stage-specific Crlz1 gene is caused by one distal LEF-1 and multiple proximal Ets sites. Molecules and Cells Volume 32 Number 1: 67-76, 2011

Parker R. & Sheth U. P bodies and the control of mRNA translation and degradation. Mol Cell 25: 635–646 (2007).

Parkes T.L., et al. Extension of Drosophila lifespan by overexpression of human SOD1 in motorneurons. Nat Genet.: 19(2): 171-4 (1998).

Parton M.J., et al.. Mediated Amyotrophic Lateral Sclerosis: A Single Founder for All Cases With Evidence for a Cis-acting Disease Modifier in the Recessive Haplotype. Human Mutation (2002).

Pasinelli P., Brown R.H.. Molecular biology of amyotrophic lateral sclerosis: insights from genetics. Nat. Rev. Neurosci. 7: 710–723 (2006).

Pasinelli P., et al. Caspase-1 and -3 are sequentially activated in motor neuron death in Cu,Zn superoxide dismutase-mediated familial amyotrophic lateral sclerosis. Proc Natl Acad Sci U S A.: 97(25): 13901-6 (2000).

Pasinelli P., et al.. Amyotrophic Lateral Sclerosis-Associated SOD1 Mutant Proteins Bind and Aggregate with Bcl-2 in Spinal Cord Mitochondria. Neuron Vol. 43: 19–30 (2004).

Pasinelli P., et al.. Caspase-1 is activated in neural cells and tissue with amyotrophic lateral sclerosis-associated mutations in copper-zinc superoxide dismutase. Proc. Natl. Acad. Sci. U.S.A. 95: 15763–15768 (1998).

Passini M.A., et al.. CNS-targeted gene therapy improves survival and motor function in a mouse model of spinal muscular atrophy. The Journal of Clinical Investigation Vol. 120 (2010).

Pedrini S., et al.. ALS-linked mutant SOD1 damages mitochondria by promoting conformational changes in Bcl-2. Hum Mol Genet 19(15): 2974-86 (2010).

Pellegrini M., Strasser A.. A portrait of the Bcl-2 protein family: life, death, and the whole picture. J Clin Immunol 19: 365-77 (1999).

Pesaresi M.G, et al.. Mitochondrial redox signalling by p66Shc mediates ALS-like disease through Rac1 inactivation. Human Molecular Genetics: 1–13 (2011).

Piepers S., et al.. Randomized Sequential Trial of Valproic Acid in Amyotrophic Lateral Sclerosis. Ann Neurol 66: 227–234 (2009).

Pillai R.S.. MicroRNA function: multiple mechanisms for a tiny RNA? RNA 11: 1753–1761 (2005).

Polumenidou M., et al.. Long pre-mRNA depletion and RNA missplicing contribute to neuronal vulnerability from loss of TDP-43. Nat. Neurosci. 14: 459–468 (2011).

Potter S.Z. and Valentine J.S.. The perplexing role of copper-zinc superoxide dismutase in amyotrophic lateral sclerosis (Lou Gehrig's disease). J Biol Inorg Chem 8: 373–380 (2003).

Pramatarova A., et al.. Neuron-Specific Expression of Mutant Superoxide Dismutase 1 in Transgenic Mice Does Not Lead to Motor Impairment. The Journal of Neuroscience 21(10): 3369–3374 (2001).

Puls I., et al.. Mutant dynactin in motor neuron disease. Nature genetics Vol. 33 (2003).

Pun S., et al.. Selective vulnerability and pruning of phasic motoneuron axons in motoneuron disease alleviated by CNTF. Nat. Neurosci. 9: 408–419 (2006).

Rabin S.J., et al.. Sporadic ALS has compartment-specific aberrant exon splicing and altered cell-matrix adhesion biology. Hum. Mol. Genet. 19: 313–328 (2010).

Rabizadeh S., et al.. Mutations associated with amyotrophic lateral sclerosis convert superoxide dismutase from an antiapoptotic gene to a proapoptotic gene: studies in yeast and neural cells. Proc Natl Acad Sci U S A.: 92(7): 3024-8 (1995).

Reaume A.G., et al.. Motor neurons in Cu/Zn superoxide dismutasedeficient mice develop normally but exhibit enhanced cell death after axonal injury. Nat. Genet. 13: 43–47 (1996).

Restagno G., et al.. The IVS1 +319 t > a of SOD1 gene is not an ALS causing mutation. Amyotroph. Lateral Scler. Other Motor Neuron. Disord. 6: 45–49 (2005).

Robberecht W., et al.. D90A heterozygosity in the SOD1 gene is associated with familial and apparently sporadic amyotrophic lateral sclerosis. Neurology 47: 1336–1339 (1996).

Rosen D.R., et al.. Mutations in Cu/Zn superoxide dismutase gene are associated with familial amyotrophic lateral sclerosis. Nature 362 (6415): 59-62 (1993).

Rosenfeld J., et al.. Expression of Superoxide Dismutase Following Axotomy. Experimental neurology 147: 37–47 (1997).

Rosenfield J., et al.. Expression of superoxide dismutase following axotomy. Exp. Neurol. 147: 37-47 (1997).

Roth M.B., et al.. A conserved family of nuclear phosphoproteins localized to sites of polymerase II transcription. J. Cell Biol.115: 587-596 (1991).

Rothstein J.D., et al.. Chronic inhibition of superoxide dismutase produces apoptotic death of spinal neurons. Proc Natl Acad Sci U S A.: 91(10): 4155-9 (1994).

Rothstein J.D., et al.. Selective loss of glial glutamate transporter GLT-1 in amyotrophic lateral sclerosis. Ann. Neurol. 38: 73±84 (1995).

Rothstein J.D.. Current hypotheses for the underlying biology of amyotrophic lateral sclerosis. Ann. Neurol. 65 (Suppl 1): S3–S9 (2009).

Roy J., et al.. Glutamate Potentiates the Toxicity of Mutant Cu/Zn-Superoxide Dismutase in Motor Neurons by Postsynaptic Calcium-Dependent Mechanisms. The Journal of Neuroscience 18(23): 9673–9684 (1998).

Rutherford N.J., et al.. Novel Mutations in TARDBP (TDP-43) in Patients with Familial Amyotrophic Lateral Sclerosis. PLoS Genetics (2008).

Sambrook J., et al. Molecular Cloning, A Laboratory Manual, Cold Spring Harbor Press, Cold Spring Harbor, NY Hierarchical Interactions Control CD4 Gene Expression during Thymocyte Development (1989).

Samir K.S. Progranulin and TDP-43: Mechanistic Links and Future Directions. J Mol Neurosci (2011).

Sato T., et al.. Axonal ligation induces transient redistribution of TDP-43 in brainstem motor neurons. Neuroscience 164: 1565–1578 (2009).

Saudou F., et al.. Huntingtin acts in the nucleus to induce apoptosis but death does not correlate with the formation of intranuclear inclusions. Cell 95: 55–66 (1998).

Savettieri G., et al.. A case-control study of amyotrophic lateral sclerosis. Neuroepidemiology 10(5-6): 242-5 (1991).

Schmidt S., et al.. Association of ALS with head injury, cigarette smoking and APOE genotypes. J Neurol Sci 291(1-2): 22-9 (2010).

Schultz D.R. and Harrington W.J.. Apoptosis: Programmed Cell Death at a Molecular Level. Seminars in Arthritis and Rheumatism Vol. 32 No. 6: 345-369 (2003).

Sekizawa T., et al.. Cerebrospinal fluid interleukin 6 in amyotrophic lateral sclerosis: immunological parameter and comparison with inflammatory and non-inflammatory central nervous system diseases. Journal of Neurological Sciences 154: 194–199 (1998).

Sephton C.F., et al.. Identification of neuronal RNA targets of TDP-43-containing ribonucleoprotein complexes. J Biol Chem 286: 1204–1215 (2011).

Sephton C.F., et al.. Identification of neuronal RNA targets of TDP-43-containing ribonucleoprotein complexes. J. Biol. Chem. 286: 1204–1215 (2011).

Shaw P.J.. Molecular and cellular pathways of neurodegeneration in motor neurone disease. J Neurol Neurosurg Psychiatry 76: 1046–1057 (2005).

Shaw P.J., et al.. CSF and plasma amino acid levels in motor neuron disease: elevation of CSF glutamate in a subset of patients. Neurodegeneration 4: 209–16 (1995).

Sheth U. & Parker R.. Decapping and decay of messenger RNA occur in cytoplasmic processing bodies. Science 300: 805–808 (2003).

Shi S.G., et al.. Identification of the mutation of SOD1 gene in a familial amyotrophic lateral sclerosis. Zhonghua Yi Xue Yi Chuan Xue Za Zhi 21: 149–152 (2004).

Shibata N.. Transgenic mouse model for familial amyotrophic lateral sclerosis with superoxide dismutase-1 mutation. Neuropathology 21(1): 82-92 (2001).

Siklos L., et al.. Ultrastructural evidence for altered calcium in motor nerve terminals in amyotropic lateral sclerosis, Ann. Neurol. 39: 203–216 (1996).

Simmons M.J., et al.. Bfl-1/A1 functions, similar to Mcl-1, as a selective tBid and Bak antagonist. Oncogene 27: 1421–1428 (2008).

Singh R. & Valcarcel J.. Building specificity with nonspecific RNA-binding proteins. Nat Struct Mol Biol 12: 645–653 (2005).

Sjalander A., et al.. The D90A mutation results in a polymorphism of Cu,Zn superoxide dismutase that is prevalent in northern Sweden and Finland. Hum. Mol. Genet. 4: 1105–1108 (1995).

Smits C., et al.. Structural plasticity underpins promiscuous binding of the prosurvival protein A1. Structure 16: 818–829 (2008).

Spalloni A., et al.. Cu/Zn-superoxide dismutase (GLY93→ALA) mutation alters AMPA receptor subunit expression and function and potentiates kainite-mediated toxicity in motor neurons in culture. Neurobiology of Disease 15: 340–350 (2004).

Spreux-Varoquaux O., et al.. Glutamate levels in cerebrospinal fluid in amyotrophic lateral sclerosis: a reappraisal using a new HPLC method with coulometric detection in a large cohort of patients. Journal of the Neurological Sciences 193: 73–78 (2002).

Sreedharan, J., et al. TDP-43 mutations in familial and sporadic amyotrophic lateral sclerosis. Science 319: 1668–1672 (2008).

Strong M.J., Volkening K.. TDP-43 and FUS/TLS: sending a complex message about messenger RNA in amyotrophic lateral sclerosis? FEBS J. 278(19): 3569-77 (2011).

Strong, M.J., et al.. TDP43 is a human low molecular weight neurofilament (hNFL) mRNA-binding protein. Mol. Cell. Neurosci. 35: 320–327 (2007).

Susin S.A., et al.. Bcl-2 inhibits the mitochondrial release of an apoptogenic protease. J Exp Med 184: 1331-41 (1996).

Takeuchi H., et al.. Hsp70 and Hsp40 improve neurite outgrowth and suppress intracytoplasmic aggregate formation in cultured neuronal cells expressing mutant SOD1. Brain Research 949: 11–22 (2002).

Takeuchi H., et al.. Mitochondrial Localization of Mutant Superoxide Dismutase 1 Triggers Caspase-dependent Cell Death in a Cellular Model of Familial Amyotrophic Lateral Sclerosis. The journal of biological chemistry Vol. 277 No. 52: 50966–50972 (2002).

Tatom J.B., et al.. Mimicking aspects of frontotemporal lobar degeneration and Lou Gehrig's disease in rats via TDP-43 overexpression. Mol. Ther. 17: 607–613 (2009).

Thomsen D.R., et al.. Promoter-regulatory region of the major immediate early gene of human cytomegalovirus. Proc. Natl. Acad. Sci. USA 81: 659-663 (1984).

Ticozzi N., et al.. Genetics of familial amyotrophic lateral sclerosis. Archives Italiennes de Biologie 149: 65-82 (2011).

Tollervey J.R., et al.. Characterizing the RNA targets and position-dependent splicing regulation by TDP-43. Nat. Neurosci. 14, 452–458 (2011).

Tomkins J., et al.. Novel insertion in the KSP region of the neurofilament heavy gene in amyotrophic lateral sclerosis (ALS). Neuroreport 9: 3967–70 (1998).

Traub R., et al.. Rowland. Research Advances in Amyotrophic Lateral Sclerosis, 2009 to 2010. Curr Neurol Neurosci Rep 11: 67–77 (2011).

Turner B.J., Talbot K.. Transgenics, toxicity and therapeutics in rodent models of mutant SOD1-mediated familial ALS. Progress in Neurobiology 85: 94–134 (2008).

Udar N., et al.. SOD1: A Candidate Gene for Keratoconus. IOVS Vol. 47 No. 8 (2006).

Ulleras E., et al.. NFAT but not NF-kappaB is critical for transcriptional induction of the prosurvival gene A1 after IgE receptor activation in mast cells. Blood 111: 3081–3089 (2008).

Urushitani M., et al.. Therapeutic effects of immunization with mutant superoxide dismutase in mice models of amyotrophic lateral sclerosis. PNAS Vol. 104 No. 7: 2495–2500 (2007).

Valentine J.S. and Hart P.J.. Misfolded CuZnSOD and amyotrophic lateral sclerosis. PNAS Vol. 100 No. 7: 3617–3622 (2003).

Valentine J.S., et al.. Copper-Zinc Superoxide Dismutase and Amyotrophic Lateral Sclerosis. Annu Rev Biochem 74: 563–593 (2005).

Valentine J.S.. Do oxidatively modified proteins cause ALS?. Free Radical Biology & Medicine Vol. 33 No. 10: 1314–1320 (2002).

Van Deerlin V.M., et al. TARDBP mutations in amyotrophic lateral sclerosis with TDP-43 neuropathology: a genetic and histopathological analysis. Lancet Neurol. 7: 409–416 (2008).

Virgo L., de Belleroche J.. Induction of the immediate early gene c-jun in human spinal cord in amyotrophic lateral sclerosis with concomitant loss of NMDA receptor NR-1 and glycine transporter mRNA. Brain Res. 676: 196–204 (1995).

Vlug A.S., et al.. ATF3 expression precedes death of spinal motoneurons in amyotrophic lateral sclerosis-SOD1 transgenic mice and correlates with c-Jun phosphorylation, CHOP expression, somato-dendritic ubiquitination and Golgi fragmentation. Eur. J. Neurosci. 22: 1881–1894 (2005).

Vukosavic S., et al.. Bax and Bcl-2 interaction in a transgenic mouse model of familial amyotrophic lateral sclerosis. J Neurochem. 73(6): 2460-8 (1999).

Wang C.Y., et al.. NF-kappaB induces expression of the Bcl-2 homologue A1/Bfl-1 to preferentially suppress chemotherapy-induced apoptosis. Mol. Cell. Biol. 19: 5923–5929 (1999).

Wang I.F., et al.. TDP-43: an emerging new player in neurodegenerative diseases. Trends Mol. Med. 14: 479–485 (2008).

Wang J, et al.. Copper-binding-site-null SOD1 causes ALS in transgenic mice: aggregates of non-native SOD1 delineate a common feature. Human Molecular Genetics Vol. 12 No. 21: 2753–2764 (2003).

Wang X., et al.. Degradation of TDP-43 and its pathogenic form by autophagy and the ubiquitin-proteasome system. Neurosci. Lett. 469: 112–116 (2010).

Warraich S.T., et al.. TDP-43: A DNA and RNA binding protein with roles in neurodegenerative Diseases. The International Journal of Biochemistry & Cell Biology 42: 1606–1609 (2010).

Watanabe M., et al.. Histological Evidence of Protein Aggregation in Mutant SOD1 Transgenic Mice and in Amyotrophic Lateral Sclerosis Neural Tissues. Neurobiology of Disease 8: 933–941 (2001).

Wegorzewska I., et al.. TDP-43 mutant transgenic mice develop features of ALS and frontotemporal lobar degeneration. Proc. Natl Acad. Sci. USA 106: 18809–18814 (2009).

Weisskopf M.G., et al. Prospective study of occupation and amyotrophic lateral sclerosis mortality. Am J Epidemiol 162(12): 1146-52 (2005).

Weisskopf M.G., et al.. Smoking may be considered an established risk factor for sporadic ALS. Am J Epidemiol160 (1): 26-33 (2004).

Werner A.B., et al.. Bcl-2 family member Bfl-1/A1 sequesters truncated bid to inhibit is collaboration with pro-apoptotic Bak or Bax. J. Biol. Chem. 277: 22781–22788 (2002).

Wiedemann F.R., et al.. Mitochondrial DNA and respiratory chain function in spinal cords of ALS patients. Journal of Neurochemistry 80: 616-625 (2002).

Williamson T.L. and Cleveland D.W.. Slowing of axonal transport is a very early event in the toxicity of ALS-linked SOD1 mutants to motor neurons. Nature neuroscience Vol. 2 No. 1 (1999).

Wils H., et al.. TDP-43 transgenic mice develop spastic paralysis and neuronal inclusions characteristic of ALS and frontotemporal lobar degeneration. Proc. Natl Acad. Sci. USA (2010).

Winton M.J., et al.. Disturbance of nuclear and cytoplasmic TAR DNA-binding protein (TDP-43) induces disease-like redistribution, sequestration, and aggregate formation. J. Biol. Chem. 283: 13302–13309 (2008).

Wong P.C., et al.. An adverse property of a familial ALS-linked SOD1 mutation causes motor neuron disease characterized by vacuolar degeneration of mitochondria. Neuron 14: 1105–16 (1995).

Xiao S., et al.. RNA targets of TDP-43 identified by UV-CLIP are deregulated in ALS. Mol. Cell. Neurosci. 47: 167–180 (2011).

Xing R.H., Rabbani S.A.. Overexpression of urokinase receptor in breast cancer cells results in increased tumor invasion, growth and metastasis. Int J Cancer 67:423-429 (1996).

Xu Z, et al.. Increased expression of neurofilament subunit NF-L produces morphological alterations that resemble the pathology of human motor neuron disease. Cell 73: 23–33 (1993).

Yang J., et al.. Prevention of apoptosis by Bcl-2: release of cytochrome c from mitochondria blocked. Science 275: 1129-32 (1997).

Yang WS, et al.. C-terminal region of Bfl-1 induces cell death that accompanies caspase activation when fused with GFP. J Cell Biochem. 94(6): 1234-47 (2005).

Yang Y., et al.. The gene encoding alsin, a protein with three guanine-nucleotide exchange factor domains, is mutated in a form of recessive amyotrophic lateral sclerosis. Nature genetics Vol. 29 (2001).

Yeo G.W., et al.. An RNA code for the FOX2 splicing regulator revealed by mapping RNA-protein interactions in stem cells. Nat. Struct. Mol. Biol. 16: 130–137 (2009).

Yim M.B., et al.. Copper,zinc superoxide dismutase catalyzes hydroxyl radical production from hydrogen peroxide. Biochemistry Vol. 87: 5006-5010 (1990).

Yokoseki A., et al.. TDP-43 mutation in familial amyotrophic lateral sclerosis. Ann. Neurol. 63: 538–542 (2008).

Zhang Y.J., et al.. Aberrant cleavage of TDP-43 enhances aggregation and cellular toxicity. Proc. Natl Acad. Sci. USA 106: 7607–7612 (2009).

Zhang Y.J., et al.. Progranulin mediates caspase-dependent cleavage of TAR DNA binding protein-43. J. Neurosci. 27: 10530–10534 (2007).

Zhu S., et al.. Minocycline inhibits cytochrome c release and delays progression of amyotrophic lateral sclerosis in mice. Nature 417: 74–78 (2002).

Zinman L., Cudkowicz M.. Emerging targets and treatments in amyotrophic lateral Sclerosis. Lancet Neurol; 10: 481–90 (2011).

Zinszner H., et al.. A topogenic role for the oncogenic N-terminus of TLS: nucleolar localization when transcription is inhibited. Oncogene 14: 451–461 (1997).

Zong W.X., et al.. The prosurvival Bcl-2 homolog Bfl-1/A1 is a direct transcriptional target of NF-kappaB that blocks TNFalpha-induced apoptosis. Genes Dev. 13: 382–387 (1999).